

IDÓJÁRÁS

QUARTERLY JOURNAL
OF THE HUNGARIAN METEOROLOGICAL SERVICE

CONTENTS

<i>Andrzej Doroszewski, Katarzyna Żyłowska, Anna Nieróbca, and Tytus Berbeć: Agricultural autumn drought and crop yield in 2011 in Poland.....</i>	361
<i>Zuzanna Bielec-Bąkowska, Katarzyna Piotrowicz, and Ewa Krępa-Adolf: Trends in the frost-free season with parallel circulation and air-mass statistics in Poland.....</i>	375
<i>Czesław Koźmiński and Bożena Michalska: Wind Speed and Direction on the Polish Baltic Coast and Conditions for Recreation.....</i>	393
<i>Tin Lukić, Biljana Basarin, Tanja Micić, Dajana Bjelajac, Tiemen Maris, Slobodan B. Marković, Dragoslav Pavić, Milivoj B. Gavrilov, and Minučer Mesaroš: Rainfall erosivity and extreme precipitation in the Netherlands</i>	409
<i>Tatjana Popov, Slobodan Gnjato, and Goran Trbić: Analysis of extreme precipitation over the Peripannonian region of Bosnia Hercegovina.....</i>	433
<i>Evhen V. Samchuk: Methodology of objective three- dimensional identification and tracking of the cyclones and anticyclones in the low and middle troposphere</i>	453

IDŐJÁRÁS

Quarterly Journal of the Hungarian Meteorological Service

Editor-in-Chief
LÁSZLÓ BOZÓ

Executive Editor
MÁRTA T. PUSKÁS

EDITORIAL BOARD

- | | |
|---------------------------------------|--|
| ANTAL, E. (Budapest, Hungary) | MIKA, J. (Eger, Hungary) |
| BARTHOLY, J. (Budapest, Hungary) | MERSICH, I. (Budapest, Hungary) |
| BATCHVAROVA, E. (Sofia, Bulgaria) | MÖLLER, D. (Berlin, Germany) |
| BRIMBLECOMBE, P. (Hong Kong, SAR) | PINTO, J. (Res. Triangle Park, NC, U.S.A.) |
| CZELNAI, R. (Dörgicse, Hungary) | PRÁGER, T. (Budapest, Hungary) |
| DUNKEL, Z. (Budapest, Hungary) | PROBÁLD, F. (Budapest, Hungary) |
| FERENCZI, Z. (Budapest, Hungary) | RADNÓTI, G. (Reading, U.K.) |
| GERESDI, I. (Pécs, Hungary) | S. BURÁNSZKI, M. (Budapest, Hungary) |
| HASZPRA, L. (Budapest, Hungary) | SZALAI, S. (Budapest, Hungary) |
| HORVÁTH, Á. (Siófok, Hungary) | SZEIDL, L. (Budapest, Hungary) |
| HORVÁTH, L. (Budapest, Hungary) | SZUNYOGH, I. (College Station, TX, U.S.A.) |
| HUNKÁR, M. (Keszthely, Hungary) | TAR, K. (Debrecen, Hungary) |
| LASZLO, I. (Camp Springs, MD, U.S.A.) | TÄNCZER, T. (Budapest, Hungary) |
| MAJOR, G. (Budapest, Hungary) | TOTH, Z. (Camp Springs, MD, U.S.A.) |
| MÉSZÁROS, E. (Veszprém, Hungary) | VALI, G. (Laramie, WY, U.S.A.) |
| MÉSZÁROS, R. (Budapest, Hungary) | WEIDINGER, T. (Budapest, Hungary) |

Editorial Office: Kitaibel P.u. 1, H-1024 Budapest, Hungary

P.O. Box 38, H-1525 Budapest, Hungary

E-mail: journal.idojaras@met.hu

Fax: (36-1) 346-4669

**Indexed and abstracted in Science Citation Index Expanded™ and
Journal Citation Reports/Science Edition**

Covered in the abstract and citation database SCOPUS®

Included in EBSCO's databases

Subscription by mail:

IDŐJÁRÁS, P.O. Box 38, H-1525 Budapest, Hungary

E-mail: journal.idojaras@met.hu

IDŐJÁRÁS

*Quarterly Journal of the Hungarian Meteorological Service
Vol. 122, No. 4, October – December, 2018, pp. 361–374*

Agricultural autumn drought and crop yield in 2011 in Poland

**Andrzej Doroszewski, Katarzyna Żylowska, Anna Nieróbca,
and Tytus Berbeć***

*Institute of Soil Science and Plant Cultivation - State Research Institute,
Czartoryskich 8, 24-100 Puławy, Poland*

Corresponding author E-mail: tberbec@iung.pulawy.pl

(Manuscript received in final form November 15, 2017)

Abstract—Over the recent years, drought has been occurring with an ever increasing frequency in Poland. The longer the rainless period lasts, the more acute its impacts are. Agricultural drought manifests itself as a prolonged period of water shortage for agricultural crops during their growth season resulting in yield reduction. Extent of drought was evaluated by the climatic water balance (*CWB*). Climatic water balance is an indicator that determines the state of humidification of the environment using data measured at meteorological stations. It is defined as the difference between atmospheric precipitation and evapotranspiration (in millimeters) calculated by an empirical formula taking into account: temperature, sunshine, and length of the day. *CWB* was calculated using meteorological data from 294 weather stations and weather posts across Poland. Spatial data from point measurements were interpolated using the Geographic Information System (GIS) software. Yield forecasts were made for major crops in Poland using agro-meteorological yield models and weather indices (*WI*). Yield figures were based on data from the Central Statistical Office of Poland (GUS).

The autumn of 2011 was the driest in several dozen years in many localities of south-eastern Poland. For instance, at the weather station in Puławy, the lowest level of precipitation had been recorded since 1871. Weather conditions prevailing in the growing season of 2012 were very beneficial for winter cereals and winter rapeseed. As for sugar beet, the weather also favored high yields over most of the growing season, except the final stage of growth. Notwithstanding the extreme drought in the autumn of 2011, the good weather conditions in the remaining part of the growth period caused the yields of winter crops and sugar beet to be high.

The very scant autumn precipitation, even though it had negative impact on the germination of cereals, seedling emergence, and seedling growth, did not cause any major losses to yields. Water supplies from September precipitation combined with frequent morning mists, fogs, and dew mitigated the impact of prolonged drought and were sufficient to sustain the yields at an acceptable level.

Key-words: agricultural drought, atmospheric drought, climatic water balance (*CWB*), precipitation, yields

1. Introduction

The climate change precipitates events of extreme nature, drought being one of them (*Łabędzki*, 2006). Drought can be very acute, especially if prolonged. As the rainless spell continues, the first to appear is the atmospheric drought, and it is followed by hydrological drought.

In the field, drought and its intensity can be determined by means of teledetection techniques and using meteorological data. The method used to determine the occurrence of drought is the standardized precipitation index (SPI) (*Dhakar et al.*, 2013; *Li et al.*, 2012; *Vergin and Todisco*, 2011). There are also other modified indicators to measure the extent of drought such as standardized precipitation evapotranspiration index (SPEI) (*Meza*, 2013) and agricultural drought index (ADI) (*Brunini et al.*, 2005), both of which utilize evapotranspiration data. A different group of methods employs satellite image-based data by using the normalized difference vegetation index (NDVI) or its variants (*Ezzine et al.*, 2014; *Rhee et al.*, 2010; *Son et al.*, 2012; *Wu et al.*, 2013).

In this study, the *CWB* index that takes account the evapotranspiration and atmospheric precipitation figures (*Doroszewski et al.*, 2012, 2016; *Łabędzki et al.*, 2008, 2011) was used to ascertain the occurrence of drought.

Agricultural drought becomes manifest as a long and profound shortage of water available to plants during their growth, whose final outcome is yield reduction. High air temperatures, heavy insolation, and high wind velocities combine to increase the rate of evaporation of water from plants and soil. In Poland, drought in the growing season occurs at various times, but most frequently in the spring and much less frequently in the autumn (*Farat et al.*, 1995). The previous extreme drought spells were recorded in 1951 and 1959 in south-eastern Poland (*Mitosek*, 1960).

Losses to agricultural drought are important economic problems nationwide because of massive reduction in crop yields (*Lipiec et al.*, 2013; *Martyniak et al.*, 2007). They are also major economic issues for farmers themselves, as they generate a decrease in gross financial returns made from farming (*Lawes and Kingwell*, 2012).

The objective of the study was to describe the meteorological conditions behind the extreme atmospheric drought in the autumn of 2011, and to assess the drought's impact on the yields of winter cereals and sugar beets in Poland.

2. Materials and methods

The drought-related meteorological conditions were determined using the climatic water balance (*CWB*) i.e., as a difference between the atmospheric precipitation and potential evaporation (*Doroszewski et al.*, 2012, 2014; *Harmsen et al.*, 2009; *Kanecka-Geszke and Smarzyńska*, 2007; *Legates and McCabe*, 2005; *Łabędzki*, 2006; *Łabędzki et al.*, 2011; *Paltineanu et al.*, 2011; *Rojek*, 1987).

$$CWB = P - ETP, \quad (1)$$

where P is the atmospheric precipitation (mm) and ETP is the evapotranspiration (mm).

Potential evapotranspiration was calculated using formula (*Doroszewski and Górska, 1995*) based on Penman's algorithm (*Penmann, 1948*):

$$ETP = -89.6 + 0.0621 t^2 + 0.00448 h^{1.66} + 9.1 f, \quad (2)$$

where t is the mean air temperature 2 mm above ground level ($^{\circ}\text{C}$), h is the insolation (h), and f is the daylength (h).

Data on atmospheric precipitation came from 54 weather stations and 163 precipitation-measuring posts operated by IMGW-PIB (Institute of Meteorology and Water Management – National Research Institute), 50 weather stations run by COBORU (Research Center for Cultivar Testing), and 27 automated weather stations operated by IUNG-PIB (Institute of Soil Science and Plant Cultivation-State Research Institute). Potential evapotranspiration (ETP) was determined based on weather data collected by 54 IMGW-PIB weather stations and 27 IUNG-PIB weather stations. Altogether, CWB was calculated based on data from 295 sites across Poland. Spatial data from on-site measurements were interpolated using GIS (Geographic Information System).

Yield predictions for major crops in Poland were made using agrometeorological yield models – weather indices were developed by IUNG-PIB (*Górska et al., 1997*). Actual yield figures for the crops under study were obtained from data published by GUS (Main Statistical Office of Poland) (*Statistical yearbooks of Agricultural, 2003–2013*).

3. Results and discussion

The first signs of an imminent drought were recorded as early as in August 2011 in the south-eastern part of Poland (*Fig. 1*). An unequivocal water deficit also occurred in September. Water deficits in both months (August and September) were as high as 120 to 150 mm over large areas of some provinces: southern part of Mazowieckie, eastern part of Świętokrzyskie, northern part of Podkarpackie, and nearly across the whole area of the province of Lubelskie (*Figs. 1 and 2*). In those areas, average long-term CWB values ranged from –50 to –20 mm (*Rojek, 1987*).

The weather conditions were very conducive to drought: the air temperature in the southern part of Poland in August was $1.5\ ^{\circ}\text{C}$ above the long-term average, whereas precipitation-wise the month was dry, very dry, or extremely dry over most of the country. The precipitation in the south-eastern part of the country accounted for 30 to 40% of that averaged over the period from 1971 to 2000 (*Bulletin of the National Hydrological and Meteorological Services, 2011*).

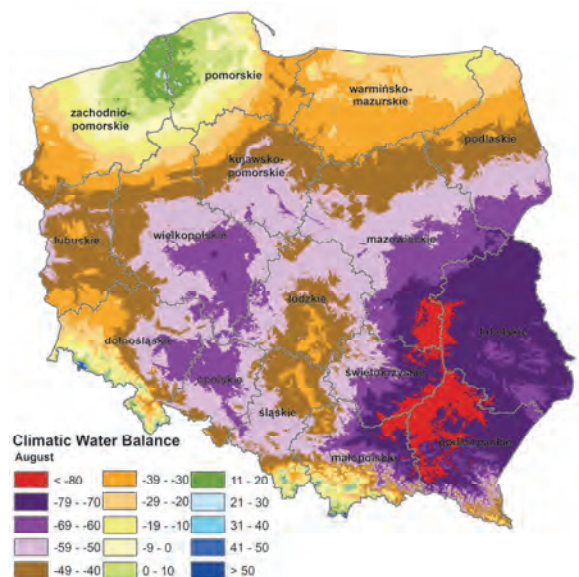


Fig. 1. Climatic water balance in August 2011.

September was also very warm throughout the country. The temperature exceeded the long-term average by 2 °C. Except for the western and north-western parts, where precipitation of 30 to 100 mm was recorded, the remaining area of Poland received substantially less rainfall: from 2 to 30 mm. In the central and eastern parts of Poland, September was extremely dry, very dry, or dry. In Puławy (province of Lubelskie), the precipitation was 6.2 mm (12% of the long-term average). In Kozienice (province of Mazowieckie), it was 2.9 mm (5.6% of the long-term average). Across the country, the average monthly precipitation was approximately the 50% of the long-term average. Those thermal and moisture conditions brought a substantial shortage of water in south-eastern Poland, which ranged from 40 to 60 mm (*Fig. 2*). Such a heavy deficit caused the top layer of soil to become exceedingly dry (*Bulletin of the National Hydrological and Meteorological Services*, 2011).

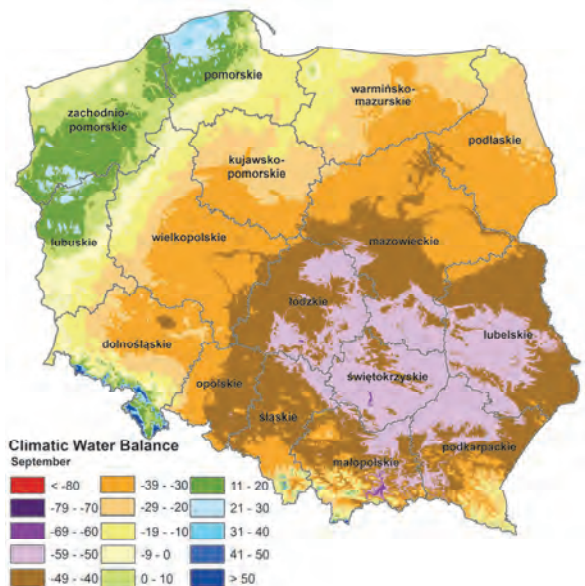


Fig. 2. Climatic water balance in September 2011.

In October, the heaviest water deficit occurred in central Poland, ranging from 10 to 20 mm (Fig. 3). The long rainless period aggravated even further the shortage of the soil water. Over a large area of the country, the parching of topsoil continued to be recorded. The monthly average temperature of October was 0.3 °C in excess of the regular temperature for the month. In thermal terms it was qualified as normal. October was dry to very dry over most of the country, becoming extremely dry in the north-eastern and central parts (*Bulletin of the National Hydrological and Meteorological Services*, 2011).

In November, the thermal conditions approached the long-term average (*Bulletin of the National Hydrological and Meteorological Services*, 2011). Except for north-eastern Poland, where the precipitation was the highest, the remaining part of the country received very little, if any, of it (Table 2). Scant precipitation combined with low evapotranspiration (Table 3) caused the water deficit (CWB) to be as low as 10 mm over a large portion of the country, especially in its southern part (Fig. 4). Precipitation-wise, the month was rated across the nation as extremely dry, and the heavy shortage of precipitation aggravated only the moisture conditions of the soil also (*Bulletin of the National Hydrological and Meteorological Services*, 2011).

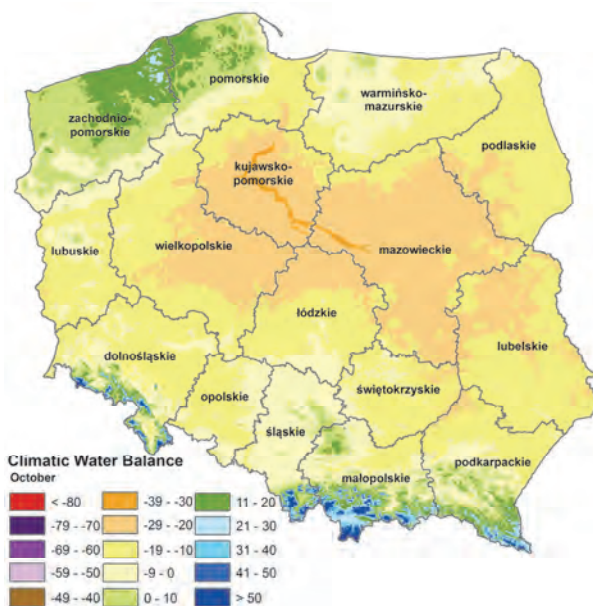


Fig. 3. Climatic water balance in October 2011.

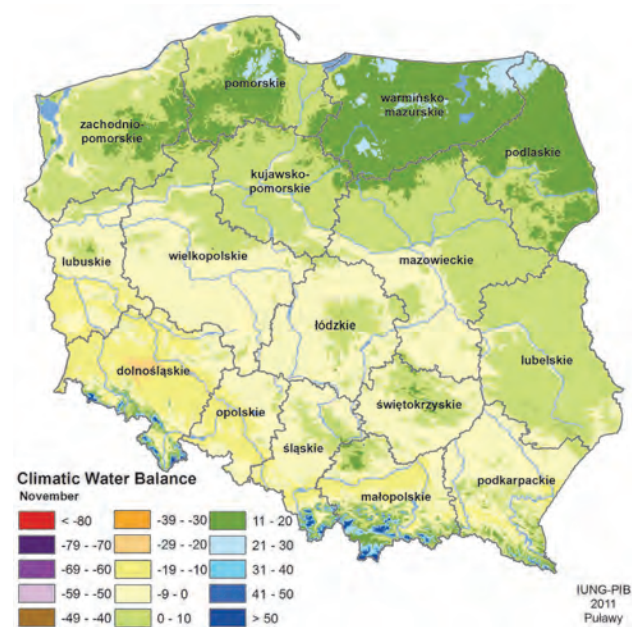


Fig. 4. Climatic water balance in November 2011.

Difficult weather conditions in the autumn period were depicted by the CWB map for the periods August to November (*Fig. 5*) and September to November (*Fig. 6*). The cumulative maps show the area of the country, where the drought occurred.

At many localities of south-eastern Poland, the autumn of 2011 was the driest in many years (*Tables 1, 2, and 3*). The meteorological station in Puławy is one of the oldest in Poland. On the basis of data obtained from observations conducted since 1871, it was possible to find out how often drought occurred in this area. In Puławy, extreme autumn atmospheric drought with precipitation that falls short of 50% of the long-term average appears once in about 15 years, on average. However, such low precipitation as that in 2011 had not been recorded since 1871 (*Table 1*). Particularly low precipitation, below 30% of the long-term average, occurred in the years 1951, 1959, and 2011, but that below 30 mm occurred only once, in 2011, which is an absolute record in the 142-year-long history of that station.

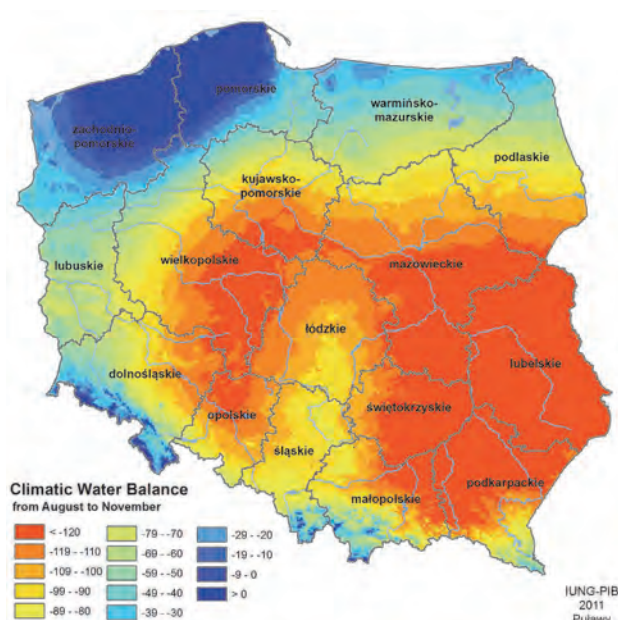


Fig. 5. Climatic water balance for the entire period from August to November in 2011.

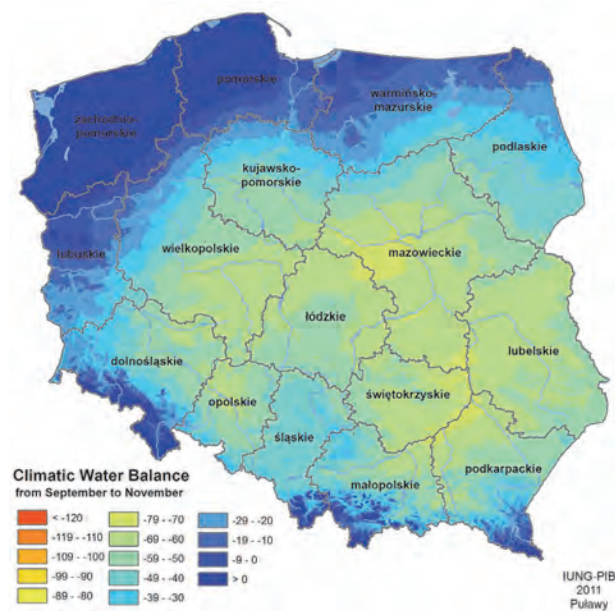


Fig. 6. Climatic water balance for the entire period from September to November in 2011.

Table 1. Years of lowest rainfall in autumn (September-November) in the period of 1871-2012 in Pulawy.

No.	Years	Precipitation, month, season								
		Sept (mm)	Sept (% of norm)*	Oct (mm)	Oct (% of norm)*	Nov (mm)	Nov (% of norm)*	Autumn (mm)	Autumn (% of norm)**	
1	1891	14	28	11	26	35	90	60	45	
2	1908	30	60	22	51	13	33	65	49	
3	1942	7	14	32	74	26	67	65	49	
4	1911	17	34	21	49	15	38	53	40	
5	1951	2	4	1	2	31	79	34	26	
6	1959	7	14	8	19	16	41	31	23	
7	1965	21	42	9	21	35	90	65	49	
8	2005	33	66	3	7	28	72	64	48	
9	2011	6	12	22	51	0 (0.2)	0 (1)	28	21	
1871–2012		50	100	43	100	39	100	132	100	

*Months: 25–49.9% - very dry; <25% - extremely dry (Kaczorowska, 1962; Łabędzki, 2006).

**Season: 50–74.9% - very dry; <50% - extremely dry (Kaczorowska, 1962; Łabędzki, 2006).

Tables 2 and 3 show data from selected meteorological stations in south-eastern Poland, where very low values of precipitation (Table 2) and potential evapotranspiration (Table 3) occurred in the autumn of 2011. The evapotranspiration (Table 3) in November was very close or even equal to zero.

Table 2. Monthly precipitation values in 2011 and long-term monthly averages in selected meteorological stations of south-eastern Poland.

No.	Station names	Aug (mm)	% of norm*	Sept (mm)	% of norm*	Oct (mm)	% of norm*	Nov (mm)	% of norm*	Sept- Nov norm** (mm)
1	Puławy (lubelskie)	41.1	56	5.9	13	20.5	53	0.2	1	26.6
2	Osiny (lubelskie)	42.8	58	4.7	10	31.5	81	1.4	4	37.6
3	Palikije (lubelskie)	12.7	17	6.9	14	23.2	54	0.5	1	30.6
4	Rogalów (lubelskie)	42.2	58	4.2	9	21.7	50	1.7	4	27.6
5	Rogów (lubelskie)	46.0	63	3.6	7	28.2	67	2.3	6	34.1
6	Werbkowice (lubelskie)	48.5	66	16.4	34	23.0	53	2.5	6	41.9
7	Błonie-Topola (łódzkie)	25.2	38	30.9	70	21.3	58	1.3	4	53.5
8	Borusowa (małopolskie)	43.0	58	9.6	20	28.3	71	1.9	5	39.8
9	Bodaczki (podlaskie)	45.8	62	9.3	20	9.6	23	10.0	24	28.9
10	Annoślaw (łódzkie)	60.9	86	8.7	20	23.8	64	2.9	8	35.4
11	Gołąbki (lubelskie)	40.1	53	17.6	37	16.7	44	2.5	7	36.8
12	Grabów (lubelskie)	28.8	36	4.0	5	19.7	45	1.2	3	24.9
13	Bratoszewice (łódzkie)	107.6	152	7.1	15	26.6	67	2.8	7	36.5
14	Dobra (łódzkie)	110.9	156	19.9	42	24.0	60	0.7	2	44.6
15	Kielce (świętokrzyskie)	40.7	53	4.6	8	24.4	58	0.3	1	29.3
16	Kraków (małopolskie)	64.8	85	14.2	24	29.7	60	0.2	1	44.1
17	Lublin (lubelskie)	30.7	45	5.1	9	26.9	62	1.0	3	33.0
18	Łódź (łódzkie)	65.5	106	11.1	22	29.3	74	0.3	1	40.7
19	Rzeszów (podkarpackie)	29.3	43	8.6	14	30.0	63	0.4	1	39.0
20	Terespol (lubelskie)	45.4	74	16.6	31	23.6	63	4.6	14	44.8
21	Warszawa (mazowieckie)	61.8	105	7.0	14	9.4	25	0.4	1	16.8

*Months: 25–49.9% - very dry; <25% - extremely dry (Kaczorowska, 1962; Łabędzki, 2006)

**Seasons: 50–74.9% - very dry; <50% - extremely dry (Kaczorowska, 1962; Łabędzki, 2006)

The optimum sowing date for winter rapeseed in drought-endangered areas is between the 10th and 20th of September (Walkowski *et al.*, 2002). In 2011, following a very rainy July, the soil was relatively well supplied with water, and there were no problems with emergence and rosette formation. Those conditions

caused the rapeseed to enter the overwintering season in a good condition, the plants developed 12–14 leaves, and the thickness of root crowns was also sufficient: 2–3 cm (*Walkowski et al.*, 2002).

Table 3. Monthly evapotranspiration values in 2011, south-eastern Poland

No.	Station names	Aug (mm)	Sept (mm)	Oct (mm)	Nov (mm)	Sept-Nov (mm)
1	Puławy (lubelskie)	116	70	27	1	98
2	Osiny (lubelskie)	116	70	27	1	98
3	Palikije (lubelskie)	114	69	28	0	97
4	Rogalów (lubelskie)	115	69	26	1	96
5	Rogów (lubelskie)	116	69	29	0	98
6	Werbkowice (lubelskie)	116	68	29	0	97
7	Błonie- Topola (lódzkie)	107	72	28	3	103
8	Borusowa (małopolskie)	116	74	26	2	102
9	Bodaczki (podlaskie)	112	63	25	0	88
10	Anosław (lódzkie)	116	69	25	2	96
11	Gołąbki (lubelskie)	117	67	31	0	98
12	Grabów (lubelskie)	117	64	28	2	94
13	Bratoszewice (lódzkie)	117	70	26	3	99
14	Dobra (lódzkie)	113	70	27	6	103
15	Kielce (świętokrzyskie)	111	71	23	1	95
16	Kraków (małopolskie)	115	73	26	2	101
17	Lublin (lubelskie)	114	69	28	0	97
18	Łódź (lódzkie)	117	70	25	3	98
19	Rzeszów (podkarpackie)	116	74	26	2	102
20	Terespol (lubelskie)	122	76	31	0	107
21	Warszawa (mazowieckie)	118	64	29	2	95

The optimum seeding date in drought-affected areas in 2011 (south-eastern Poland) was from the 16th to 25th of September (*Grabiński et al.*, 2007) for rye and from the 21th of September to the 1st of October for wheat (*Podolska and Holubowicz-Kliza*, 2005). In that period, a considerable shortage of water occurred, which may have caused very poor emergence. Because of substantial water deficit in the soil in the drought-affected areas, the tillering of rye in the autumn of 2011 was very poor (*Bulletin of the National Hydrological and Meteorological Services*, 2011) or, in extreme cases, non-existent. As a result of improved weather conditions, the tillering became more profuse only at the beginning of the winter season.

Among winter cereals, rye has the best developed root system, while the root system of barley develops slightly less, and that of wheat and triticale even more inferior. Notwithstanding, the yield forecast by IUNG-PIB envisaged

slightly higher yield losses for rye than for winter wheat (*Table 4*). Since rye was sown in September, earlier than wheat, it was much more exposed to drought than wheat. At the time of rye seeding (the second half of September) and in the first weeks after sowing, there was considerably less rainfall than when wheat was sown (the second half of September and the beginning of October). In October, in particular, moisture (*Figs. 2 and 3*) and precipitation conditions were much superior to those in September (*Table 2*). In Poland, rye is grown on soils which are much poorer and more prone to drought than those on which wheat is cultivated. The disadvantageous seeding date and the impact of poor soils were taken in account in the predictions, which foresaw that rye would respond with a slightly greater yield reduction than wheat (*Table 4*).

Table 4. Forecasted yields of winter crops in 2012 and sugar beet in 2011 (in %) relative to the long-term average yields

No.	Voivodeship	Rye	Winter wheat	Winter triticale	Winter rape	Sugar beet
1	Dolnośląskie	100	100	100	103	112
2	Kujawsko-Pomorskie	99	100	99	99	110
3	Lubelskie	98	99	97	104	103
4	Lubuskie	101	101	101	99	107
5	Łódzkie	99	99	98	105	107
6	Małopolskie	99	100	99	104	102
7	Mazowieckie	97	98	97	102	100
8	Opolskie	98	99	98	102	108
9	Podkarpackie	99	100	99	102	101
10	Podlaskie	100	100	99	106	107
11	Pomorskie	101	101	101	102	95
12	Śląskie	100	100	100	105	105
13	Świętokrzyskie	97	99	97	99	95
14	Warmińsko-Mazurskie	100	100	99	105	106
15	Wielkopolskie	99	99	99	102	108
16	Zachodniopomorskie	101	101	101	100	109
	Poland	99	100	99	103	105

The substantial water deficit, although it has an adverse impact on the germination and seedling emergence of winter crops, did not cause important yield losses. Also, the very low rainfall did not cause much harm at the beginning of the growing season, when the winter cereals were at the seedling stage and had few tillers. At that stage the plants did not require much water, as there was still enough available moisture from the September rainfall and from frequently occurring mists

and dew which mitigated the effects of prolonged drought, and which were plentiful enough to prevent heavy yield decrease (*Table 4*).

The impact of water deficit (low *CWB* values) and low rainfall in south-eastern Poland was reflected by yield predictions as decreased weather index (*WI*) values (*Table 4*). In areas where water shortage was acute, *WI* values were lower compared to those in the remaining parts of the country. However, the predicted yield reductions on long term-averages were not large, amounting from 2 to 3%. Thus, the adverse weather pattern in the autumn of 2011 did not cause substantial losses to the yields of the crops under study.

The autumn drought occurred chiefly in south-eastern Poland. In the north-western part of the country, the moisture conditions were much superior to those of the remaining areas. In the case of rapeseed, the 3% yield reduction in the north-east was caused by excessive rainfall (*Table 4*). Water deficit in the autumn of 2011 in the south-eastern part of Poland can be described as extreme atmospheric drought (*Kaczorowska, 1962*), whereas, because of relatively small yield losses, it is not qualified as agricultural drought (*Doroszewski et al., 2008, 2012; The Act, 2005*).

The drought of 2011 in Poland, although it was extreme in meteorological terms (*Kaczorowska, 1962*), did not cause excessive losses to winter cereals or sugar beets (*Tables 4*), since weather conditions prevailing in the advanced part of the growing season favored winter crops. *WI* values showed that the impact of the extremely low values of autumn precipitation in south-eastern Poland did not cause a significant yield reduction on long-term averages, as the yields of winter crops in 2012 and those of sugar beets in 2011 were high (*Table 4*).

In the autumn of 2011, the precipitation in south-eastern Poland was extremely low, amounting to 25 to 50 mm of the long-term average. However, the crop yields in drought-affected areas approached the long-term figures or even exceeded them in the case of winter rapeseed and sugar beets. Such a situation was caused by the favorable pattern of the remaining weather elements that positively affected yields: temperature and air humidity, mists, fogs, and dew. In November, when extremely low precipitation value was recorded, evapotranspiration was also very low (close to zero) thus, as a result, *CWB* figures were close to zero and no substantial water deficit occurred. The frequent occurrence of fogs, mists, and dew (*Bulletin of the National Hydrological and Meteorological Services, 2011*) caused the water shortages to be considerably mitigated as, under those conditions, precipitation accounted for 10–25% of the total amount of water available to plants.

4. Conclusions

In the autumn of the year 2011 (particularly in September and November) extremely low values of precipitation occurred in south-eastern Poland. The

occurrence of an extreme atmospheric drought did not cause considerable reduction of crop yields in the five drought-affected provinces. Unfavorable weather conditions did not cause yield reduction on long-term average figures for rapeseed, sugar beets, and winter cereals: wheat, barley, triticale, cereal mixtures. Low air temperature combined with a frequent occurrence of fogs, mists, and dew mitigated the adverse effect of drought and positively influenced the crop yields.

Acknowledgements: This work was supported by the research project „System of monitoring of agricultural drought in Poland” of Polish Ministry of Agriculture and Rural Development.

References

- Brunini, O., Dias da Silva, P.L., Griman, A.M., Assad Delgado, E., and Boken, V.K., 2005. Agricultural drought phenomena in Latin America with focus on Brazil. In (Eds.: Boken, V.K., Cracknell, A.P., Heathcote, R.L.) Monitoring and predicting agricultural drought: A Global Study. Oxford University Press, 156–168.
- Bulletin of the National Hydrological and Meteorological Services, IMGW-PIB.* 2011. 8–13; 106–111
- Statistical yearbook of Agricultural,* 2003-2013. Central Statistical Office of Poland (GUS), Warsaw.
- Dhakar, R., Sehgal, V.K., and Pradhan, S., 2013. Study on inter-seasonal and intra seasonal relationship of meteorological and agricultural drought indices in the Rajasthan State of India. *J. Arid Environ.* 97, 108–119. <https://doi.org/10.1016/j.jaridenv.2013.06.001>
- Doroszewski, A. and Górska, T., 1995. Prosty wskaźnik ewapotranspiracji potencjalnej. *Rocz. AR Pozn.*, CCLXXI, *Melior. Inż. Środ.*, 16, 3–8. (In Polish)
- Doroszewski A., Jóźwicki T., Wróblewska E., and Kozyra J., 2014. Susza rolnicza w Polsce w latach 1961-2010, Puławy, ISBN 978-83-7562-171-6. (In Polish)
- Doroszewski, A., Kozyra, J., Pudelko, R., Stuczyński, T., Jadczyszyn, J., Koza, P., and Łopatka, A., 2008. Monitoring suszy rolniczej w Polsce. *Wiad. Mel. i Łąk.*, 416, 35–38. (In Polish)
- Doroszewski, A., Jadczyszyn, J., Kozyra, J., Pudelko, R., Stuczyński, T., Mizak, K., Łopatka, A., Koza, P., Górska, T., Wróblewska, E., 2012. Podstawy Systemu Monitoringu Suszy Rolniczej. *Woda Środ. Obsz. Wiej.* (IV-VI), 12, 2(38), 77–91. (In Polish)
- Doroszewski A., Wróblewska E., Pudelko R., Żyłowska K., Koza P., and Nieróbca A., 2016. System monitoringu suszy rolniczej w Polsce – podstawy metodologiczne i możliwości zastosowań. In: (Eds. Dembek W., Kuś J., Wiatkowski M., Żurek G. Brwinów) Innowacyjne metody gospodarowania zasobami gospodarki wodnej w rolnictwie. 105–128.(In Polish)
- Ezzine, H., Bouziane, A., and Ouazar, D., 2014. Seasonal comparisons of meteorological and agricultural drought indices in Morocco using open short time-series data. *International Journal of Applied Earth Observation and Geoinformation* 26, 36–48. <https://doi.org/10.1016/j.jag.2013.05.005>
- Farat, R., Kępińska-Kasperek, M., Kowalczyk P., and Mager, P., 1995. Susze na obszarze Polski w latach 1951-1990. Mater. Bad. IMGW Gosp. Wodna i Ochrona Wód. Vol. 16, 59-72 (In Polish)
- Górska, T., Demidowicz, G., Deputat, T., Górska, K., Marcinkowska, I., and Spoz-Pać, W., 1997. Empiryczny model plonowania pszenicy ozimej w funkcji czynników meteorologicznych. *Zesz. Nauk. AR, Wrocław*, 313, 99–109. (In Polish)
- Grabiński, J., Holubowicz-Kliza, G., and Brzóska, F., 2007. Uprawa i wykorzystanie żyta ozimego. IUNG PIB, IŻ PIB, User's of Dissemination, 138. 1-80. (In Polish)
- Harmsen, E.W., Miller, N.L., Schlegel, N.J., and Gonzalez, J.E., 2009. Seasonal climate change impacts on evapotranspiration, precipitation deficit and crop yield in Puerto Rico. *Agric. Water Manage.* 96, 1085–1095. <https://doi.org/10.1016/j.agwat.2009.02.006>
- Kaczorowska, Z., 1962. Opady w Polsce w przekroju wieloletnim. Ed. Wyd. Geol. Warszawa, Prace Geogr. Instytut Geogr. PAN, 33. (In Polish)

- Kanecka-Geszke, E. and Smarzyńska, K., 2007. Ocena suszy meteorologicznej w wybranych regionach agroklimatycznych Polski przy użyciu różnych wskaźników. *Acta Sci. Pol. Formatio Circumiectus* 6(2), 41–50. (In Polish)
- Lawes, R.A. and Kingwell, R.S., 2012. A longitudinal examination of business performance indicators for drought-affected farms. *Agric. Syst.* 106, 94–101.
<https://doi.org/10.1016/j.agsy.2011.10.006>
- Legates, D.R., and McCabe, G.J., 2005. A re-evaluation of the average annual global water balance. *Phys. Geogr.* 26, 467–479. <https://doi.org/10.2747/0272-3646.26.6.467>
- Li, Y., Zheng, X., Lu, F., and Ma, J., 2012. Analysis of drought evolvement characteristics based on Standardized Precipitation Index in the Huaihe River Basin. *Procedia Engineering* 28, 434–437.
<https://doi.org/10.1016/j.proeng.2012.01.746>
- Lipiec, J., Doussan, C., Nosalewicz, A., and Kondracka, K., 2013. Effect of drought and heat stresses on plant growth and yield: a review. *Int. Agrophys.* 27, 463–477.
<https://doi.org/10.2478/intag-2013-0017>
- Łabędzki, L., 2006. Susze rolnicze – zarys problematyki oraz metody monitorowania i klasyfikacji. Rozpr. Nauk. Monografie, Falenty: IMUZ, Woda-Środowisko-Obszary-Wiejskie, 17, 107. (In Polish)
- Łabędzki, L., Bąk, B., Kanecka-Geszke, E., Kasperska-Wołowicz, W., and Smarzyńska, K., 2008. Związek między suszą meteorologiczną i rolniczą w różnych regionach agroklimatycznych Polski. Rozpr. Nauk. Monografie, Falenty: IMUZ, Woda-Środowisko-Obszary-Wiejskie 25. (In Polish)
- Łabędzki, L., Kanecka-Geszke, E., Bąk, B., and Słowińska, S., 2011. Estimation of reference evapotranspiration using the FAO Penman-Monteith method for climatic Conditions of Poland. Evapotranspiration. Ed. Prof. Leszek Łabędzki, *InTech*. 275–294.
- Martyniak, L., Dabrowska-Zielinska, K., Szymczyk, R., and Gruszczynska, M., 2007. Validation of satellite-derived soil-vegetation indices for prognosis of spring cereals yield reduction under drought conditions – case study from central-western Poland. *Adv. Space Res.* 39, 67–72.
<https://doi.org/10.1016/j.asr.2006.02.040>
- Meza, F.J., 2013. Recent trends and ENSO influence on droughts in Northern Chile: An application of the Standardized Precipitation Evapotranspiration Index. *Weather Climate Extr.* 1, 51–58.
<https://doi.org/10.1016/j.wace.2013.07.002>
- Mitosek, H., 1960. Letnia-jesienna susza 1959 r. *Post. Nauk Rol.*, 1(61), 53–64. (In Polish)
- Paltineanu, C., Chitu, E., and Mateescu, E., 2011. Changes in crop evapotranspiration and irrigation water requirements. *Int. Agrophys.* 25, 369–373.
- Penmann, H.L., 1948. Natural evaporation from open water, bare soil and grass. *Proc. Roy. Soc. of London.* 193, 120–145. <https://doi.org/10.1098/rspa.1948.0037>
- Podolska, G. Holubowicz-Kliza, G., 2005. Uprawa pszenicy ozimej na cele młyńskie. IUNG-PIB. User's of Dissemination, 106. (In Polish)
- Rhee, J., Im, J., and Carbone, G.J., 2010. Monitoring agricultural drought for arid and humid regions using multi-sensor remote sensing data. *Remote Sens. Environ.* 114, 2857–2887.
<https://doi.org/10.1016/j.rse.2010.07.005>
- Rojek, M., 1987. Rozkład czasowy i przestrzenny klimatycznych i rolno-klimatycznych bilansów wodnych na terenie Polski. *Zesz. Nauk. AR.* Wrocław, 62, 67. (In Polish)
- Son, N.T., Chen, C.F., Chen, C.R., Chang, L.Y., Minh, V.Q., 2012. Monitoring Agricultural drought in the Lower Mekong Basin using Modis NDVI and land surface temperature data. *International Journal of Applied Earth Observation and Geoinformation*, 18, 417–427.
<https://doi.org/10.1016/j.jag.2012.03.014>
- Ustawa z 2005. O dodatkowych opłatach za ubezpieczenie upraw rolnych i zwierząt gospodarskich Art.150, 1249 ze zmianami.(In Polish)
- Walkowski, T., Bartkowiak-Broda, I., Krzymański, J., Wielebski, F., Wójtowicz, M., Mrówczynski, M., Korbas, M., Paradowski, A., and Ochocki, P., 2002: Rzepak ozimy. Ed. IHAR Poznań. (In Polish)
- Wu, J., Zhou, L., Liu, M., Zhang, J., Leng, S., and Diao, C., 2013. Establishing and assessing the Integrated Surface Drought Index (ISDI) for agricultural drought monitoring in mid-eastern China. *Int. J. Appl. Earth Obs. Geoinf.* 23, 397–410. <https://doi.org/10.1016/j.jag.2012.11.003>
- Vergni, L., and Todisco, F., 2011. Spatio-temporal variability of precipitation, temperature and agricultural drought indices i Central Italy. *Agric. For. Meteorol.* 151, 301–313.
<https://doi.org/10.1016/j.agrformet.2010.11.005>

IDŐJÁRÁS

*Quarterly Journal of the Hungarian Meteorological Service
Vol. 122, No. 4, October – December, 2018, pp. 375–392*

Trends in the frost-free season with parallel circulation and air mass statistics in Poland

Zuzanna Bielec-Bąkowska¹, Katarzyna Piotrowicz^{2*}, and Ewa Krępa-Adolf³

¹ Faculty of Earth Science, University of Silesia,
Będzińska str. 60, 41-200 Sosnowiec, Poland

² Institute of Geography and Spatial Management, Jagiellonian University,
Gronostajowa str. 7, 30-387 Kraków, Poland

³ Public Primary School No. 7
Budowlanych str. 40, 47-122 Opole, Poland

* Corresponding author E-mail: k.piotrowicz@uj.edu.pl

(Manuscript received in final form November 18, 2017)

Abstract—This study describes the regularities in spatial and multiannual variations in the occurrence of last spring frost (LSF), first fall frost (FFF) and the length of the frost-free season (FFS). In the paper, daily minimum and maximum air temperatures recorded at 20 stations in Poland in 1951–2015 and a calendar of synoptic situations were used. It was found that at 75% of the analyzed stations the FFS period grew longer and the changes were statistically significant. Clearly, the longer length of the season is attributable to the earlier LSF dates. The frosts under investigation were recorded most frequently in anticyclonic situations, especially in the presence of an anticyclonic wedge (Ka) and a central anticyclone situation (Ca). LSFs and FFFs were predominantly accompanied by arctic (PA), polar maritime cold (PPms), and polar continental (PPk) air masses.

Key-words: frost-free season, atmospheric circulation, air masses, Niedźwiedź's calendar of synoptic situations, Poland

1. Introduction

Freeze events in spring and autumn (hereafter frost in spring, frost in autumn, or frost), which are defined as days with the minimum temperature below 0 °C and the maximum temperature above 0 °C (Kunkel *et al.*, 2004; Tomczyk *et al.*, 2015), have not only a significant influence on the growth of plants, but are also

crucial for the natural environment and human activity. For example, frosts can cause damages to trees, bushes, and other plants which have already started their vegetative growth, including flowers and/or fruiting buds (*Chmielewski and Rötzer, 2000; Menzel, 2000; Scheifinger et al., 2002*); they are added to the freeze-thaw processes thus accelerating frost weathering and influencing the life-cycle of insects and the spread of pests into new areas (*Juszczak et al., 2019*). Frosts also have impact on the transport and construction industries.

Long-term changes in the frost occurrence and the length of the frost-free season determine changes in the early and late phenological phases of various plants, determine the size of crops and fructification, and effect the thermal conditions of the vegetation period (*Kożuchowski and Żmudzka, 2000; Żmudzka, 2003; Graczyk and Kundzewicz, 2016; Wypych et al., 2017*). In turn, these changes force processes of adaptation including the need to use specific types of crops, methods, and dates of agrotechnical works, or the application of plant protection products at specific periods of the year.

Climatological and particularly agroclimatological studies tend to focus on the thermal and precipitation conditions prevailing the vegetative period. Multiannual variations in frost-free seasons, which are much shorter than vegetation seasons, are studied far less frequently. In Poland, the differences between the seasons reach as many as 50–60 days in southern and south-eastern Poland (except in mountainous areas), and they are the least pronounced (approximately 20 days) along the Baltic coast (*Wypych et al., 2017*).

Spring frosts can be particularly dangerous in forestry, agriculture, and above all in fruit farming and horticulture. They appear every year over large areas of Poland, most often in April and May (on average, between April 20 and May 25), and occasionally, also in early June (*Czarnecka et al., 2009; Ustrmł et al., 2014; Tomczyk et al., 2015*). Spring frosts usually occur on single days, but there are cases when they can last for more than 2 days. Most frequently, such frosts are mild in nature with the minimum temperature ranging between -0.1 and -2.0 $^{\circ}\text{C}$, while strong frosts ($\text{tmin} < -6$ $^{\circ}\text{C}$) occur very rarely in Poland (*Tomczyk et al., 2015*). In general, fall frosts cause much less damage to crops than spring frosts. They occur most frequently in September and October, sometimes in November, and along the Baltic coast, in extreme cases, even as late as December. Thus, on average, the first fall frosts are recorded between September 20 and November 5 (*Tomczyk et al., 2015; Wypych et al., 2017*). Plants are gradually preparing for their winter dormancy, therefore, they can be damaged only by early frosts involving large air temperature drops.

The length of the frost-free season, which lasts on average 160–180 days in Poland, depends on local conditions (altitude, landform, land cover, and distance from water bodies). However, given the multiannual and seasonal changes in air temperatures observable in Poland and worldwide (nearly all seasons are warmer), it is certain that these changes will also be reflected in the dates of the

first and last frost, and the length of the frost-free season (*Yu et al.*, 2014; *Zhang et al.*, 2014; *Modala et al.*, 2017).

The presence of frost within a given area is related, among other factors, to the synoptic situation (type of circulation and/or inflow of cool air masses), as well as the landform. The following types of frosts are distinguished: 1) radiation frost, associated with a high-pressure system, when the heat radiates from the surface into the atmosphere on a clear night and 2) advection frost, when wind moves air from cold regions. A third, mixed type of frost may be distinguished as radiation-advection frost (3).

Studies, e.g., by *Yu et al.* (2014) and *Zhang et al.* (2014) prove that in the Great Lakes region of the United States, there is a significant correlation between the last spring frost (LSF) and the Pacific North American (PNA) pattern index and between both the first fall frost (FFF) and the length of the frost-free season (FFS) and the Pacific Decadal Oscillation (PDO) indices (*Yu et al.*, 2014), whereas on the Tibetan Plateau the length of the FFS depends on the Northern Hemisphere Polar Vortex indices (*Zhang et al.*, 2014). In Central Europe and Poland, multi-annual variations in the FFS relative to the atmospheric circulation have not been extensively studied. *Tomczyk et al.* (2015) based such studies on values of the sea level pressure (SLP) and the height of the 500 hPa isobaric surface derived from reanalyses, and the types of circulation of the Grosswetterlagen classification. *Ustrnul et al.* (2014) narrowed down their research to the relationships between the occurrence of the last spring frost (LSF) and types of circulation using three classifications, the Grosswetterlagen, Lityński, and Niedzwiedź classifications. However, the above studies do not take into account the multiannual changeability in the types of circulation and air masses, which determines the occurrence of frost in this part of Europe. For this reason, the present study aims to investigate the spatiotemporal changes in the occurrence of the first and last frost and in the length of the frost-free season in Poland in 1951–2015, and to determine the frequency and changes in the types of circulation and air masses co-occurring with spring and fall frosts.

2. Data and methods

The study is based on daily minimum and maximum air temperature values read at 2 m above ground level at 20 synoptic stations of the Institute for Meteorology and Water Management in Poland in 1951–2015 (*Fig. 1, Table 3*). The only exception was data from Rzeszów and Lesko, which covers the period starting in 1952 and 1955, respectively. Data have been checked, and they are homogeneous. The homogeneity of records was tested by means of the *Alexandersson* (1986) test. A frost day in spring and autumn is defined as one when the minimum temperature is lower than 0 °C and the maximum

temperature is higher than 0 °C (*Kunkel et al.*, 2004; *Tomczyk et al.* 2015). In the individual years, the date of the last spring frost (LSF) and the date of the first fall frost (FFF) were determined for each station. These dates were the beginning and end dates of the frost-free season, respectively, used as the basis for determining the duration of the FFS. The trends of change in the beginning and end dates and the length of the frost-free season were determined using an equation of a linear regression, whereas trend significances were calculated using the Mann-Kendall test (*Mann*, 1945; *Kendall*, 1975).



Fig. 1. Meteorological stations used in the study.

Explaining the impact of atmospheric circulation on the occurrence of LSFs and FFFs requires the determination of mesoscale circulation and air mass types. For this reason, a calendar of synoptic situations developed by *Niedźwiedź* (2016a; *Table 1* and *2*), based on the period of 1873–2015 was used. Types of atmospheric circulation and air masses performed on the basis of synoptic maps came from the forecasting offices were determined. The identified synoptic situations are characteristic of the atmospheric conditions present in the basin of the upper Vistula (covering south-east Poland). Because some authors state that they can be used for identifying the synoptic weather conditions over the entire territory of Poland, relevant data was compared to verify this. For this purpose, a similar version of the calendar of synoptic situations for nine regions of Poland

spanning the period 2001–2015 was applied (*Niedźwiedź*, 2016b). The obtained results show that the differences between the frequency of the circulation types occurring on the frost days under study identified for the individual regions and for the basin of the upper Vistula may reach as much as 33%. As a consequence, the part of the analysis in question was conducted only for frost days occurring in Bielsko-Biała, Katowice, Zakopane, Rzeszów, and Lesko.

Table 1. Types of synoptic situations (according to catalogue of *Niedźwiedź*, 2016a)

Types of synoptic situations			
Anticyclonic situations		Cyclonic situations	
Symbol	Direction of advection	Symbol	Direction of advection
Na	North	Nc	North
NEa	North–East	NEc	North–East
Ea	East	Ec	East
SEa	South–East	SEc	South–East
Sa	South	Sc	South
SWa	South–West	SWc	South–West
Wa	West	Wc	West
NWa	North–West	NWc	North–West
Ca	Central anticyclonic situation (high center)	Cc	Central cyclonic situation (low center)
Ka	Anticyclonic wedge or ridge of high pressure	Bc	Through of low pressure
X	unclassified situations or pressure col		

Table 2. Types of air masses (according to catalogue of *Niedźwiedź*, 2016a)

Air masses	
PA	Arctic
PPm	Polar maritime (fresh)
PPmc	Polar maritime warm
PPms	Polar maritime old (transformed)
PPk	Polar continental
PZ	Tropical
rmp	Various air masses in day

3. The beginning, end, and length of the frost-free season

In Poland, in the years 1951–2015, on average the LSF fell on April 29, and the FFF fell on October 13. The FFS began the earliest in the northern (along the Baltic coast), western, and central parts of Poland (Fig. 2). On average, the LSF occurred as late as the first half of May in the north-east and south-east parts of Poland, in the mountains and intermontane valleys (Zakopane, Jelenia Góra), as well as in Toruń and Chojnice (Fig. 2). When analyzing the individual stations it was found that the earliest LSFs were recorded in Świnoujście, Hel, Kalisz, and Bielsko-Biała (March 12–30), while the latest ones were observed in Jelenia Góra and Włodawa (June 11–12) (Table 3).

Table 3. Dates of the last (LSF) and first frost day (FFF) and length of frost-free season (FFS) at selected stations in Poland (see also their coordinates) in the period of 1951–2015

Station	Φ [N]	λ [E]	H m a.s.l.	LSF			FFF			Length of FFS [days]				
				min	average	max	min	average	max	year	min	average	max	year
Bielsko-Biała	48°49'	19°00'	398	30.03	25.04	2.06	14.09	18.10	1.12	1973	118	175	235	2000
Chojnice	53°42'	17°31'	164	10.04	1.05	31.05	18.09	16.10	14.11	1977	109	167	202	1986
Hel	54°36'	18°48'	1	28.03	27.04	1.06	27.09	9.11	19.12	1976	152	195	253	2000
Jelenia Góra	50°54'	15°47'	342	17.04	16.05	12.06	6.09	27.09	21.10	1991	93	134	173	2002
Kalisz	51°46'	18°04'	138	20.03	21.04	20.05	14.09	17.10	23.11	1954	141	178	225	1998
Katowice	50°14'	19°01'	284	10.04	29.04	7.06	14.09	13.10	17.11	1973	118	166	210	1961
Legnica	51°11'	16°12'	122	3.04	23.04	20.05	8.09	15.10	10.11	1991	135	175	212	1961
Lesko	49°27'	22°20'	420	10.04	3.05	7.06	14.09	9.10	2.11	1977	114	159	200	2012
Łódź	51°43'	19°24'	187	9.04	28.04	1.06	17.09	15.10	15.11	1966	109	169	214	2000
Poznań	52°25'	16°50'	83	7.04	28.04	28.05	19.09	15.10	19.11	1957	120	169	222	2000
Rzeszów	50°06'	22°01'	195	4.04	1.05	2.06	14.09	9.10	12.11	1977	107	159	221	1989
Słubice	52°20'	14°35'	21	1.04	28.04	6.06	3.09	5.10	10.11	1977	108	159	203	2001
Suwałki	54°07'	22°56'	184	9.04	5.05	3.06	16.09	7.10	12.11	1982	114	154	189	1957
Szczecin	53°23'	14°37'	1	5.04	27.04	29.05	16.09	17.10	28.11	1952	116	172	222	2014
Świnoujście	53°55'	14°14'	6	12.03	16.04	12.05	13.10	8.11	28.12	1971	167	205	276	2006
Toruń	53°02'	18°35'	69	15.04	8.05	7.06	14.09	6.10	7.11	1977	113	149	197	1989
Warszawa	52°09'	20°57'	106	5.04	25.04	25.05	27.09	14.10	18.11	1964	134	171	222	2008
Włodawa	51°33'	23°31'	177	7.04	28.04	11.06	12.09	6.10	29.10	1973	115	159	199	2008
Wrocław	51°06'	16°54'	120	1.04	27.04	30.05	8.09	13.10	19.11	1991	114	167	222	1961
Zakopane	49°17'	19°57'	855	13.04	10.05	4.06	4.09	30.09	24.10	1966	109	142	186	2006
Poland				12.03	29.04*	12.06	03.09	13.10*	28.12	1991	93	166*	276	2006

Notation for dates in the second and third columns: 30.03 stands for March 30, etc.;

* average from 20 stations, min – the earliest date or the shorter frost-free period max – the latest date or the longest frost-free period

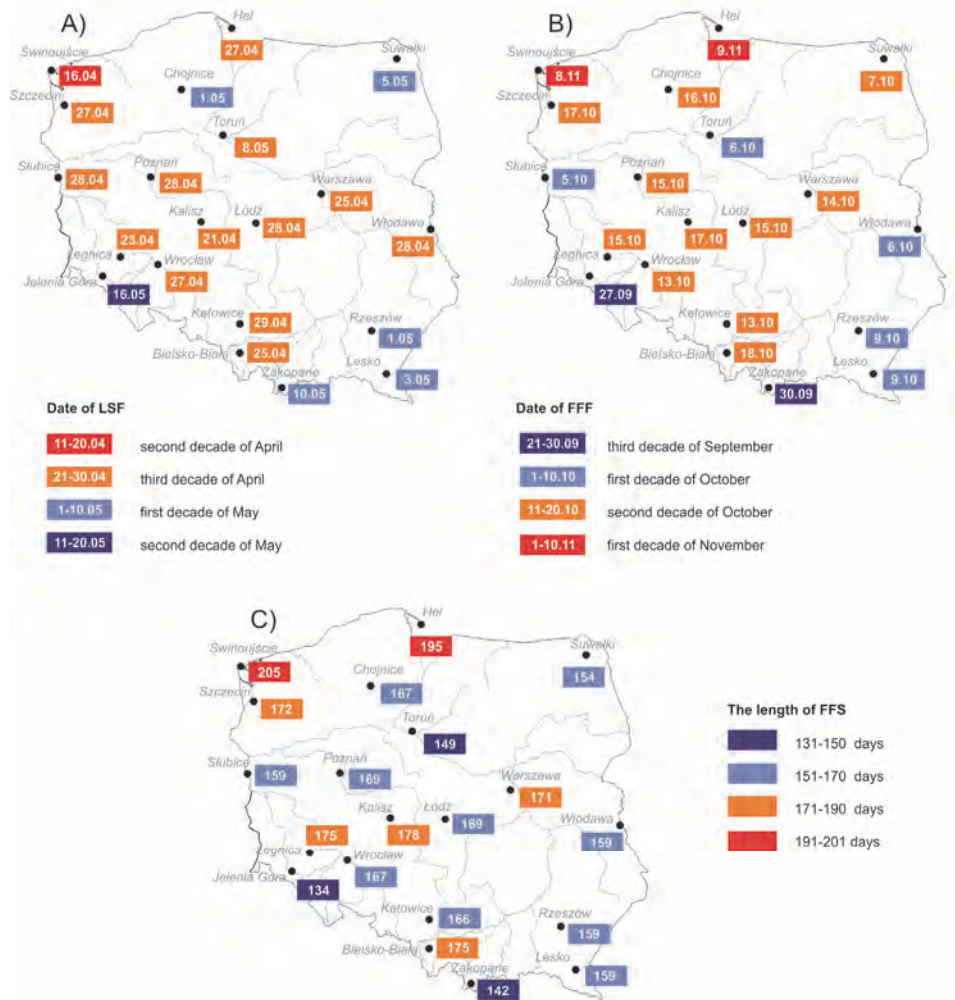


Fig. 2. Date of the last spring frost (A), first fall frost (B), and length of frost-free season (C) in Poland in the period of 1951–2015.

As a rule, the earliest FFFs occurred at stations located in eastern and southern Poland, including those lying in mountain valleys (Zakopane and Jelenia Góra – September 27–30), but also in Słubice, Toruń, Włodawa, Suwałki, Rzeszów, and Lesko (in the first decade of October) (Fig. 2). On the

other hand, the latest FFFs occurred at those sites, where the earliest beginning dates of the FFS were recorded, i.e., coastal stations (Hel and Świnoujście – November 8–9). In extreme cases, the FFF occurred on the first days of September (Słubice, Zakopane –September 3–4) or as late as the second half of December (Hel, Świnoujście –December 19–28) (*Table 3*).

Based on the extreme beginning and end dates of the FFS at the individual stations (*Table 3*), it was found that in Poland, in the period concerned, a potential FFS could last as many as 291 days (LSF recorded on March 12, 2014 in Świnoujście – FFF recorded on December 28, 2006 in Świnoujście). This means that in the last 9 years, the length of the season increased by 6 days (Bielec-Bąkowska and Piotrowicz, 2011). At the same time, the season without a single frosty day remained unchanged, spanning the period between June 13 and September 2, i.e., 82 days (LSF recorded on June 12, 1955 in Jelenia Góra – FFF recorded on September 3, 2003 in Słubice).

In the period under analysis, the FFS lasted 166 days on average (*Table 3*). The spatial differences in the length of the season clearly indicate a significant impact of local conditions. While at most stations the length of the season ranged between 160 and 180 days, it was shorter by 20–25 days at the stations located in intermontane valleys (134 days in Jelenia Góra, 142 days in Zakopane). By contrast, the moderating effect of the Baltic Sea lengthened the FFS to 195 days in Hel, and even to 205 days in Świnoujście (*Fig. 2*). Naturally, in the individual years, the length of the FFS was determined by the weather conditions prevailing over a given area, even though it is difficult to identify a single year which would be particularly conducive to the occurrence of short- or long-lasting frosts. The examples could be the particularly short FFS recorded in Jelenia Góra in 1991, which lasted only 93 days, and the exceptionally long season in Świnoujście in 2006, which lasted more than 9 months (276 days).

4. Frost-free season change trends

Fifteen of the stations included in the study (75%) recorded increasingly early beginning dates of the FFS (statistically significant trend, $p < 0.05$), and another two stations observed indications of similar changes (*Fig. 3*). The greatest change was observed at the Hel station, where the LSF occurred earlier by an average of 3.9 days per 10 years. At the other sites, mainly those located in the southern and central-west parts of Poland, the change ranged between –1.4 days/decade in Warsaw and –3.1 days/decade in Kalisz. It was only the Suwałki station that recorded a slight shift towards later occurrence of LSF of 0.1 days/decade.

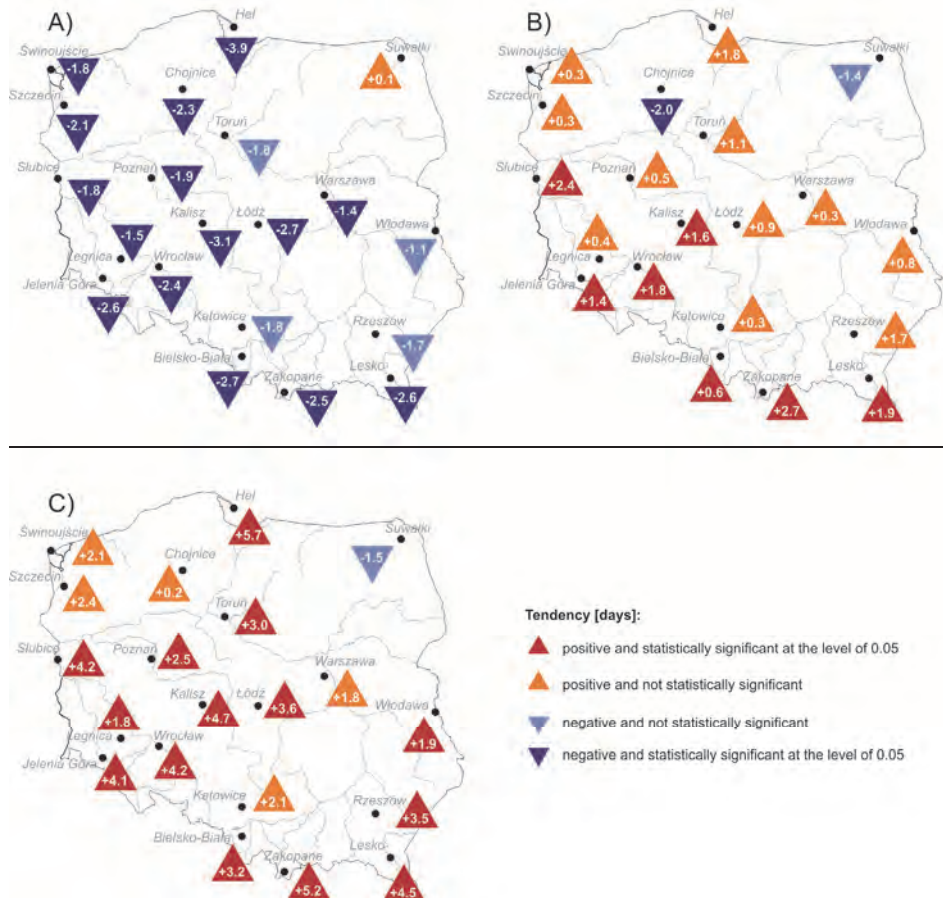


Fig. 3. Trends of shift in the beginning (A), end (B), and length (C) of the frost-free season (FFS) at selected stations in Poland in the period of 1951–2015.

The multiannual changes in the end dates of the frost-free season (FFF) are not so noticeable as in the case of the beginning dates (LSF). At only 7 stations (35%), most of which are located in the southern and south-western parts of Poland, the differences had proven to be positive and statistically significant at the level of 0.05 (Fig. 3). This means that the FFF occurred there at increasingly late dates. The values of these trends ranged between 1.4 in Jelenia Góra and 2.7 days/decade in Zakopane. 12 stations (60%) also show indications of later occurrence of the end of the FFS, even though the tendencies are not statistically significant. At the other two stations located in the northern part of the country

(Chojnice and Suwałki), FFF occurred slightly earlier towards the end of the period under study than in the mid-20th century (-2.0 and -1.5 days/decade, respectively), even though the changes had proven to be statistically significant only in Chojnice (Fig. 3).

As a result of the above shifts in the beginning and end dates of the FFS, the length of the season has changed. Except for Suwałki, it was clearly longer at all stations, with statistically significant changes at the level of 0.05 recorded at 14 of them (75%) (Fig. 3). The changes ranged between 1.8 days/decade in Legnica and 5.7 days/decade in Hel.

The described changes in the occurrence of spring and autumn frosts and in the length of the frost-free season (FFFs) are related to changes in the air temperature during the twentieth century. In a large part of Europe, increase in temperature was observed (Brázdil *et al.*, 1996; Wibig and Glowicki, 2002; Yan *et al.*, 2002; Alexander *et al.*, 2006; Moberg *et al.*, 2006). The pace of these changes was the fastest within the last quarter of the century (Klein Tank and Können, 2003).

Results of the research on seasonal air temperature changes in various regions of Europe have shown that the values of the change tendency were different (Brázdil *et al.*, 1996; Wibig and Glowicki, 2002; Yan *et al.*, 2002; Alexander *et al.*, 2006; Moberg *et al.*, 2006). Studies of seasonal variability of air temperature in Central and Eastern Europe indicate that the temperature increased the most in wintertime – up to $3.5\text{ }^{\circ}\text{C}/10$ years (Brázdil *et al.*, 1996). Summer temperature trends showed a small increase, while spring and autumn temperature trends did not indicate a similar direction of change; however, temperature predominantly tended to increase rather than decrease.

Average trends, for 75 stations mostly representing the western part of Europe, showed a warming also for the maximum and minimum temperatures (Moberg *et al.*, 2006). According to Alexander *et al.* (2006), in Europe the changes in the minimum temperature extremes are higher than the changes of the maximum temperature extremes. Winter has, on average, warmed more ($1.0\text{ }^{\circ}\text{C}/100$ years) than summer ($0.8\text{ }^{\circ}\text{C}/100$ years), both for daily maximum and minimum temperatures (Moberg *et al.*, 2006). The value of the trends was also generally greater for the minimum temperature (Alexander *et al.*, 2006).

5. Synoptic conditions of the beginning and end of the frost-free season

The occurrence of frosts marking the beginning and end of the frost-free season is usually associated with specific synoptic situations, which include anticyclonic types of circulation and advection of very cold air masses (Ustrnul *et al.*, 2014; Tomczyk *et al.*, 2015). Thus, the multiannual change in the FFS in Poland and worldwide, as described in the literature and mentioned above, should be associated with changes in the atmospheric circulation over a given area.

This part of the study checks what types of atmospheric circulation and air masses co-occurred most often with LSFs and FFFs in the multiannual period under study. As it was already stated above, the analysis comprises only 5 sites located in south-eastern Poland. Because nearly all the cases of frosts in question occurred as follows: spring frosts in April (46.9%) and May (50.0%), fall frosts in September (26.6%) and October (67.8%) (*Table 4*), the analysis is narrowed down to these periods of the year.

Table 4. Monthly distribution of the number of days with the last (LSF) and first (FFF) frost day at selected stations in Poland in the period of 1951–2015

Months	LSF				FFF				Sum	
	Bielsko-Biała	Katowice	Rzeszów	Lesko	Zakopane	Bielsko-Biała	Katowice	Rzeszów	Lesko	
Jan	0	0	0	0	0	0	0	0	0	0
Feb	0	0	0	0	0	0	0	0	0	0
Mar	1	0	0	0	0	0	0	0	0	1
Apr	41	35	30	28	16	0	0	0	0	150
May	22	29	33	31	45	0	0	0	0	160
June	1	1	1	2	4	0	0	0	0	9
July	0	0	0	0	0	0	0	0	0	0
Aug	0	0	0	0	0	0	0	0	0	0
Sep	0	0	0	0	0	4	11	19	17	85
Oct	0	0	0	0	0	51	50	42	43	217
Nov	0	0	0	0	0	9	4	3	1	17
Dec	0	0	0	0	0	1	0	0	0	1

During the analyzed period, the occurrence of the last spring frost and particularly the first fall frost, was usually associated with the presence of the anticyclonic type of circulation over a given region. In spring, the frequency of such circulation ranged from 68.9% in Lesko to 80.0% in Katowice, while in fall – from 86.2% in Bielsko-Biała to 90.8% in Zakopane. However, it must be stressed that it would be hard to identify a single frequency distribution pattern for the types of circulation in question across the stations. Also, when comparing the occurrence of frost in fall and spring, it can be observed that the frequency of

the synoptic situations differ noticeably. This is attributable to the local nature of frosts which modifies the general tendencies in the distribution of air temperatures in an area.

Last spring frosts occurred most frequently during the presence of a ridge of high pressure over south-eastern Poland (from 17.2% in Rzeszów to 30.8% of the cases in Katowice and Bielsko-Biała) (*Fig. 4*). The other most distinguishable anticyclonic types included SEa, Sa, SWa (especially in Lesko and Rzeszów), Ca, while in Bielsko-Biała also Na, NEa and Ea. In fall, the predominant types of circulation involving first frosts were anticyclonic wedges and central anticyclonic situations (Ka and Ca; *Fig. 4*). The respective frequencies of their occurrence ranged from 13.8% in Bielsko-Biala to 25.0% in Katowice and from 12.3% in Lesko to 21.9% in Rzeszów. Against this background, Bielsko-Biała stands out in terms of the occurrence of fall frost, where they appeared with similar frequency during the types Na, Ea and SEa (12.3–13.8%). The combination of the three elements of circulation strongly determines the type of weather on a given day, in particular the radiation and thermal conditions.

In the years of 1951–2015, both LSFs and FFFs were chiefly recorded during the advection of arctic (PA), polar maritime cold (PPms), and polar continental (PPk) air masses (*Fig. 5*). In spring, a slightly higher frequency was observed for frosts occurring in PPms masses (31.3% of all cases), and the lowest was observed in PPk masses (25.9%). By contrast, in fall, the highest numbers of frost days were registered during the presence of PA masses (34.4%), and the lowest – when PPms was present over a given area (23.4%). However, the frequency of frost in the air masses analyzed here varied considerably from site to site. This is best illustrated by the frequency of occurrence of LSF in PA masses, which ranged between 21.3% in Lesko and 40.0% in Bielsko-Biała, or of occurrence of FFF in PPk masses, which ranged from 18.5% in Zakopane to 42.2% in Rzeszów (*Fig. 5*).

The correlations described above mean that an increase or decline in the number of days with a specific type of circulation or air mass should be reflected by a corresponding growth or decline in the number of frost days. However, given the small number of the days with frost under study, the correlations are not always noticeable or strong (*Table 5* and *6*). This is exemplified by the increase in the number of LSFs during SEa and Ka circulation patterns, and in the number of FFFs occurring during a ridge of high pressure (Ka). The number of frost days during such types of circulation from the beginning of the analyzed period increased as follows: for LSF by 1.0 and 0.9, and FFF by 1.3. A clear correlation, indeed the strongest one, is noticeable for air masses in fall: there is a correlation between the decline in the frequency of occurrence of polar maritime fresh air masses (PPm) and the decline in the number of days with FFF, as well as, between the growth in the number of days with polar continental air (PPk) and the growth in the number of days with FFF (*Table 6*).

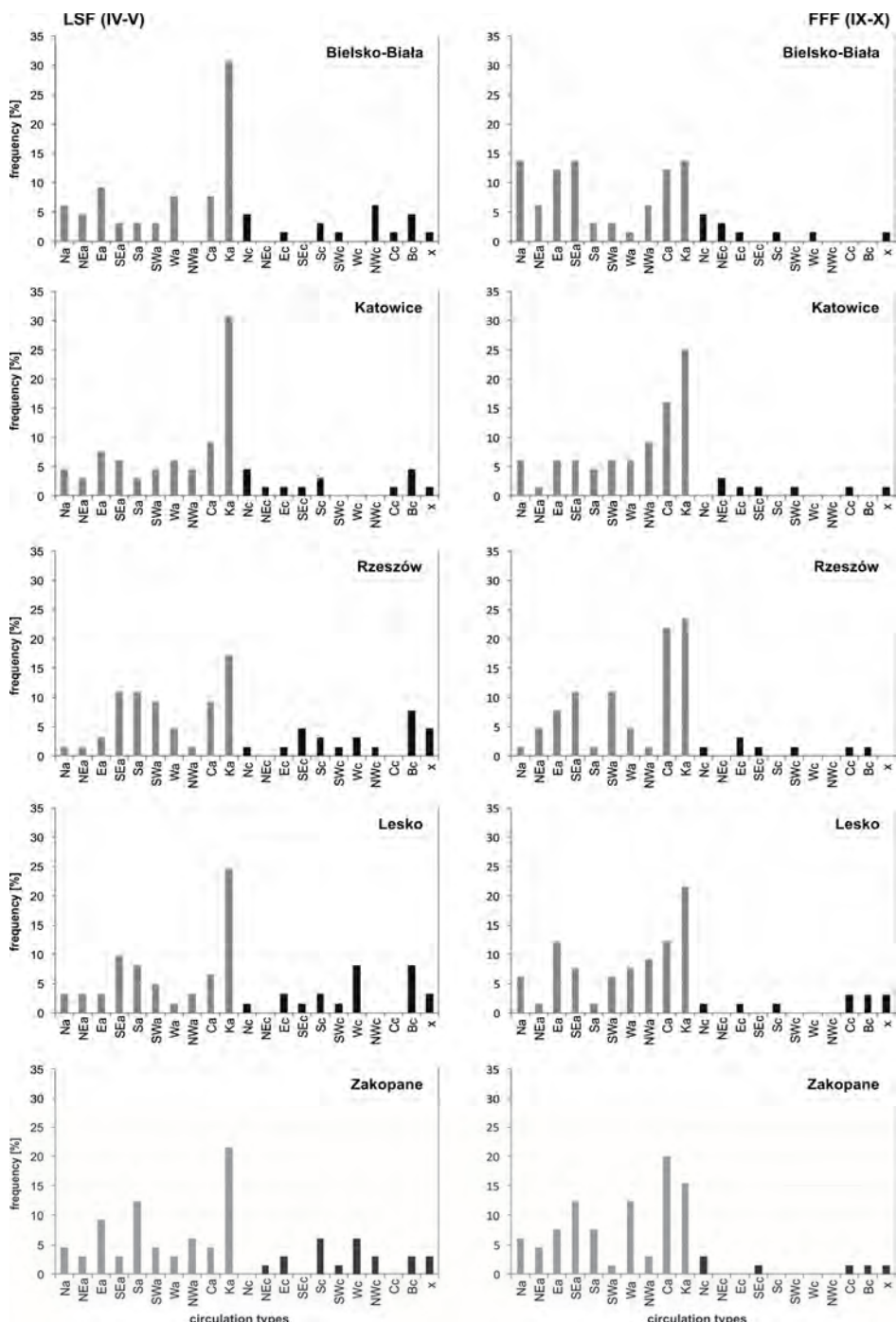


Fig. 4. Frequency of the last spring frost (LSF) and first fall frost (FFF) occurrence in the particular circulation types at selected stations in Poland in the period of 1951–2015.

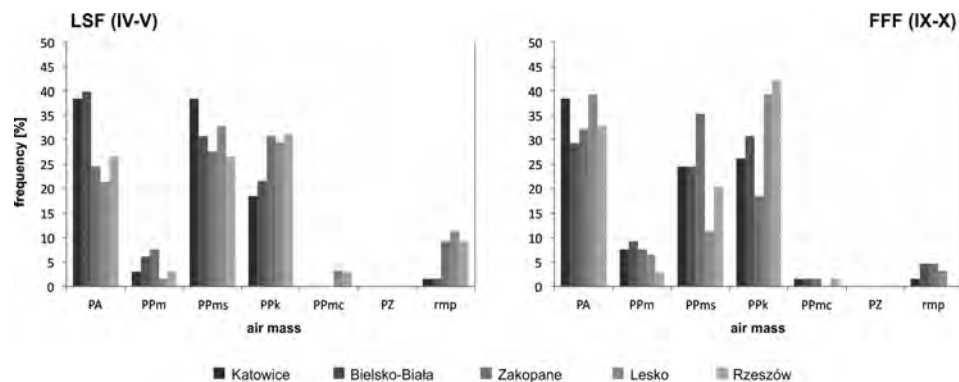


Fig. 5. Frequency of the last spring frost (LSF) and first fall frost (FFF) occurrence in the particular types of air masses at selected stations in Poland in the period of 1951–2015.

Table 5. Tendency of the number of days with circulation types and number of days with the last (LSF) and first (FFF) frost day during particular types of circulation at 5 stations in Poland in the period of 1951–2015

Period	Circulation type (see Table 1)	Tendency [days/10 years]	
		Number of days with particular circulation type	Number of days with frost during particular circulation types
Apr.–May	Na	-0.11	-0.02
	NEa	0.24	0.03
	Ea	-0.21	-0.08
	SEa	0.46	0.16
	Sa	-0.70	0.02
	SWa	0.56	0.00
	Wa	-0.01	-0.01
	NWa	0.03	-0.13
	Ca	-0.49	-0.05
	Ka	0.85	0.13
Sept.–Oct.	Na	-0.05	-0.09
	NEa	0.08	0.02
	Ea	-0.35	-0.06
	SEa	0.24	0.02
	Sa	-0.45	0.04
	SWa	0.26	0.07
	Wa	-0.03	-0.08
	NWa	0.17	0.01
	Ca	-0.30	0.06
	Ka	0.79	0.21

Table 6. Tendency of the number of days with types of air masses and number of days with the last (LSF) and first (FFF) frost day during particular types of air masses at 5 stations in Poland in the period of 1951–2015

Period	Air masses (see Table 2)	Tendency [days/10 years]	
		Number of days with particular type of air masses	Number of days with frost during particular air mass types
Apr– May	PPm	−0.02	0.01
	PPms	−0.61	−0.01
	PPk	−0.06	0.16
	PPmc	0.68	−0.03
	PZ	−0.57	—
	rmp	0.89	0.02
Sep– Oct	PA	0.15	−0.08
	PPm	−0.93	−0.10
	PPms	−0.74	−0.10
	PPk	0.60	0.36
	PPmc	0.63	−0.02
	PZ	−0.36	—
	rmp	0.64	−0.01

6. Discussion and conclusions

The results of the research indicate that, in the period in question, there was a clear trend towards earlier occurrence of LSF dates over most of the territory of Poland. For FFF dates, the changes were not pronounced and were statistically insignificant over a large proportion of the area. Nevertheless, shifts in the beginning and end dates of the FFS increased the length of the season at 95% of the stations included in the study, with 70% of them recording statistically significant changes.

The greatest changes in the beginning dates and length of the frost-free season took place in the southern and west-central parts of Poland and in Hel. Similar correlations may be found in studies by *Ustrnul et al.* (2014), *Tomczyk et al.* (2015), and *Wypych et al.* (2017). However, in some regions of Europe, especially in the southern, south-eastern, and north-eastern parts of the continent, the changes may be opposite in nature (*Chmielewski and Rötzer*, 2000; *Tomczyk et al.*, 2014). It should be stressed here, that the average length of the FFS remained similar to that identified for the years of 1951–2006 (*Bielec-*

Bakowska and Piotrowicz 2011), and it changed by no more than 1–2 days at the different stations.

To find the causes underlying the trends, the authors investigated the long-term variability of the occurrence of air masses and types of circulation and their correlation with changes in the occurrence of LSFs and FFFs. As it was found by other authors (*Ustrnul et al.*, 2014; *Tomczyk et al.*, 2015), the results of the present analysis indicate that the frosts in question are most often associated with anticyclonic situations, especially in fall. LSFs were recorded exceptionally frequently during the presence of an anticyclonic wedge (Ka), whereas FFFs occurred most often in September and October during the Ka and Ca types. The frosts in question appeared most often during the advection of the following air masses: arctic, polar continental, and polar maritime transformed. Even though the frequency differed from station to station and from season to season, on average it ranged between 23–34% of all the cases across the stations (attaining the highest values in spring in Bielsko–Biała – 40% in a PA mass, and in autumn in Rzeszów – 42% in a PPk air mass).

The positive and mostly statistically significant correlations between the types of circulation or the above types of air masses and the occurrence of LSFs and FFFs would indicate, that it is possible to use forecasts of changes in the types of synoptic situations to predict the overall trends in the occurrence of the frosts under study. However, the low number of frost cases in the individual types of synoptic situations and a comparison of their long-term variability with changes in the types of circulation and air masses do not clearly indicate such relationship. It is also worth stressing that, even though the entire period saw an overall increase in the frequency of the types of circulation accompanied by a large percentage of frosts (Ka, SEa, SWa and NEa), Poland has seen a clear drop in pressure values and also a drop in the number of strong anticyclones (*Bielec–Bąkowska, 2016*) since the 1990s, which may partly explain the longer FFSs. Most probably, however, the main cause of the changes is the increase in air temperatures, which is particularly noticeable in spring (*Kożuchowski and Żmudzka, 2000*). Hence, it seems that a more accurate explanation of the changes discussed in the paper requires the investigation of the temporal frequency, thermal characteristics, and air masses of the individual types of circulation.

The regularities obtained will certainly change the phenology of plants, which will consequently cause changes in agricultural production (*Wypych et al., 2017*). The growing length of the frost-free season, which is influenced most strongly by its increasingly earlier beginning date (LSF), may contribute to an increase in the crop production and a fall in the occurrence of late, May frosts, which very frequently causes damages to fruit plants and trees in bloom. Nevertheless, the risk of such a frost remains high, particularly in eastern Poland.

References

- Alexander, L.V., Zhang, X., Peterson, T.C., Caesar, J., Gleason, B., Klein Tank, A.M.G., Haylock, M., Collins, D., Trewin, B., Rahimzadeh, F., Tagipour, A., Rupa Kumar, K., Revadekar, J., Griffiths, G., Vincent, L., Stephenson, D.B., Burn, J., Aguilar, E., Brunet, M., Taylor, M., New, M., Zhai, P., Rusticucci, M., and Vazquez-Aguirre, J.L., 2006: Global observed changes in daily climate extremes of temperature and precipitation. *J. Geophys. Res.* 111, D05109. <https://doi.org/10.1029/2005JD006290>
- Alexandersson, H. 1986: A homogeneity test applied to precipitation data. *J. Climate* 6, 661–675. <https://doi.org/10.1002/joc.3370060607>
- Bielec-Bąkowska, Z. 2016: Long-term variability of the frequency and persistence of strong highs over Poland. *Environ Socio-econ Stud* 4(1), 12–23, DOI: 10.1515/environ-2016-0002. <https://doi.org/10.1515/environ-2016-0002>
- Bielec-Bąkowska, Z. and Piotrowicz K. 2011: Wieloletnia zmienność okresu bezprzymrozowego w Polsce w latach 1951–2006. *Prace i Studia Geograficzne* 47, 77–86. (In Polish)
- Brázdil, R., Budíková, M., Auer, I., Böhm, R., Cegnar, T., Faško, P., Lapin, M., Gajic-Čapka, M., Zaninović, K., Koleva, E., Niedzwiedź, T., Ustrnul, Z., Szalai, S., and Weber, R.O. (1996) Trends of maximum and minimum daily temperatures in Central and Southeastern Europe. *Int J Climatol* 16, 765–782. [https://doi.org/10.1002/\(SICI\)1097-0088\(199607\)16:7<765::AID-JOC46>3.0.CO;2-O](https://doi.org/10.1002/(SICI)1097-0088(199607)16:7<765::AID-JOC46>3.0.CO;2-O)
- Chmielewski, F.M. and Rötzer, T. 2000: Phenological trends in Europe in relation to climatic changes. *Agrarmeteorologische Schriften* 7, 1–15.
- Czarnecka, M., Koźmiński, C., and Michalska, B. 2009: Climatic risk for plant cultivation in Poland. *Acta Agrophysica* 169, 78–96.
- Graczyk, D. and Kundzewicz, Z.W. 2016: Changes of temperature-related agroclimatic indices in Poland. *Theor Appl Climatol* 124, 401–410. <https://doi.org/10.1007/s00704-015-1429-7>
- Juszczak, R., Leśny, J., Serba, T., and Olejnik, J. 2009: Cumulative degree-days as an indicator of agroclimatic condition changes in the Wielkopolska Region. Implications for codling moth development. *Acta Agrophysica* 169, 122–136.
- Kendall, M.G. 1975: Rank correlation methods. 4th edn Charles Griffin, London.
- Klein Tank, A.M.G. and Könen, G.P. 2003: Trends in indices of daily temperature and precipitation extremes in Europe, 1946–1999. *J. Climate* 16, 3665–3680. [https://doi.org/10.1175/1520-0442\(2003\)016<3665:TIIODT>2.0.CO;2](https://doi.org/10.1175/1520-0442(2003)016<3665:TIIODT>2.0.CO;2)
- Kożuchowski, K. and Źmudzka, E. 2000: Vegetation and climate in Poland in the 1990's: Variation of the normalized difference vegetation index, air temperature, sunshine and precipitation. *Prace Geograficzne* 107, 235–242.
- Kunkel, K.E., Easterling, D.R., Hubbard, K., and Redmond, K. 2004: Temporal variations in frost-free season in the United States. *Geophys. Res. Lett.* 31, 1895–2000. <https://doi.org/10.1029/2003GL018624>
- Mann, H.B. 1945: Non-parametric tests against trend. *Econometrica* 13, 245–259. <https://doi.org/10.2307/1907187>
- Menzel, A. 2000: Trends in phenological phases in Europe between 1951 and 1996. *Int J Biometeorol.* 44, 76–81. <https://doi.org/10.1007/s004840000054>
- Moberg, A., Jones, P.D., Lister, D., Walther, A., Brunet, M., Jacobbeit, J., Alexander, L.V., Della-Marta, P.M., Luterbacher, J., Yiou, P., Chen, D., Klein Tank, A.M.G., Saladiée, O., Sigró, J., Aguilar, E., Alexandersson, H., Almarza, C., Auer, I., Barriendos, M., Begert, M., Bergström, H., Böhm, R., Butler, C.J., Caesar, J., Drebs, A., Founda, D., Gerstengarbe, F.-W., Micela, G., Maugeri, M., Österle, H., Pandzic, K., Petrakis, M., Srnec, L., Tolasz, R., Tuomenvirta, H., Werner, P.C., Linderholm, H., Philipp, A., Wanner, H., and Xoplaki, E. 2006: Indices for daily temperature and precipitation extremes in Europe analyzed for the period 1901–2000. *J. Geophys Res* 111, D22106. <https://doi.org/10.1029/2006JD007103>

- Modala, N.R., Ale, S., Goldberg, D.W., Olivares, M., Munster, C.L., Rajan, N., Feagin, R.A.* 2017: Climate change projections for the Texas High Plains and Rolling Plains. *Theor. Appl. Climatol.* 129, 263–280. <https://doi.org/10.1007/s00704-016-1773-2>
- Niedźwiedź, T.*, 2016a: Calendar of Circulation Types for territory of Southern Poland, Uniwersytet Śląski, Katedra Klimatologii, Sosnowiec. <http://klimat.wnoz.us.edu.pl/#!/glowna> (accessed 01.09.2016).
- Niedźwiedź, T.*, 2016b: Calendar of Circulation Types for Poland. Uniwersytet Śląski, Katedra Klimatologii, Sosnowiec.
- Scheifinger, H., Menzel, A., Koch, E., Peter, Ch., and Ahas, R.* 2002: Atmospheric mechanisms governing the spatial and temporal variability of phenological phases in Central Europe. *Int. J. Climatol.* 22, 1739–1755. <https://doi.org/10.1002/joc.817>
- Tomczyk, A.R., Szyga-Pluta, K., and Majkowska, A.* 2015: Frost periods and frost-free periods in Poland and neighbouring countries. *Open Geosci* 7, 812–823. <https://doi.org/10.1515/geo-2015-0061>
- Ustrnul, Z., Wypych, A., Winkler, J.A., and Czekierda, D.* 2014: Late spring freezes in Poland in relation to atmospheric circulation. *Quaestiones Geographicae* 33, 165–172. <https://doi.org/10.2478/quageo-2014-0039>
- Wibig, J. and Głowicki, B.* 2002: Trends of minimum and maximum temperature in Poland. *Clim. Res.* 20, 123–133. <https://doi.org/10.3354/cr020123>
- Wypych, A., Sulikowska, A., Ustrnul, Z., and Czekierda, D.* 2017: Variability of growing degree days in Poland in response to ongoing climate changes in Europe. *Int. J. Biometeorol.* , 61 49–59. <https://doi.org/10.1007/s00484-016-1190-3>
- Yan, Z., Jones, P.D., Davies, T.D., Moberg, A., Bergström, H., Camuffo, D., Cocheo, C., Maugeri, M., Demarée, G.R., Verhoeve, T., Thoen, E., Barriendos, M., Rodríguez, R., Martín-Vide, J. and, Yang, C.* 2002: Trends of extreme temperatures in Europe and China based on daily observations. *Clim. Change* 53, 355–392. <https://doi.org/10.1023/A:1014939413284>
- Yu, L., Zhong, S., Bian, X., Heilman, W.E., and Andresen, J.A.* 2014: Temporal and spatial variability of frost-free seasons in the Great Lakes region of the United States. *Int. J. Climatol.* 34, 3499–3514. <https://doi.org/10.1002/joc.3923>
- Zhang, D., Xu, W., Li, J., Cai, Z., and An, D.* 2014: Frost-free season lengthening and its potential cause in the Tibetan Plateau from 1960 to 2010. *Theor. Appl. Climatol.* 115, 441–450. <https://doi.org/10.1007/s00704-013-0898-9>
- Żmudzka, E.* 2003: The circulation-related conditioning for the variability of the spring date of air temperature passage through the +5°C threshold in Poland. *Acta Universitatis Wratislaviensis, Studia Geograficzne* 75, 250–261.

IDÓJÁRÁS

*Quarterly Journal of the Hungarian Meteorological Service
Vol. 122, No. 4, October – December, 2018, pp. 393–408*

Wind speed and direction on the Polish Baltic coast and conditions for recreation

Czesław Koźmiński¹ and Bożena Michalska^{2*}

¹*Department of Tourism and Recreation, University of Szczecin,
Mickiewicza 16, 70-383 Szczecin, Poland,*

²*Department of Meteorology and Green Areas Management,
West Pomeranian University of Technology in Szczecin.
Papieża Pawła VI 3, 71-459 Szczecin, Poland,*

Corresponding author E-mail: bozena.michalska@zut.edu.pl

(Manuscript received in final form November 15, 2017)

Abstract— Using the results of daily measurements of wind from 6 meteorological stations (Świnoujście, Kołobrzeg, Koszalin, Ustka, Łeba, Hel) operated by the Institute of Meteorology and Water Management of Poland (IMGW) for the period 2000–2016, the study presents the assessment of temporal and spatial variation of wind speed and direction on the Polish Baltic coast with respect to conditions for recreation and tourism. For the purpose of assessing bioclimatic conditions, additional measurements were taken at 12 UTC in the period 2006–2015, which provided grounds for determination of thermal sensation using Hill's index and heat load experienced by a person staying at the seaside. The analysis of wind speed and direction on the Polish Baltic coast shows high spatial variability and variation, which determines the stimuli character of this region. Considering thermal sensation expressed with Hill's index, the most favorable conditions for recreation on the Polish Baltic coast occur in the Bay of Pomerania and the Bay of Gdańsk, favorable conditions are recorded in the area of Rewal to Dąbki, and less favorable in the area of Darłowo to Władysławowo.

Key-words: wind, the Baltic sea coast, speed, direction, load, thermal sensations

1. Introduction and aims

Wind speed is a significant element of bioclimatic conditions of a given area, particularly the Baltic coastal zone – in addition to sunshine duration, air, and water temperature. Wind can further aggravate thermal discomfort in the case of low air temperature, as well as increase thermal comfort in the conditions of high air temperature and humidity. Therefore, wind speed recorded in a given area determines the conditions of aerotherapy as being mild, stimulating, or loaded (*Kozłowska-Szczęsna et al.*, 2002; *Koźmiński and Michalska*, 2011; *Chojnacka-Ożga*, 2013). The classification by *Knoch* (*Jankowiak and Parczewski*, 1978) is used in bioclimatology to describe the wind speed of $0.0\text{--}1.0 \text{ ms}^{-1}$ as calm, $1.1\text{--}4.0 \text{ ms}^{-1}$ as light, $4.1\text{--}8.0 \text{ ms}^{-1}$ as moderate, and $>8.0 \text{ ms}^{-1}$ as strong wind causing negative effects on the human organism. The wind of moderate speed ($4.1\text{--}8.0 \text{ ms}^{-1}$) has a positive effect on the human organism in summer, as it results in a micromassage of exposed body area leading to the improvement of thermoregulatory mechanisms (*Bogucki*, 1999; *Kozłowska-Szczęsna et al.*, 1997).

In comparison to the southern regions of Poland (apart from the mountain area), mean wind speed on the Baltic coastal zone is by $1.0\text{--}2.5 \text{ ms}^{-1}$ higher, particularly in winter and spring (*Koźmiński and Michalska*, 2002). The Baltic coast area is characterized by particularly strong stimuli due to heavy wind, significant air cooling power, relatively low subjective temperature, and large weather variations (*Kozłowska-Szczęsna et al.*, 2002; *Szyga-Pluta*, 2011). According to *Woś* (1999), the coastline is marked by the highest frequency of days with cool and cloudy weather, as well as cool weather without precipitation. High wind speed contributes to formation of waves on the surface of the sea, and intensifies wave breaking in the coastal zone, which results in an increased release of aerosols and oxygen to the atmosphere. Particularly during storm, the aerosols are enriched with iodine, selenium, calcium, magnesium, bromine, and other microelements significant to human health (*Garbalewski*, 1999; *Marks*, 2016).

High wind speed ($>3 \text{ ms}^{-1}$) is favored for water sports, e.g., sailing, windsurfing, or kitesurfing, which are becoming increasingly popular among tourist spending their vacation on the seaside or lakes. The appeal of this particular form of recreation often results in an increased health risk, as the wave of more than 1 m in height may lead to water aspiration, exhaustion, or cramps while swimming (*Zalewski*, 2016). The wind speed considered to be favorable for windsurfing ranges from approximately 3 to 6 ms^{-1} , and as much as from 6 to 8 ms^{-1} for the more experienced surfers. Participating in water sports activities depends not only on wind speed, but also on its direction, e.g., wind along, towards or from the coastline. Particular wind direction has an effect on

water temperature at the beach and the phenomenon of upwelling, which is especially present in the region of Kołobrzeg, Łeba, and Władysławowo.

At the border of two environments, such as water and land, weather conditions show high variability, including speed and direction of wind, formation of sea breeze transporting oxygen and aerosols from the sea towards the beach (Marks, 2016). Considering the energy of wind, this element is included in various indices and bioclimatic models, such as the heat balance of the human body.

The aim of the present paper is the analysis of temporal and spatial (Matzarakis, 2006; Blażejczyk and Kunert, 2011) distribution of wind speed and direction on the Polish Baltic sea coast with respect to conditions of recreation.

2. Materials and methods

The study makes use of daily measurements of wind speed and direction recorded in the period 2000–2006, obtained from six of the Institute of Meteorology and Water Management of Poland (IMGW) meteorological stations located in Świnoujście (dune), Kołobrzeg (residential area), Ustka, Łeba, and Hel (in the vicinity of a beach), and Koszalin (airport). The characteristics of wind speed is presented using mean and extreme values and coefficient of variation. Additionally, wind speed is analyzed per seasons of a year according to the 12-grade Beaufort scale. For the purpose of analyzing tourism and water sports the following wind speed classification was adopted: 3–5, 6–8, and $>8\text{ ms}^{-1}$. 16 wind directions were taken into account in the study, and monthly frequencies of individual directions were illustrated in figures per selected stations. The assessment of the effect of wind on the human organism and conditions for recreation was made using the Hill's index taking into account wind speed and air temperature values measured at 12 UTC in the period 2006–2015. Thermal sensation was determined using the scale by Petrović and Kacvinsky (Table 1) and the heat load according to the scale by Conrad (Table 2), (Blażejczyk and Kunert, 2011).

For the purpose of establishing the dates of the beginning, termination and duration of periods with given heat load conditions (Conrad scale), mean values of the Hill's index were determined for subsequent days in a year (12 UTC), and the trend lines were identified in the form of polynomial of degree 5.

Table 1. Petrovič and Kacvinsky scale

H [Wm ⁻²]	Thermal sensation
≤ 210.0	very hot
210.1–420.0	hot
420.1–630.0	mild
630.1–840.0	slightly cool
840.1–1260.0	cool
1260.1–1680.0	cold
1680.1–2100.0	very cold
2100.1<	extremely cold and windy

Table 2. Conrad scale

H [Wm ⁻²]	Heat load
≤ 420.0	risk of hyperthermia
420.1–840.0	mild conditions (comfort)
840.1–1260.0	slightly loaded conditions
1260.1–1680.0	strongly loaded conditions
1680.1<	risk of hypothermia

3. Results and discussion

On the Polish Baltic coast, in a year, the most prevalent direction of wind is from the south-west, west, and north-east, yet there is a clear variation as to wind direction between the stations and seasons (*Fig. 1*). In the area of Świnoujście, from August till March, the wind from the south-west prevails, while from April to July there is a marked increase in the frequency of the wind from the north-east direction. The least frequent is the wind from the north, in particular from October till February. The stations in Łeba show slightly different distribution of wind direction frequencies, as from March till September, the most frequent is the wind from the west, and in April and May –

also from the north-east. In the autumn and winter months, the wind from the south-west is recorded most frequently, and the wind from the north and east is recorded least frequently.

Spatial variability of wind speed on the Polish Baltic coast is greater between the analyzed stations than the temporal variability between the individual months (*Table 3*). In the cold half-year (October-March), the seaside is characterized by wind which is often accompanied by air temperature considered low for a given period. This combination causes a significant inconvenience for tourists involved in leisure activities such as hiking, cycling, and others (*Koźmiński and Michalska, 2004*). In the conditions of low air temperature and high humidity, an increase in wind speed results in aggravation of the feeling of chill. This discourages tourist from walking along the beach despite the fact that the increase in wind speed and formation of waves at the shoreline fosters release of aerosols and oxygen (*Garbalewski, 1999; Marks, 2016*). Along the Polish Baltic coast, the winds from the south-west and west are predominant. Mean annual speed in Świnoujście amounts to 3.2 ms^{-1} and increases in Ustka to 5.3 ms^{-1} (*Table 3*). The biggest difference in monthly wind speed between Świnoujście and Ustka are marked from October to February – more than 2.0 ms^{-1} , and in December and January even more than 2.6 ms^{-1} . In the cold half-year, wind speed can be as high as several meters per second in the western and central part of the coast, and approximately 20 meters per second in the eastern part. The lowest spatial variability in monthly wind speed between the eastern and western part of the coastline was found in May – 1.5 ms^{-1} . The amplitudes between the lowest and the highest mean monthly wind speed in a year range from 0.7 ms^{-1} in Świnoujście to 1.3 ms^{-1} in Hel. Significant variability in wind speed from one year to another was found for the station in Świnoujście, whereas the station in Hel shows the lowest variability. Considering the values of coefficient of variation presented in *Table 3*, a tourist coming to the seaside should expect high fluctuation in wind speed from one day to another.

Świnoujście

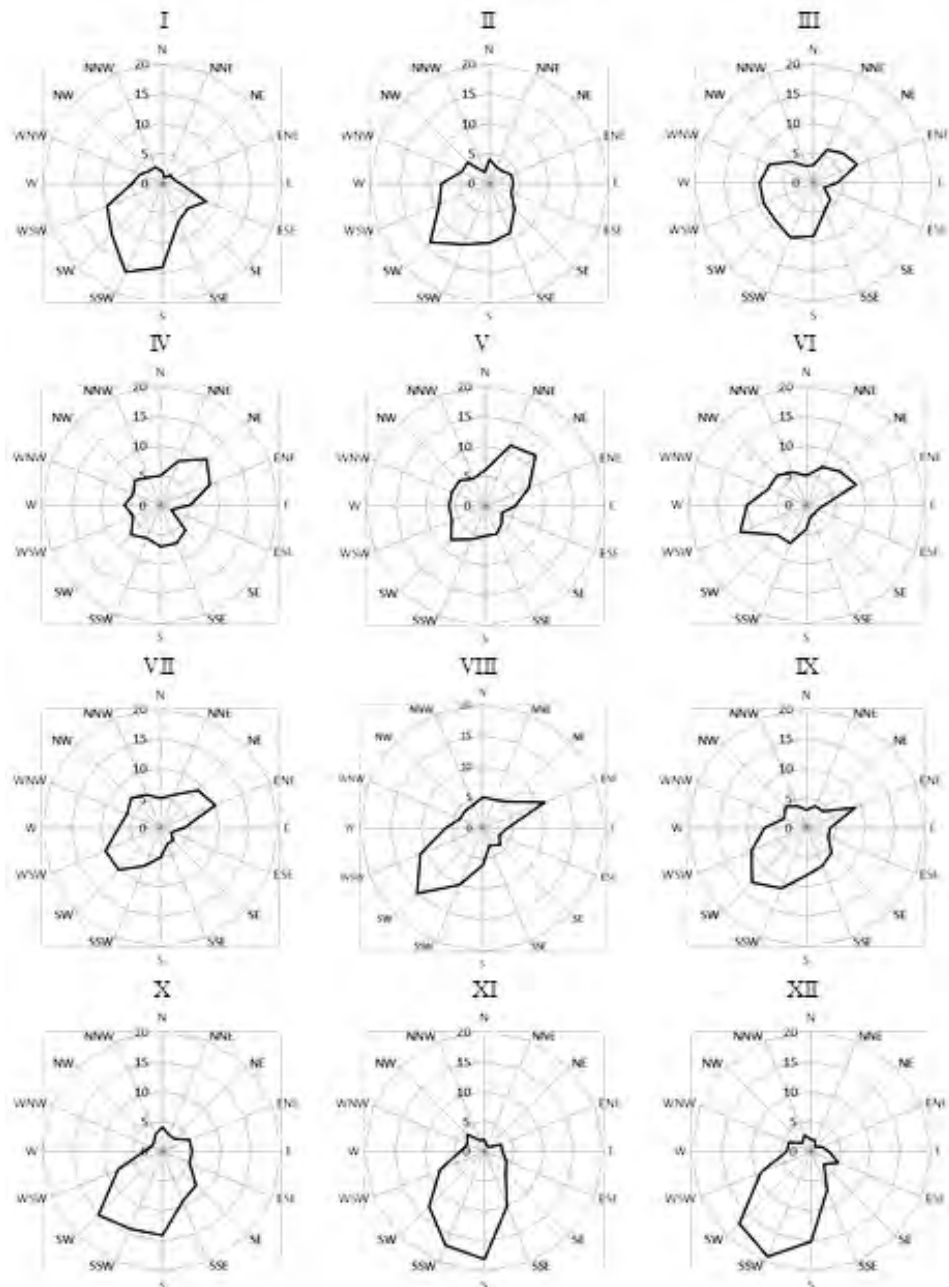


Fig. 1. Frequency (%) of days with particular wind direction according to months in Świnoujście and Łeba in the period of 2000–2016.

Łeba

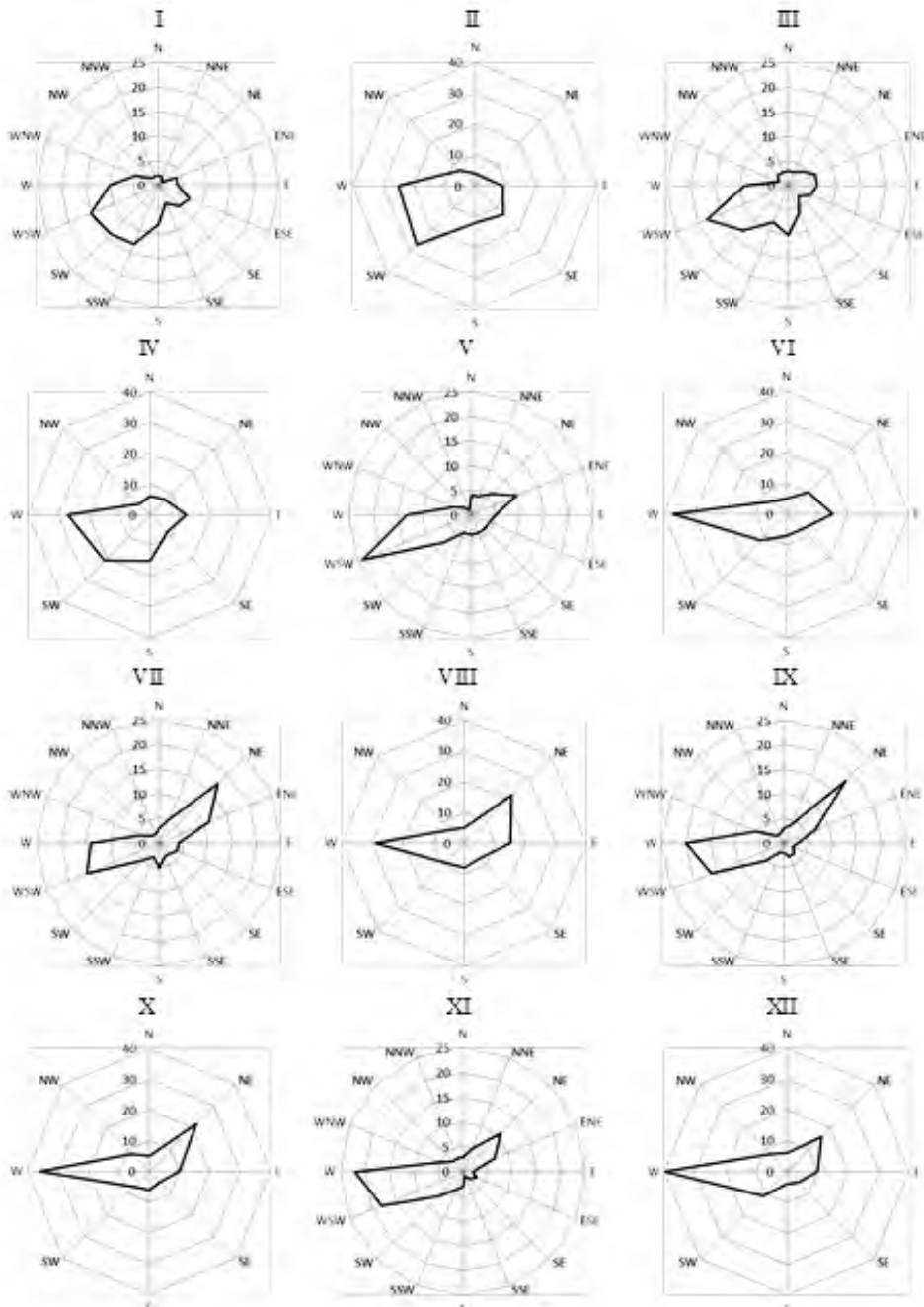


Fig. 1. (Continued from the previous page.)

Table 3. Mean daily (a), maximum (b), and minimum (c) values and coefficient of variability (d) according to months in the period of 2000–2016

Station		Jan	Feb	Mar	Apr	May	June	July	Aug	Sept	Oct	Nov	Dec	Jan-Dec
Świnoujście	a	3.3	3.3	3.6	3.5	3.2	3.2	3.1	2.9	3.1	3.0	3.0	3.2	3.2
	b	13.6	11.0	13.4	12.3	14.4	10.6	11.5	10.2	12.5	13.9	12.1	13.2	12.4
	c	0.6	0.5	0.8	1.0	0.4	1.0	1.1	0.8	0.6	0.5	0.4	0.6	0.7
	d	47.7	55.7	54.8	55.3	52.2	47.9	47.2	45.4	57.6	59.2	53.1	49.1	52.1
Kołobrzeg	a	3.8	3.7	3.6	3.4	3.0	3.0	2.9	2.8	2.8	2.8	3.4	3.7	3.2
	b	12.9	10.6	11.3	12.5	8.5	10.9	12.3	10.7	13.6	9.9	12.3	11.6	11.4
	c	0.5	0.6	0.8	0.9	0.6	1.0	0.8	0.5	0.6	0.6	0.3	0.3	0.6
	d	51.3	48.2	45.2	44.4	42.0	49.0	50.0	54.2	58.1	51.5	52.7	46.2	49.4
Koszalin	a	3.8	3.6	3.5	3.3	3.0	3.1	2.9	2.8	2.8	2.9	3.5	3.6	3.2
	b	10.0	10.3	9.7	9.8	8.0	9.2	8.3	8.8	9.1	9.5	10.7	11.5	9.6
	c	0.4	0.3	1.0	0.8	0.8	0.8	0.9	0.9	0.4	0.0	0.5	0.0	0.6
	d	48.5	45.4	44.8	40.6	37.7	39.1	36.0	37.8	41.7	46.5	44.0	43.3	42.1
Ustka	a	5.9	5.6	5.6	5.1	4.7	5.0	4.7	4.7	5.0	5.2	5.5	5.8	5.3
	b	16.7	14.8	13.8	17.3	15.4	13.3	13.0	13.9	18.3	21.0	17.4	20.8	16.3
	c	1.2	0.4	0.9	0.8	1.0	1.7	1.5	1.4	1.4	1.7	1.5	0.8	1.2
	d	47.1	46.6	44.0	43.9	42.0	41.0	38.1	40.3	44.9	48.5	48.5	44.4	44.1
Łeba	a	5.4	5.1	5.0	4.4	4.3	4.7	4.3	4.2	4.2	4.4	4.8	5.2	4.7
	b	16.7	16.5	16.7	13.3	12.1	14.0	12.8	14.3	12.1	13.9	13.9	14.4	14.2
	c	0.8	0.1	0.6	1.1	1.2	1.5	0.5	0.4	0.9	0.6	0.4	0.4	0.7
	d	56.3	57.1	51.1	47.2	46.0	47.1	45.5	47.5	47.7	51.4	51.4	51.0	49.9
Hel	a	4.6	4.2	3.9	3.4	3.3	3.5	3.3	3.4	3.7	4.0	4.4	4.5	3.9
	b	8.8	7.7	7.6	6.1	5.9	6.3	5.7	6.6	6.8	7.0	7.8	10.5	7.2
	c	2.1	1.7	1.8	1.8	1.9	1.9	1.8	1.8	1.9	1.7	1.9	1.1	1.8
	d	36.0	35.9	35.0	29.9	27.6	30.8	29.0	32.1	32.8	35.0	32.8	35.0	32.7

Those, who practice water sports such as windsurfing or kitesurfing, often adopt wind speed assessment according to the Beaufort scale. In the western and central part of the Polish Baltic sea, wind speed from 1.6 to 3.3 ms^{-1} (2°B) is the most frequent, and in the eastern section of the coast (stations in Ustka and Łeba) – the wind speed is from 3.4 to 5.4 ms^{-1} (3°B). The station in Hel shows occurrence of both scale 2 and 3 winds (*Fig. 2*). It must be emphasized, that in the area of Ustka and Łeba, strong wind of more than 8 ms^{-1} shows higher mean frequency – approximately 10% of the total number of days per season. In summer, wind below 3.4 ms^{-1} is prevalent on the entire coast. In winter, higher frequency of days with wind speed over 3.3 ms^{-1} is recorded in the western and central section, of the coast, and wind speed over 5.4 ms^{-1} in the east. According to data presented in *Fig. 2*, the area of Ustka, Łeba and Władysławowo is characterized by the most favorable conditions for water sports on the Polish Baltic coast, whereas the area of Świnoujście shows less favorable conditions.

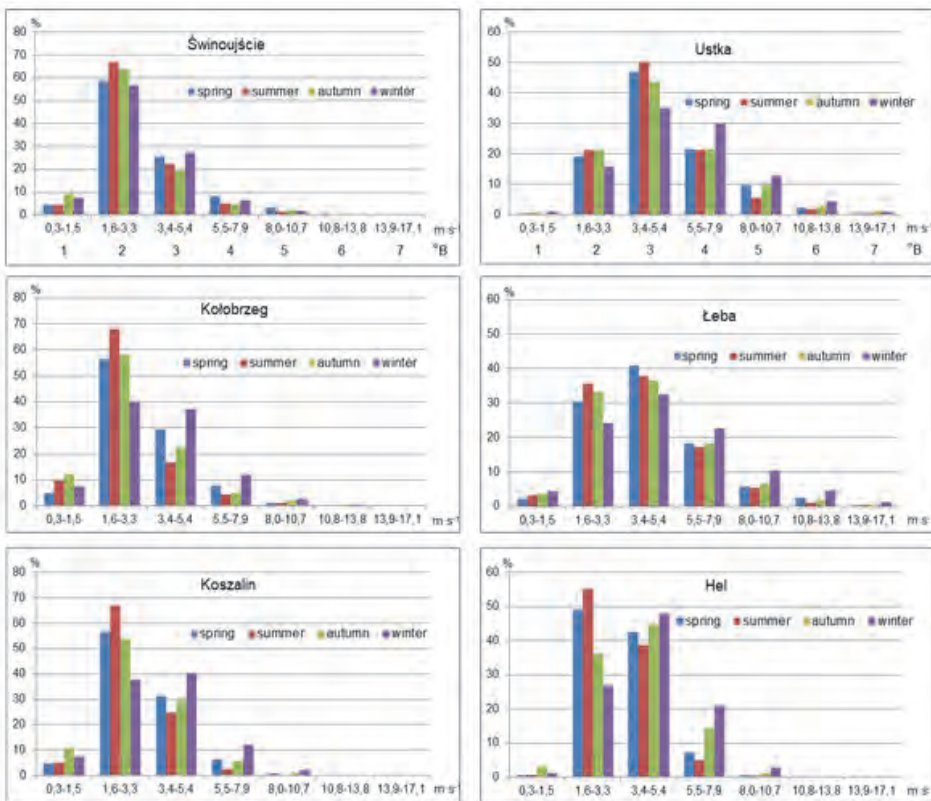


Fig. 2. Frequency (%) of daily wind of various speed values according to the Beaufort scale in four seasons of a year in the period of 2000–2016.

Data from 12 UTC, i.e., the time of high tourist activity, is used in bioclimatology for the assessment of meteorological conditions for recreation. The wind speed recorded on the coastal zone at 12 UTC is generally 3–5 ms⁻¹. Such wind is considered mild and shows the highest frequency in the warm half-year, on average 20 to 24 days per month in Hel, 16 to 20 days in Świnoujście, and significantly less, 11 to 14 days in Ustka (*Table 4*). A high average number of days with mid wind speed can also result from a frequent occurrence of sea breeze of average speed of 5 ms⁻¹ (*Radomski, 1987*). The moderate wind speed of 6–8 ms⁻¹ is most frequently recorded in Ustka and Łeba – 8–12 days, less frequently in Hel – 2–8 days, and very rarely in Świnoujście and Kołobrzeg – 1–6 days in a month. The wind speed of more than 8 ms⁻¹ is recorded mainly in the stations located in Ustka and Łeba, on average 4–7 days in a month. Such wind speed values, particularly when combined with low air temperature, may

discourage from leisure activities (walks along the beach) in the northern part of the coastline. According to Araźny *et al.*, (2007), wind speed values $>8 \text{ ms}^{-1}$ recorded in Central Europe show a statistically significant increase in the number of days by 0.7 days for 10 years, which results in increasing frequency of extreme weather phenomena. In the western and central part of the Baltic coast, wind speed $>8 \text{ ms}^{-1}$ taken at 12 UTC is recorded sporadically, on average 1 to 2 days in a month, yet, as the study by Tarnowska (2011) shows, between 12 and 3 p.m. on particular days, there is a risk of increased occurrence of strong wind. Data presented in *Table 4* show increased stimuli of the bioclimate in the northern sector of the Baltic coast from Darłowo to Władysławowo, where in the summer season, the temperature of seawater is below 14°C . One of the safety criteria of mini swimming marathons is the water temperature which must be above 14°C , preferably over 18°C , and the wind speed must be below 5 on the Beaufort scale.

Table 4. Mean number of days with wind speed 3–5, 6–8, and $> 8 \text{ ms}^{-1}$ at 12 UTC according to months in the period of 2006–2015

Station	ms ⁻¹	Jan	Feb	Mar	Apr	May	June	July	Aug	Sep	Oct	Nov	Dec
Świnoujście	3–5	18	14	16	16	21	19	21	19	18	17	16	18
	6–8	2	3	5	6	4	5	4	4	3	1	2	2
	> 8	2	1	2	2	1	1	1	1	1	1	1	1
Kołobrzeg	3–5	17	16	19	19	19	17	17	17	16	16	16	17
	6–8	4	5	4	3	3	3	3	2	2	2	2	5
	> 8	2	1	1	2	1	1	1	2	1	1	1	1
Koszalin	3–5	18	16	19	20	23	22	21	22	21	18	17	19
	6–8	6	6	7	7	5	5	6	4	5	5	5	6
	> 8	1	1	2	1	1	1	1	0	0	0	1	1
Ustka	3–5	13	12	11	11	12	12	14	13	12	13	13	11
	6–8	10	10	11	10	12	10	9	11	11	10	9	12
	> 8	6	4	7	7	5	5	6	5	5	4	5	5
Łeba	3–5	14	12	13	14	14	15	13	13	13	14	13	12
	6–8	9	8	10	10	11	9	10	11	11	9	8	8
	> 8	5	4	6	5	4	5	5	4	4	4	5	6
Hel	3–5	19	18	19	21	24	23	23	23	20	20	17	18
	6–8	7	4	5	3	2	3	3	3	4	5	6	8
	> 8	1	1	1	0	0	0	0	1	0	0	1	1

The data (*Table 5*), obtained using Hill's index and thermal sensation scale by Petrović and Kacvinsky show that sensations of a person staying on the coast in a year may range from *very hot* in July and August to *extremely cold and windy* in the period from November to April. However, most frequent thermal sensations is *cool* in late spring and early autumn, followed by *cold* in the cold half year. Thermal sensation termed *slightly cool* and *mild* occur most frequently in the warm

half-year, particularly from June to August. The frequency of days with thermal sensation *slightly cold* is highest in June – 42.0% in Hel, 36.7% in Kołobrzeg, and 36% in Świnoujście. Thermal sensation *mild* is prevalent in July, and in Świnoujście and Hel also in August, whereas in Ustka and Łeba the predominant thermal sensation in July is *cool*. Considering the values of air cooling power expressed with the Hill's index, favorable bioclimatic conditions for recreation occur in the western part of the coast and the Bay of Gdańsk. The conditions are less favorable in the area of Ustka to Władysławowo. In summer, August is marked by days with thermal comfort (classes *slightly cold* and *mild*) in Świnoujście, Kołobrzeg, and Hel from 65% to 78%, and only 46.2% in Ustka (*Table 5*).

Table 5. Frequency (%) of days with thermal sensations experienced by a person staying on the seaside, determined with the use of the value of air cooling power index H (data from 12 UTC)

Month	Station	Very hot	Hot	Mild	Slightly cool	Cool	Cold	Very cold	Extremely cold and windy
January	Świnoujście	0	0	1.6	1.3	31.6	43.9	15.2	6.5
	Kołobrzeg	0	0	1.3	1.3	22.9	46.8	22.6	5.2
	Koszalin	0	0	1	0	14.5	46.1	31.3	7.1
	Ustka	0	0	0.3	0	5.8	31.8	36.4	25.6
	Łeba	0	0	0.3	0.3	11	28.7	34.2	25.5
	Hel	0	0	0	0.3	11.3	44.8	33.6	10
February	Świnoujście	0	0	0.3	3.2	37.9	36.2	12.8	9.6
	Kołobrzeg	0	0	0.7	1.4	28.1	43.5	19.9	6.4
	Koszalin	0	0	0.3	1	20.9	44.1	31.6	2.1
	Ustka	0	0	0	0	12	33	33	22
	Łeba	0	0	0.7	0.3	11.3	36.2	29.8	21.6
	Hel	0	0	1.1	0.4	17.7	45	31.2	4.6
March	Świnoujście	0	0	0	6.5	43.2	27.7	15.2	7.4
	Kołobrzeg	0	0	1	2.6	36.1	44.5	9.4	6.4
	Koszalin	0	0	0.6	1.6	31	44.5	19.4	2.9
	Ustka	0	0	0	1.6	13.6	35.8	26.4	22.6
	Łeba	0	0	0.3	1	16.5	38.3	28.1	15.8
	Hel	0	0	0.3	2.3	34.2	44.8	16.8	1.6
April	Świnoujście	0	0.3	6.3	15.7	40.7	24.7	11	1.3
	Kołobrzeg	0	0	2	11.3	49.3	28.8	6.3	2.3
	Koszalin	0	0	3.3	14.3	41	31.4	10	0
	Ustka	0	0	0	6.3	23	37	24.7	9
	Łeba	0	0	0.3	4.3	30.7	41.3	17.7	5.7
	Hel	0	0	1.7	12.3	54.7	28.3	3	0
May	Świnoujście	0	2.9	9.7	24.8	46.4	12.9	2.3	1
	Kołobrzeg	0	3.5	8.7	25.6	49	11.6	1.3	0.3
	Koszalin	0	2.3	9	22.9	48.7	16.1	1	0
	Ustka	0	1.6	3.2	9.4	39.8	34	9.7	2.3
	Łeba	0	0.3	4.2	11	48.5	27.9	7.1	1
	Hel	0	0.6	9	26.8	56.8	6.5	0.3	0

Table 5. (Continued from the previous page)

Month	Station	Very hot	Hot	Mild	Slightly cool	Cool	Cold	Very cold	Extremely cold and windy
June	Świnoujście	0	6	19.7	36	31	7	0.3	0
	Kołobrzeg	0	4.3	17.7	36.7	33.7	7	0.6	0
	Koszalin	0	4.7	17.7	28.3	44	5	0.3	0
	Ustka	0	0.7	7	18.6	49.7	21.3	2.7	0
	Łeba	0	1.3	7.7	21.1	49.2	19.1	1.7	0
	Hel	0	1	22.3	42	32.7	2	0	0
July	Świnoujście	2.7	12.9	34.4	32.7	17.1	0.6	0	0
	Kołobrzeg	1	11.7	35.9	31.7	16.8	2.9	0	0
	Koszalin	1.9	11.7	29.5	27.8	27.2	1.9	0	0
	Ustka	1	3.9	20.1	24.6	42.7	7.7	0	0
	Łeba	1.6	6.2	17.3	27.4	39.4	7.8	0.3	0
	Hel	0.7	9.4	39.4	32.9	16.3	1.3	0	0
August	Świnoujście	1.3	9	38.1	35.5	15.5	0.6	0	0
	Kołobrzeg	1.3	11.6	31.3	33.9	18.7	3.2	0	0
	Koszalin	1	11	31.7	29.7	25.8	1	0	0
	Ustka	0.3	5.2	18.1	28.1	42.2	6.1	0	0
	Łeba	0.3	5.5	19.2	30.2	38.0	6.5	0.3	0
	Hel	0	5.2	42.3	36.1	15.8	0.6	0	0
September	Świnoujście	0	2.3	26.0	28.7	35.4	7.3	0.3	0
	Kołobrzeg	0	3.0	25.1	34.4	31.8	5.0	0.7	0
	Koszalin	0	1.0	19.3	29.0	45.0	5.7	0	0
	Ustka	0	0.7	10.0	19.1	44.2	24.4	1.3	0.3
	Łeba	0	0	8.7	21.3	50.0	19.3	0.7	0
	Hel	0	0.3	14.0	39.0	43.0	3.7	0	0
October	Świnoujście	0	0	8.7	25.8	52.9	9.0	2.3	1.3
	Kołobrzeg	0	0	7.1	27.4	53.6	10	1.9	0
	Koszalin	0	0.3	3.5	15.6	60.6	19.4	0.6	0
	Ustka	0	0	3.2	6.1	48.5	31.9	9.0	1.3
	Łeba	0	0	1.6	8.4	45.9	36.9	6.5	0.7
	Hel	0	0	1.9	15.8	57.1	22.6	2.6	0
November	Świnoujście	0	0	1.0	15.0	52.3	24.3	4.7	2.7
	Kołobrzeg	0	0	0.6	9.0	52.4	29.3	7.0	1.7
	Koszalin	0	0	0.6	3.3	36.9	45.8	12.4	1.0
	Ustka	0	0	0	2.0	27.4	41.9	22.7	6.0
	Łeba	0	0	1.0	2.7	29.4	37.8	24.4	4.7
	Hel	0	0	0.7	3.3	36.8	45.8	12.4	1.0
December	Świnoujście	0	0	0.3	3.5	44.9	40.0	7.1	4.2
	Kołobrzeg	0	0	1.3	2.6	28.7	48.7	16.8	1.9
	Koszalin	0	0	1.0	1.6	21.0	54.2	18.7	3.5
	Ustka	0	0	0	0.3	11.3	32.9	42.6	12.9
	Łeba	0	0	1.0	1.3	12.9	34.9	34.7	15.2
	Hel	0	0	0.3	1.0	18.7	51.3	22.3	6.4

By way of example, the course of mean values of the Hill's index according to days (12 UTC) in a year is presented in Fig. 3 for two stations

(Świnoujście and Łeba). The largest variation from one day to another is recorded in the period from November to May, particularly in February and March, and the smallest in the summer season, from June to August. Even though the results for the period of 10 years are given as average, in many instances the variations in the values at both stations occur on the same days. According to the Conrad scale, the heat load in the cold half-year may shift within a few days from *strongly loaded* to *slightly loaded* conditions, and vice versa. In summer, the fluctuations from one day to another are markedly smaller and within the category of *mild* conditions.

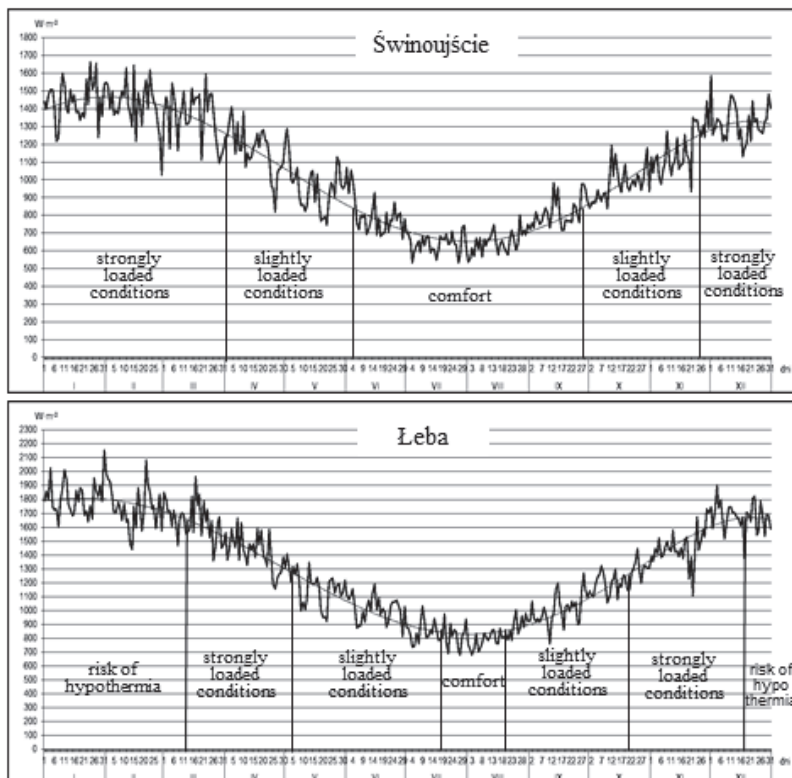


Fig. 3. The course of daily Hill's index values in a year in Świnoujście and Łeba with indicated dates of occurrence of particular heat load according to the Conrad scale in the period 2006–2015.

For the purpose of assessment of bioclimatic conditions, the dates of beginning and termination of particular heat loads in the coastal zone were

determined from the trend lines for the six analyzed stations (*Table 6*). In a year, in the western part of the coast and the Bay of Gdańsk, the period with *strongly loaded* conditions shows the longest duration, from 129 days in Świnoujście to 142 days in Hel, whereas in the northern part of the coast, the number of days amounts to 102 in Ustka and 110 in Łeba. However, the stations in Ustka and Łeba are marked by additional occurrence of heat load category *risk of hypothermia*, from 85 days in Łeba to 105 days in Ustka. Relatively low spatial variation in a year is recorded in a period with *slightly loaded* conditions, from 109 days in Hel to 138 days in Łeba. The most favorable bioclimatic conditions for the human organism are the conditions with heat load termed as *mild (comfort)*. Duration of a period with such conditions is the longest, i.e., more than 110 days in the western and central part of the coast and in the area of Hel, whereas in Ustka and Łeba, the duration is four times shorter, 28 and 32 days, respectively (*Table 6*).

Table 6. Mean date of beginning (a), termination (b), and the duration (in days) (c) of periods with heat load according to the Conrad scale in the period of 2006–2015

Station	Heat load ($\text{W} \cdot \text{m}^{-2}$)				
	Risk of hyperthermia	Comfort	Slightly loaded conditions	Strongly loaded conditions	Risk of hypothermia
	≤ 420.0	$420.1\text{--}840.0$	$840.1\text{--}1260.0$	$1260.1\text{--}1680.0$	>1680.0
Świnoujście	a-b	June 4–Sept 27	Mar 31–June 3	Nov 22–Mar 30	
	c	116	65	129	
	e	a-b	Sep 28–Nov 21		
	c		55		
Kołobrzeg	a-b	June 5–Sep 26	Apr 2–June 4	Nov 21–Apr 11	
	c	114	64	132	
	a-b		Sep 27–Nov 20		
	c		55		
Koszalin	a-b	June 9–Sep 16	Apr 8–June 8	Nov 10–Apr 7	
	c	100	62	149	
	a-b		Sep 17–Nov 9		
	c		54		
Ustka	a-b	July 23–Aug 19	May 5–July 22	Mar 21–May 14	Dec 6–Mar 20
	c	28	69	55	105
	a-b		Aug 20–Oct 19	Oct 20–Dec 5	
	c		61	47	
Łeba	a-b	July 18–Aug 18	May 5–July 17	Mar 13–May 4	Dec 18–Mar 12
	c	32	74	53	85
	a-b		Aug 19–Oct 10	Oct 22–Dec 17	
	c		64	57	
Hel	a-b	May 26–Sep 16	Mar 30–May 25	Nov 8–Mar 29	
	c	114	57	142	
	a-b		Sep 17–Nov 7		
	c		52		

4. Conclusion

In summer, in the western part of the coast, the prevalent direction of wind is from the south-west and north-east, while in the central and eastern part it is from the west and north-east. In the winter months, the coastal zone is characterised by wind from the south-west.

Mean annual wind speed shows an increase from the west to the east, from 3.2 ms^{-1} in Świnoujście to 5.3 ms^{-1} in Ustka, reaching its highest values in the cold half-year, when in the eastern part of the coast, wind speeds in a day exceeds 20 ms^{-1} .

In the western and central parts of the Polish Baltic coast, the most frequently recorded daily wind speed is from 1.6 to 3.3 ms^{-1} (2°B), and in the eastern part represented by the stations in Ustka and Łeba the prevalent daily wind speed is from 3.4 to 5.4 ms^{-1} (3°B). The area of Hel is marked by the occurrence of wind of both Beaufort scales (2 and 3).

Wind speed recorded on the coast at 12 UTC is mostly from 3 to 5 ms^{-1} , and in the area of Ustka and Łeba, it is 6 – 8 ms^{-1} . Such wind speed values create conditions which facilitate taking part in water sports activities in the warm half year, though the frequent occurrence of cool days in summer may create unfavorable conditions for outdoor activities.

In summer, the most frequently recorded heat load on the coast is the *mild (comfort)* category and *slightly loaded* conditions, although on individual days, there may occur *strongly loaded* conditions. In winter, the dominant atmospheric conditions range from *strongly loaded* to *risk of hypothermia*.

Among several heat load categories recorded on the coast, *mild* conditions show the greatest spatial variation in terms of duration, from 28 in the area of Ustka to 116 in Świnoujście. In the analyzed period, the weather condition *risk of hyperthermia* were recorded only sporadically.

Taking into consideration the thermal sensation expressed with the Hill's index, the most favorable conditions for recreation on the Polish Baltic coast occur in the Bay of Pomerania and the Bay of Gdańsk, favorable conditions are recorded in the area of Rewal to Dąbki, and less favorable in the area of Darłowo to Władysławowo.

References

- Araźny, A.; Przybylak, R.; Vizi, Z.; Kejna, M.; Maszewski, R.; and Uscka-Kowalkowska, J., 2007: Mean and Extreme Wind Velocities in Central Europe 1951–2005 on The Basis of Data from NCEP/NCAR Reanalysis. Extreme hydrometeorological events in Poland and their impact European context. Faculty of Earth Sciences University of Silesia. *Geographia Polonica* 80, 69–78.
- Blażejczyk, K. and Kunert , A., 2011: Bioklimatyczne uwarunkowania rekreacji i turystyki w Polsce. Institute of Geography and Spatial Organization, Polish Academy of Sciences, Warszawa, *Monographs*, 13, 291. (in Polish)

- Bogucki, J. (ed.),* 1999: Biometeorologia turystyki i rekreacji. Academy of Physical Education, Poznań, 347. (in Polish)
- Chojnacka-Ożga , L. and Ożga, W.,* 2013: Ocena warunków wypoczynku człowieka nad zbiornikiem wodnym w świetle wybranych wskaźników bioklimatycznych – na przykładzie Zbiornika Sulejowskiego.. *Studia i materiały CEPL in Rogowo.* 15, 37/4, 239–244. (in Polish)
- Garbalewski, C.,* 1999: Fizyka aerosolowej aktywności morza. Polish Academy of Sciences Institute of Oceanology in Sopot. *Monographs 12,* (in Polish)
- Jankowiak, J. and Parczewski, W., (ed.),* 1978: Bioklimat uzdrowisk polskich. Wyd. Komunikacji Łączności. Warszawa, 429 (in Polish)
- Kozłowska-Szczęsna, T., Błażejczyk, K., Krawczyk, B.,* 1997: Bioklimatologia człowieka. Institute of Geography and Spatial Organization, Polish Academy of Sciences, Warsaw, Monographs 1,200. (in Polish)
- Kozłowska-Szczęsna, T., Błażejczyk, K., Krawczyk, B., Limanówka, D.,* 2002: Bioklimat uzdrowisk polskich i możliwości jego wykorzystania w lecznictwie. Institute of Geography and Spatial Organization, Polish Academy of Sciences, Warsaw, Monographs 3, 611, (in Polish)
- Koźmiński, C. and Michalska, B.,* 2002: Charakterystyka prędkości wiatru i cisz w Polsce. *Acta Agrophysica* 78, 133–150. (in Polish)
- Koźmiński, C. and Michalska, B.,(ed.),* 2004: Atlas zasobów I zagrożeń klimatycznych Pomorza., Agricultural University, Szczecin, Poland. (in Polish)
- Koźmiński, C. and Michalska, B.,* 2011: Meteorologiczne uwarunkowania rozwoju turystyki I rekreacji w strefie polskiego wybrzeża Bałtyku. *Acta Balneologica, t.LIII, 1 (123),* 68–74. (in Polish)
- Koźmiński, C. and Michalska, B.,* 2015: Ocena długości sezonu kąpielowego na polskim wybrzeżu Bałtyku. *Europa Regionum, University of Szczecin, XXIV,* 55–66. (in Polish)
- Marks, R.,* 2016: Znaczenie aerosoli morskich w rekreacji I turystyce. In: Health, wellness and bioclimatic tourism, (Ed. Koźmiński, C) University of Szczecin, 198–204. (in Polish)
- Matzarakis, A.,* 2006: Weather and climate-related information for tourism". *Tourism hospital. plan. develop.* 3, 99–115.
- Radomski, C.,* 1987: Agrometeorologia. National Publishing Institute, Warsaw. (in Polish)
- Szyga-Pluta, K.,* 2011: Wielkość ochładzająca powietrza na wybrzeżu na wybrzeżu klifowym w rejonie Białej Góry w sezonie letnim 2008 i 2009 ". *Geografia fizyczna R. II, (A62),* 27–39. (in Polish)
- Tarnowska, K.,* 2011: Wiatry silne na polskim wybrzeżu Morza Bałtyckiego. *Prace i Studia Geograficzne 47,* 197–204, (in Polish)
- Woś, A.,* 1999: Klimat Polski. National Publishing Institute, Warsaw. (in Polish).
- Zalewski, T.,* 2016: Analiza wybranych aspektów bezpieczeństwa w turystyce wodnej. In (Ed.: Stankiewicz, B. and Prochorowicz, M.) Water tourism as a tourist product of the regionWest Pomeranian University of Technology in Szczecin. (in Polish)

IDŐJÁRÁS

Quarterly Journal of the Hungarian Meteorological Service
Vol. 122, No. 4, October – December, 2018, pp. 409–432

Rainfall erosivity and extreme precipitation in the Netherlands

Tin Lukic^{1,2}, Biljana Basarin¹, Tanja Micić¹, Dajana Bjelajac^{1*},
Tiemen Maris^{1,3}, Slobodan B. Marković¹, Dragoslav Pavić¹,
Milivoj B. Gavrilov¹, and Minučer Mesaroš¹

¹*Faculty of Sciences, University of Novi Sad,
Department of Geography, Tourism and Hotel Management,
Trg Dositeja Obradovića 3, 21000 Novi Sad, Serbia;*

²*Faculty of Geography, University of Belgrade,
Studentski trg 3/3, 11000 Belgrade, Serbia*

³*Nijmegen School of Management, Radboud University,
Heyendaalseweg 141 6525 AJ Nijmegen, The Netherlands*

Corresponding author E-mail: dajana.bjelajac92@gmail.com

(Manuscript received in final form October 10, 2017)

Abstract— In order to assess the rainfall erosivity of the Netherlands, several parameters which describe distribution, concentration, and variability of precipitation were used (the annual amount of precipitation, the precipitation concentration index and the modified Fournier index), as well as eleven extreme precipitation indices (maximum1-day precipitation amount, maximum 5-day precipitation amount, simple daily intensity index, number of heavy precipitation days, number of very heavy precipitation days, number of days above 25 mm, consecutive dry days, consecutive wet days, very wet days, extremely wet days, and annual total wet-day precipitation). The precipitation data for calculating the above mentioned parameters is obtained from the Royal Netherlands Meteorological Institute for the period 1957–2016. Based on statistical analysis and the calculated values, the results have been presented with the Geographic Information System (GIS) to point out the most vulnerable parts of the Netherlands with regard to pluvial erosion. This study presents the first results of combined rainfall erosivity and extreme precipitation indices for the investigated area. Trend analysis implies a shift from being largely in the low erosivity class to being completely in the moderate erosivity class in the future, thus indicating an increase in rainfall erosivity. Furthermore, the observed precipitation extremes suggest that both the amount and the intensity of precipitation are increasing. The results of this study suggest that the climate conditions in the Netherlands are changing, and that this change might have a negative influence on the rainfall erosivity of the country.

Key-words: erosion, hazard, rainfall erosivity, precipitation, extreme precipitation indices, precipitation concentration index, modified Fourier index, Netherlands

1. Introduction

Soil erosion is described as one of the biggest hazards and main environmental problems in many areas in Europe (e.g., *Vallejo et al.*, 2005; *de Luis et al.*, 2010, 2011; *Blinkov*, 2015; *Lukić et al.*, 2016). Erosion is the primary physical phenomenon which causes the movement of soil and rock particles via water, wind, ice, and gravity. *Bosco et al.* (2015) pointed out that soil erosion by water is one of the most widespread forms of soil degradation.

The major climatic variable affecting water erosion is precipitation (*Wischmeier and Smith*, 1978; *Mello et al.*, 2013). Nevertheless, soil erosion by water is a complex phenomenon. Certain authors argue that there is no exact relationship between the soil erosion and the total amount of rainfall, as well as relationship with the intensity of rainfall and its distribution in time (*Kirkby and Neale*, 1987; *de Luis et al.*, 2010; 2011). It is also pointed out in the various investigations of the respective authors, that soil erosion by rainfall can be considered as a natural hazard (*Rawat et al.*, 2011; *Berger and Rey*, 2004; *Gares et al.*, 1994; *Mather*, 1982) intrinsically entangled with many other natural hazard types (*Markantonis et al.*, 2012).

The potential of rain to generate soil erosion is known as rainfall erosivity, and its estimation is fundamental for the understanding of climatic vulnerability of a given region (*de Luis et al.*, 2011; *Mello et al.*, 2013). Therefore, erosion and precipitation distribution are important elements concerning the implications of climate variability and change. Also, the occurrence of extreme events and their impacts on society have become a fundamental issue due to the greater climate change effects on them (e.g., very heavy precipitation episodes). Analysis of precipitation events was seldom performed in climatological studies. On the other hand, the precipitation variability is one of the best indicators of climatic change (*Handmer et al.*, 1999). The predictions announced by the IPCC (Intergovernmental Panel on Climate Change) reports (*IPCC*, 2013) indicate that extreme events are very likely to change concerning their intensity, frequency, and location in the 21st century. The report points out human influence as a likely cause of global warming and changes in the hydrological cycle, with a precipitation decrease in subtropical areas and intensification of extremes (*Trenberth*, 2011). These changes in precipitation and derived extreme events have been associated with climate dynamics over different European regions (e.g., *Casanueva et al.*, 2014).

Study of *Boardman and Poesen* (2006) indicate that soil erosion by rainfall and runoff is one of the main soil threats in Europe. Due to the global climate variability, there is a great uncertainty about the future development of soil erosion by water, because the reliability of model outputs for precipitation are less accurate than those for air temperatures (*Christensen et al.*, 2007). Lately, a number of models and approaches in a GIS environment have been developed using the available database for erosion factors at the scale of Europe. This

research was focused on the countries within the European Union, but data about water erosion is often missing (Blinkov, 2015). Regional analysis of potential erosion should take into account the variability of precipitation in space and time, and this should be achieved by using dense spatial information. At present, there are many datasets on a global or continental scale (e.g., Klein-Tank *et al.*, 2002; Wijngaard *et al.*, 2003), but these are not useful at sub-regional level because of the low density of observations. This situation is especially critical in areas with high variability of rainfall in Europe.

During the last century, precipitation in the Netherlands has increased by approximately 25% (Buishand *et al.*, 2013). The increasing sea surface temperatures (Attema *et al.*, 2014) and changes in circulation (Van Haren *et al.*, 2013; Van Oldenborgh and Van Ulden, 2003) are considered to be the main reasons for this increase in precipitation. A larger increase can be seen along the West Coast region, where this is most likely caused by the enhanced coastal effect (Lenderink *et al.*, 2009), but other factors like the topography and ongoing urbanization in these areas might have contributed as well.

The rainfall regime reflects the aggressiveness of erosion on the geological substrate and soil through the volume, duration, and intensity of precipitation. In this study, a parameter based on mean monthly data averages, modified Fournier index (*MFI*), defined by Arnoldus (1980) will be used. This parameter is derived from temporal precipitation distribution, calculated using the precipitation concentration index (*PCI*). Agreement between *MFI* and *USLE R* factor (rainfall aggressivity factor) has been described in several studies (e.g., Renard and Freimund, 1994; Gabriels, 2001; Loureiro and Coutinho, 2001; Diodato and Bellocchi, 2007; de Luis *et al.*, 2010; Mello *et al.*, 2013), and as a consequence, they are commonly used as the input aggressivity factor in the development of regional models (Gregori *et al.*, 2006; Bosco *et al.*, 2015). Subsequently, the precipitation extremes (heavy precipitation events), which have great potential impacts on human society, land cover, and ecosystems in general will be investigated in this study. Thus, it can be highlighted that understanding the potential links between extreme weather events and erosion triggering factors induced by climate conditions is very important in the context of vulnerability and adaptation to climate change.

Rainfall erosivity (*R factor*) and extreme precipitation events have been widely investigated in numerous studies for different parts of the world. Beside studies that were based on *MFI* parameter (e.g., Oduro- Afriyie, 1996; Ferro *et al.*, 1999; Lujan and Gabriels, 2005; Apaydin *et al.*, 2006; Costea, 2012; Yue *et al.*, 2014; Hernando and Romana, 2015), *PCI* was also used as a stand-alone factor in analysis of precipitation distribution and concentration (Martinez-Casasnovas *et al.*, 2002; de Luis *et al.*, 2011; Zhao *et al.*, 2011; Iskander *et al.*, 2014). As far as the extreme precipitation indices are concerned, there are many papers from the respective authors from all around the world (e.g., Easterling *et*

al., 2000; *Alexander et al.*, 2006; *Van Minnen et al.*, 2013; *Donat et al.*, 2013; *Van den Hurk et al.*, 2015).

This study strives to analyze rainfall aggressiveness trends, extreme precipitation indices, and their spatial variability over the Netherlands. Results from this study can be used for development of prevention activities and for the promotion of mitigation measures at all levels. The objectives of this study are to analyze the relationship between trends of precipitation (*Pt*), extreme precipitation indices, *MFI*, and *PCI* in order to describe the evolution of rainfall aggressivity during 1957–2016 (two climatological cycles) in the Netherlands, and to look for spatial distribution patterns. This is of great importance, when assessing the risk impact not only for the present time, but for future scenarios as well. Investigation resulting from this study can aid in creating suitable strategies in order to avoid or reduce the impacts of rainfall aggressivity not only in the investigated area, but in the surrounding countries (or regions) as well.

2. Material and methods

2.1. Study area

The territory of the Netherlands is located in Western Europe, and it covers 41.543 km². It borders in the east with Germany, in the south with Belgium, and in the north and west with the North Sea. The population of Netherlands is approximately 17 million people. That gives the country a population density of 502 person per km² (*CBS*, 2017).

Fig. 1 shows a map of the investigated area, and it displays the locations of the meteorological stations which were used for the collection of precipitation data applied for this study. The stations were selected on the basis of the availability of data and its completeness for the investigated period 1957–2016. Additionally, an equal spatial distribution of the stations from north to south of the country was taken into account.

The geography of the Netherlands is unique in a way that a large part of its land has been reclaimed from the sea and lies below sea level, protected by dikes. The country can be split into two areas: the low and flat lands in the west and north, and the higher lands with minor hills in the east and south. The highest point of the Netherlands, *Vaalserberg*, is 322.7 meters above the sea level. Six geological/geomorphological agents have been active in the Netherlands: tectonics, ice, wind, rivers, sea, and life. These forces have created six different landscapes, namely the aeolian dune fields, foothills of the Ardennes, alluvial plains, peat landscape, sandur plains, and the sea clay landscape (*Lambert*, 1971; *Meijer*, 1985). The maritime climate in the Netherlands is described as temperate with cool summers and mild winters. This climate is caused by predominant southwest wind, and has a typically high humidity. Temperature values have relatively small amplitude, ranging from

3.1 °C (January) to 17.9 °C (July). Precipitation has relatively uniform distribution throughout the year, with summer and autumn months being slightly wetter (*Meijer, 1985; KNMI - the Dutch National Weather Service*).

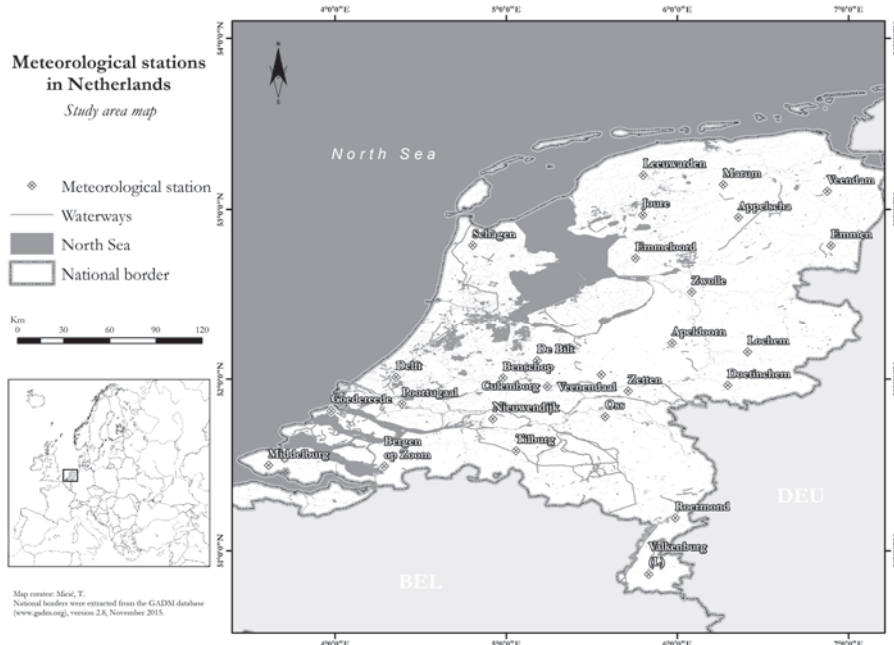


Fig. 1. Geographical location of meteorological stations in the Netherlands used in this study.

2.2. Data and methods

The daily and monthly values of precipitation were used for the calculation of extreme precipitation, as well as the rainfall erosivity indices. This data is recorded and provided by the Royal Netherlands Meteorological Institute (KNMI) in accordance with standards recommended by the World Meteorological Organization (WMO). A list of the meteorological stations is given in *Table 1*.

Table 1. List of meteorological stations and their geographical coordinates and altitudes

	Station name	Latitude	Longitude	Altitude (m)
1	Apeldoorn	52°2112' N	5°9699' E	13
2	Appelscha	52°9524' N	6°3563' E	7
3	Benschop	52°0074' N	4°9804' E	-2
4	Bergen op Zoom	51°4946' N	4°2872' E	0
5	Culemborg	51°9561' N	5°2400' E	-1
6	De Bilt	52°1093' N	5°1810' E	0
7	Delft	52°0116' N	4°3571' E	0
8	Doetinchem	51°9647' N	6°2938' E	11
9	Emmeloord	52°7121' N	5°7550' E	-2
10	Emmen	52°7858' N	6°8976' E	22
11	Goedereede	51°8181' N	3°9774' E	6
12	Joure	52°9655' N	5°7972' E	-1
13	Leeuwarden	53°2012' N	5°7999' E	-2
14	Lochem	52°1587' N	6°4098' E	11
15	Marum	53°1463' N	6°2673' E	1
16	Middelburg	51°4988' N	3°6110' E	0
17	Nieuwendijk	51°7704' N	4°9219' E	0
18	Oss	51°7836' N	5°5786' E	9
19	Poortugaal	51°8566' N	4°3950' E	0
20	Roermond	51°1913' N	5°9878' E	19
21	Schagen	52°7881' N	4°8044' E	-1
22	Tilburg	51°5853' N	5°0564' E	11
23	Valkenburg (L)	50°8652' N	5°8321' E	132
24	Veendam	53°1063' N	6°8751' E	1
25	Veenendaal	52°0263' N	5°5544' E	6
26	Zetten	51°9300' N	5°7123' E	11
27	Zwolle	52°5168' N	6°0830' E	0

Before the calculation, the homogeneity of the meteorological datasets for precipitation was examined according to the *Alexandersson* (1986) test. The homogeneity analysis indicated that the data for all observed stations are homogeneous. Precipitation concentration index (*PCI*) was calculated using the approach given by *Oliver* (1980) which was described in detail by *Michiels et al.* (1992) and *Lukić et al.* (2016). Calculation of the *PCI* on seasonal and supra seasonal scales was performed using the approach of *de Luis et al.* (2011), *Martinez-Casasnovas et al.* (2002), *Lujan and Gabriels* (2005), *Mello et al.* (2013) and *Lukić et al.* (2016). Modified Fournier index (*MFI*) was calculated according to the guidelines given by *Arnoldus* (1980).

Table 2 shows the classes of the *PCI* values and the rainfall erosivity classes determined by means of the *MFI* (e.g., *Arnoldus*, 1980; *Oliver*, 1980; *Sfiru et al.*, 2011; *Costea*, 2012; *Iskander et al.*, 2014; *Lukić et al.*, 2016). The extreme values of precipitation were calculated following the indices developed by the ETCCDI (<http://cccma.seos.uvic.ca/ETCCDI>) (*Table 3*). The RclimDex software package was used for this occasion. This is a software package designed to provide a user friendly interface to compute indices of climate extremes for monitoring and detecting climate change. Eleven precipitation indices were used for further analysis, and they are presented in *Table 3*.

Table 2. *PCI* value classes and *MFI* erosivity classes (based on *Arnoldus*, 1980)

Spatial distribution	<i>PCI</i>	Erosivity class	<i>MFI</i>
Uniform distribution	≤ 10	Very low	0 – 60
Moderate distribution	$> 10 \leq 15$	Low	60 – 90
Irregular distribution	$> 15 \leq 20$	Moderate	90 – 120
Strongly irregular distribution	> 20	High	120 – 160
		Very high	> 160

The Mann-Kendall (MK) nonparametric test was used to evaluate the presence of long-term trends in the time series of rainfall erosivity indices and precipitation indices (*Mann*, 1945; *Kendall*, 1976). The MK test compares the relative magnitudes of data rather than the data values themselves (*Gilbert*, 1987). Two hypotheses are tested in the MK test: the null hypothesis (H_0), that states there is no trend in the time series, and the alternative hypothesis (H_a) which states there is a significant trend in the series, for a certain significance level. Statistical significance (as seen as the probability p) takes values between 0 and 100 in %. In fact, p is used to test the level of confidence in H_0 . If the computed p value is lower than the chosen significance level, α (e.g., $\alpha = 5\%$), the H_0 should be rejected, and H_a should be accepted. On the other hand, if the computed p value is greater than the significance level α , the H_0 cannot be rejected (*Gilbert*, 1987).

Table 3. Definitions of 11 precipitation indices used in this study

Index ID	Indicator name	Definition	Units	Index ID	Indicator name	Definition	Units
<i>Rx1day</i>	Max 1-day precipitation amount	Monthly maximum 1-day precipitation	mm	<i>CDD</i>	Consecutive dry days	Maximum number of consecutive days with $RR < 1$ mm	days
<i>Rx5day</i>	Max 5-day precipitation amount	Monthly maximum consecutive 5-day precipitation	mm	<i>CWD</i>	Consecutive wet days	Maximum number of consecutive days with $RR \geq 1$ mm	days
<i>SDII</i>	Simple daily intensity index	Annual total precipitation divided by the number of wet days (defined as $PRCP \geq 1.0$ mm) in the year	mm/day	<i>R95p</i>	Very wet days	Annual total $PRCP$ when $RR > 95$ th percentile	days
<i>R10mm</i>	Number of heavy precipitation days	Annual count of days when $PRCP \geq 10$ mm	days	<i>R99p</i>	Extremely wet days	Annual total $PRCP$ when $RR > 99$ th percentile	mm
<i>R20mm</i>	Number of very heavy precipitation days	Annual count of days when $PRCP \geq 20$ mm	days	<i>PRCPT OT</i>	Annual total wet-day precipitation	Annual total $PRCP$ in wet days ($RR \geq 1$ mm)	mm
<i>R25mm</i>	Number of days above 25 mm	Annual count of days when $PRCP \geq 25$ mm, 25 is user defined threshold	days				

The presence of a positive serial correlation in a data set was found to increase the number of false positive results of the MK trend test (*Von Storch and Navarra*, 1995). In order to prevent this, prior to application of the MK test, *Yue-Pilon* pre-whitening test was applied (*Yue et al.*, 2002). First, the slope of the trend in each time series was estimated using the Theil-Sen approach (TSA). If the slope was found to differ from zero, the identified trend was assumed to be linear and subtracted from the sample data. The resulting residual series is

referred to as the detrended series. Next, the lag-1 serial correlation coefficient of the detrended series was computed and removed from the series. Finally, the identified trend and the modified residual series were combined, and then the MK test was applied (e.g., *Yue et al.*, 2002; *Basarin et al.*, 2016, 2017). For this purpose, the ZYP package in R (<http://www.r-project.org>) was utilized.

The Geographic Information System (GIS) and numerical modeling are becoming powerful tools not only in geographic sciences but also in climatic data processing. GIS represent a useful solution to the management of vast spatial climate datasets for a wide number of applications (*Franke*, 1982; *Lam*, 1983; *Burrough*, 1986; *Watson* and *Philip*, 1987; *McCullagh*, 1988; *Franke* and *Nielson*, 1991; *Collins* and *Bolstad*, 1996). All climatological data can be used for mapping and spatial modeling with GIS. This study uses numerical approaches for interpolating rainfall erosivity and precipitation indices applying the ArcMap software. The most suitable interpolation method for the visualization of complex data in this paperwork is the empirical bayesian kriging, which was employed through the ArcMap extension Spatial Analyst. The advantages of this interpolation (e.g., standard errors of prediction are more accurate than with other irriging methods) have been explained in detail by *Pilz* and *Spöck* (2007).

3. Results

3.1. Precipitation concentration index (PCI)

The *PCI* results for the 27 weather stations are shown in Fig. 2. The *PCI* values in the Netherlands range from 10.27 to 11.12 respectively. Thus, the Netherlands has a moderate precipitation concentration distribution. The lowest *PCI* value is found for the Valkenburg station (10.27) in the southern parts, while the highest value (11.12) is observed for the Goedereede station in the western part of the country. Trend analysis shows presence of a significant positive trend of *PCI* values for the Valkenburg station, where the *PCI* increases by 0.22 per year ($p < 0.05$), and for the Delft station where the *PCI* increases by 0.01 per year ($p < 0.1$). The obtained values are almost uniformly shifting from relatively higher values in the west to lower values in the southeastern and northeastern parts of the country. Noteworthy is that in the central parts of the Netherlands, alongside the river Rhine and the IJssel, the *PCI* exhibits slightly higher values that also belong to the class of a moderate precipitation concentration. This implies that the recorded increasing trend (for 59% of the observed stations) in the distribution of the *PCI* values could lead to a shift from moderate to irregular distribution for the future period. Calculated values of this index are of great importance for the stations with recorded statistical significance (located in the southern and western part of the country), where values of the *PCI* display an increase by 2.2 and 0.1 per decade respectively.

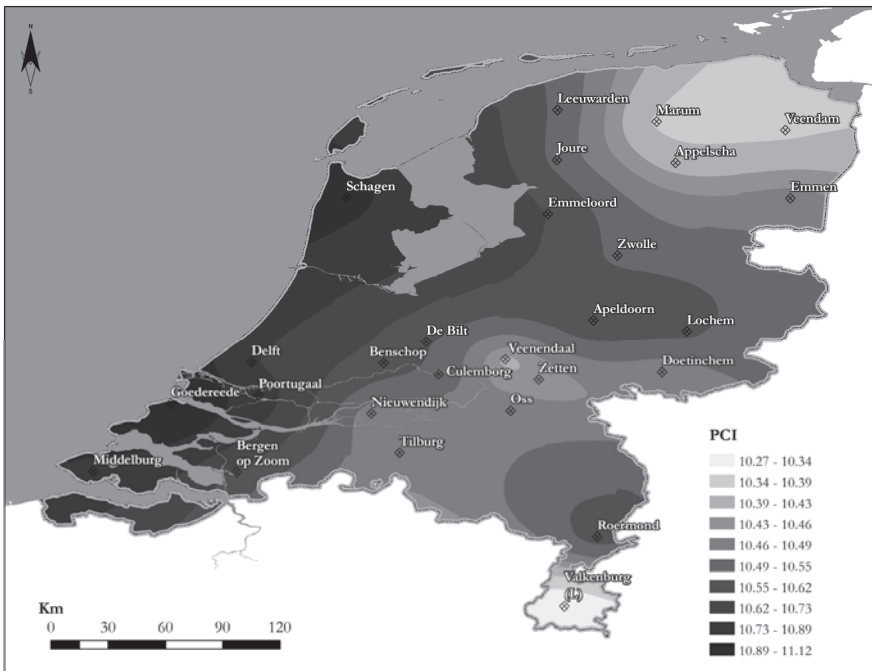


Fig. 2. Precipitation concentration index (*PCI*) on an annual basis for the observed period.

As for the distribution of precipitation during dry (Fig. 3a) and wet (Fig. 3b) periods, a clear difference can be seen. During the dry season (April-September), the *PCI* values range from 9.85 for the Valkenburg station (in the south) to 10.29 for the Apeldoorn station (in the central part of the Netherlands). Thus, it can be pointed out that during the dry season, the country falls somewhere in between the uniform precipitation distribution and the moderate precipitation concentration class. 30% of the stations exhibit an increasing trend at the given significance level of 90% ($p < 0.1$), two stations (Bergen op Zoom and Leeuwarden) display an increasing trend for the significance level of 95% ($p < 0.05$), while the stations Appelscha and Delft are showing positive trends at a significance level of 99% ($p < 0.01$). The supra-seasonal *PCI* values for the wet season (October-March) range from 10.29 for the Appelscha station to 11.46 for the Goedereede station. Therefore, it can be stated that during the wet season, the investigated area has a moderate precipitation concentration. Trend analysis show a statistically significant increasing trend for the Valkenburg station, where the value increases by 0.02 per year ($p < 0.01$), while a decreasing trend of -0.01 per year is observed for the Lochem station ($p < 0.1$). Thus, it can be observed that the precipitation distribution shows more uniformity during the dry than the wet season.

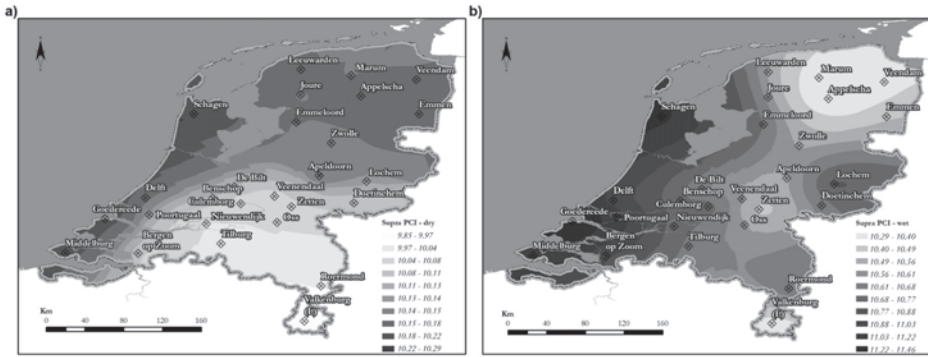


Fig. 3. Supra-seasonal *PCI* for dry (a) and wet (b) season for the observed period.

The *PCI* values during the summer season (June-August) are ranging from 3.20 for the Valkenburg station to 3.40 for the Goedereede station. Based on the trend analysis it can be noted that 26% of the stations show a decreasing trend in *PCI* value. A significant increasing trend is found for the station of Appelscha (in the north), where the *PCI* value increases by 0.01 per year ($p < 0.01$). The station of Valkenburg shows a significant rising trend (0.004 per year; $p < 0.05$), as well as the station of De Bilt, where the *PCI* value imperceptibly increases by 0.003 per year ($p < 0.1$).

During the autumn season (September-November), the values range from 3.19 for the Leeuwarden station to 3.48 for the Goedereede station. All the observed stations show an increasing trend, with the exception of the Veendam station where a minimum decline of -0.006 *PCI* value per year is detected. Only the station, in Roermond indicates a significant positive trend, where the *PCI* value increases by 0.004 per year ($p < 0.1$).

Since all the observed seasonal *PCI* values weight below 10, it can be concluded that there is a uniform precipitation distribution within the investigated area. The winter season indicates much higher *PCI* values than the other seasons, but variation within the seasons themselves is low. Nevertheless, a difference can be observed in the spatial distribution of the *PCI* values between the different seasons.

3.2. Modified Fournier index (MFI)

The results of the *MFI* and its spatial distribution are presented in Fig. 4. The *MFI* values for the Netherlands range from 77.93 for the Roermond station (in the southeast) to 97.27 for the Apeldoorn station (in the central parts). 37% of the stations have a positive trend at the given significance level of 99% ($p < 0.01$), while 26% of the stations display a significant increasing trend at the

given significance level of 95% ($p < 0.05$). The stations Culemborg and Lochem show an increasing trend at the significance level of 90% ($p < 0.1$), where the *MFI* values are experiencing an increase by 0.18 per year. The only statically significant decreasing trend ($p < 0.1$) was found for the Valkenburg station in the south of the country, where the *MFI* value declines by 0.01 per year.

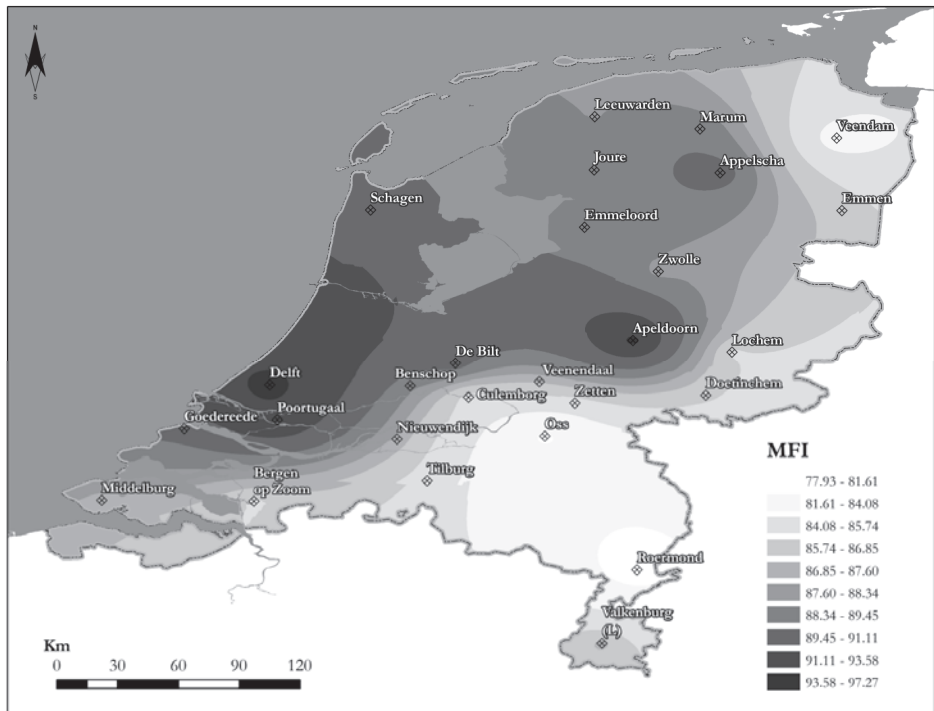


Fig. 4. Modified Fournier index (*MFI*) variability during the observed period.

It can be observed that the largest part of the Netherlands falls within the low erosivity class (with values ranging from 78 to 90). Only the regions in the northern, central and western parts of the country (30% of stations analyzed in this study) fall in the moderate erosivity class with values ranging from 90 to 97. Based on the calculated *MFI* values (Fig. 4) it can be seen that the western part of the country display higher values of erosivity. The lowest *MFI* values are

found in the region of Veendam in the northeast, and for the stations Oss and Roermond in the southeast part of the country.

This implies that the recorded significant increasing trend (for 70% of the observed stations) in *MFI* value could lead to a shift from being largely in the low erosivity class to being completely in the moderate erosivity class in the future, thus indicating an increase in rainfall erosivity.

The calculated *MFI* results are not completely in line with previous research on soil erosion in the Netherlands since soil erosion is determined by several parameters, not just rainfall erosivity. According to *Renes* (1988), soil erosion by water occurs in the Netherlands, mainly on the 40.000 ha of loess soils in the province of South-Limburg, where a hilly topography prevails. Whereas, the results of the calculated *MFI* values show higher erosivity classes for the western parts of the country. This difference can be explained by the fact that the *MFI* is a relatively simple estimator of the rainfall erosivity (*R*). Also, this index is based on the mean monthly and annual rainfall amount. Therefore, consideration of other physical factors associated with atmospheric variables must be taken into account in future investigations. Bearing in mind that the soil erosion in South-Limburg province mainly occurs on the slopes (e.g., *Winteraeken* and *Spaan*, 2010), whereas the other parts of the Netherlands are basically flat, more research is needed to improve methods for estimating soil erosion rates and variability using various models and statistical approaches, upon which mitigation strategies can be assessed and implemented.

3.3. Extreme precipitation indices

Precipitation extremes (heavy precipitation events), have been calculated for the period 1957–2016. These indices were analyzed in order to identify possible changes in precipitation related to climate extremes over the Netherlands, which could lead to increase of rainfall erosivity.

The spatial variability of the calculated *RX1day* show that all investigated stations has a positive trend, with acceptance of the Poortugaal station. The stations Delft and Veendam display a significant increasing trend ($p < 0.01$), respectively by 0.24 and 0.20 mm per year. Four stations (Goedereede, Middelburg, Roermond, and Tilburg) exhibit a significant increasing trend at a significance level of 95% ($p < 0.05$). A significant positive trend ($p < 0.1$) is found for the stations Apeldoorn (0.16 mm per year) and Nieuwendijk (0.20 mm per year).

The results of the *Rx5days* exhibit a positive trend for all of the observed stations (Fig. 5a). Four stations (Appelscha, Delft, Emmen, and Veendam) have a statistically significant trend at a confidence level of 99% ($p < 0.01$), six stations (Apeldoorn, Emmeloord, Goedereede, Leeuwarden, Middelburg, and Roermond) exhibit a positive significant trend at the given significance level of 95% ($p < 0.05$), while another six stations (De Bilt, Doetinchem, Joure, Lochem,

Nieuwendijk, and Zetten) have an increasing significant trend at a significance level of 90% ($p < 0.1$). Since the observed values display positive trend within 96% of the analyzed stations, linking precipitation extremes, their spatial variability and trends are of great importance when it comes to the erosion vulnerability assessment.

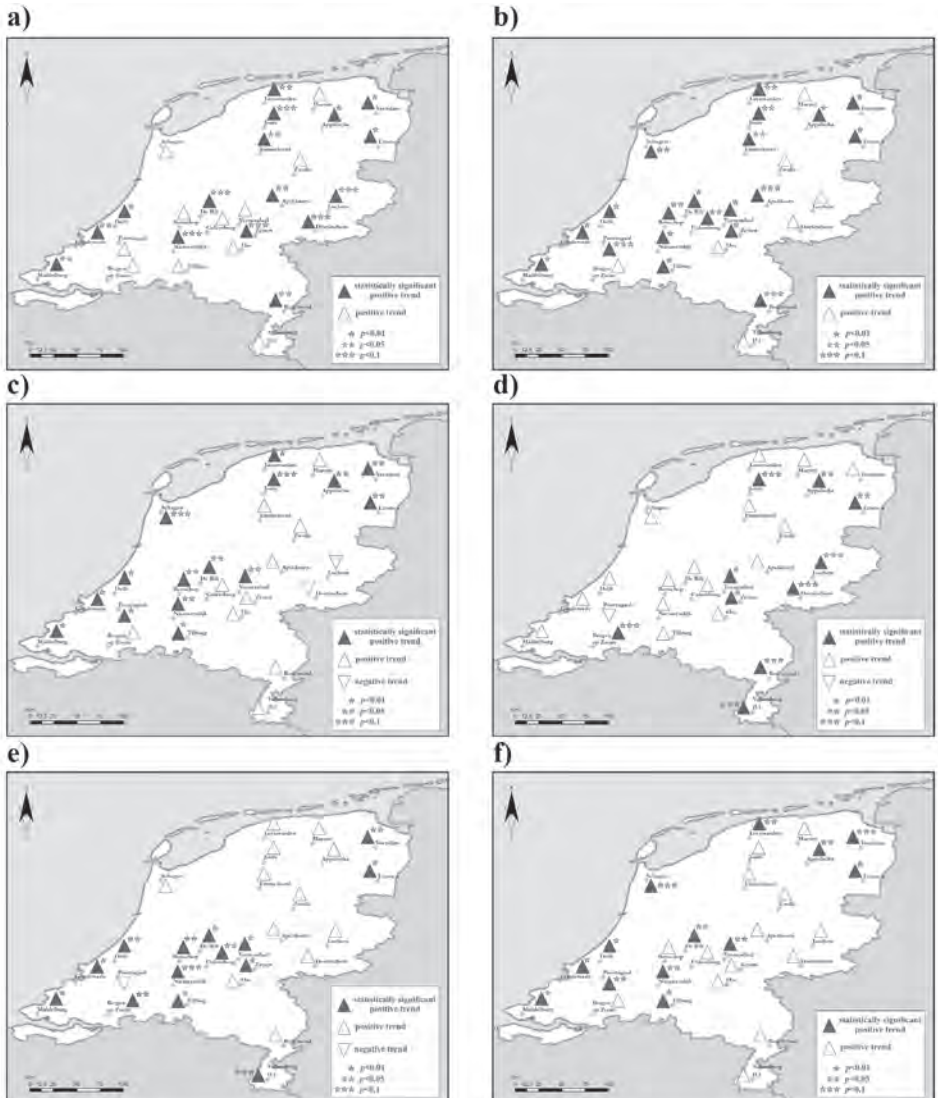


Fig. 5. Tendencies for the a) Rx5day, b) SDII, c) R10mm, d) R25mm, e) R95p, and f) PRCPTOT indices for the observed period.

Values of *SDII* are presented in *Fig. 5b*. All of the stations exhibit a positive trend, while 74% of them are displaying statistical significance at their given significance level. 41% of the analyzed stations have a significant increasing trend at the given significance level of 99% ($p < 0.01$), 22% of the observed stations show a positive trend at a significance level of 95% ($p < 0.05$), while the stations Apeldoorn, Poortugaal, and Roermond have a statically significant positive trend values by respectively 0.01 mm/day per year ($p < 0.1$). Therefore, the observed *SDII* values display a positive trend for all investigated stations for the 1957–2016 period, implying the continuous pronunciation of the observed extremes.

The results of the *R10mm* are shown in *Fig. 5c*. Six stations (Delft, Goedereede, Leeuwarden, Middelburg, Poortugaal, and Tilburg) have a significant increasing trend at $p < 0.01$, while seven stations (Appelscha, Benschop, De Bilt, Emmen, Nieuwendijk, Veendam, and Veenendaal) show a significant positive trend at a significance level of 95% ($p < 0.05$). The stations Joure and Schagen have a significant increasing trend by respectively 0.07 days per year at $p < 0.1$. The only negative trends are observed for the stations Doetinchem and Lochem, but these trends show no statistical significance.

The results of the *R20mm* show that stations Delft and Emmen have a significant increasing trend by 0.05 and 0.06 days per year, respectively, at $p < 0.01$. A total of six stations (Goedereede, Middelburg, Tilburg, Valkenburg, Veenendaal, and Zetten) show a significant positive trend at a significance level of 95% ($p < 0.05$). The stations of Schagen and Poortugal display a negative trend, but these trends have no statistical significance.

The results of the *R25mm* are shown in *Fig. 5d*. The stations of Veenendaal and Zetten display a significant increasing trend by respectively 0.04 and 0.03 days per year ($p < 0.01$), whereas the stations of Appelscha and Emmen both show a significant increasing trend by 0.02 days per year at $p < 0.05$. A total of six stations (Bergen op Zoom, Doetinchem, Joure, Lochem, Roermond, and Valkenburg) have a significant positive trend at a significance level of 90% ($p < 0.1$). The stations of Schagen and Poortugal have a negative, but not statistically significant trend. The obtained results for the *R10mm*, *R20mm*, and *R25mm* are in line with the results of previous studies (e.g., *Donat et al.*, 2013; *IPCC*, 2007, 2012, 2013), which report that many of the precipitation indices consistently indicate increases in precipitation extremes (in some cases significantly). Therefore, the frequency of heavy precipitation days and the percentage of events contributing to precipitation totals are expected to increase as confirmed by this study. This implies higher susceptibility to pluvial erosion in the Netherlands.

None of the calculated values of *CDD* indicate a significant trend. 37% of the stations display none significant positive trend, while the other 63% of the stations have none significant negative trend. The obtained results indicate the presence of wetter conditions in the investigated area.

The results for the *CWD* indicate that only two stations show a significant trend. The station Poortugaal shows a significant positive trend by 0.06 days per year at a significance level of 95% ($p < 0.05$), while Tilburg has displayed a significant positive trend by 0.03 days per year at $p < 0.1$. Both Poortugaal and Tilburg are located in the southwest of the Netherlands. A total of nine stations have a negative (but not significant trend), while fourteen stations (52%) display a positive (but not significant) trend. According to *Casanueva et al.* (2014), positive phases of the North Atlantic Oscillation (NAO) cause occurrence of heavier precipitation and a decrease in *CDD* (which also could lead to an increase in *CWD* values) in the north of Europe and the opposite in the south of the continent. For the case study of the Netherlands, an increase in *CWD* values is observed for 67% of the investigated stations. Stations with negative tendency of *CWD* values are located in northern and southeastern parts of the country.

Fig. 5e presents the spatial distribution pattern of the *R95p*. Poortugaal is the only station that shows a negative trend, but this trend is not significant. A total of six stations have a significant increasing trend at a significance level of 99% ($p < 0.01$), and four stations show a significant increasing trend at $p < 0.05$. The stations Nieuwendijk and Valkenburg have a significant positive trend by respectively 0.90 and 1.04 mm per year at $p < 0.1$. Most of the stations with a significant trend are found in the central and southwestern parts of the Netherlands. Generally, positive tendency of *R95p* is observed for 96% of the analyzed stations. These results are in agreement with the findings of *Trenberth et al.* (2007), who concluded that the number of heavy precipitation events (e.g., 95th percentile) increases within many land regions, even in regions with a reduction in total precipitation amounts. The respective authors did not pick up on sub regional and local differences in trends, because the study was focused on the whole of Europe. In addition, results from this study can give a certain focus to the regions in Western Europe, i.e., the Netherlands. According to *Casanueva et al.* (2014), the *CWD* and *CDD* are more related to large-scale atmospheric circulations, while the *R95p* has a convective origin and depends more on local processes and moisture fluxes. The annual increase of *R95p* could be related to an intensification of the hydrological cycle associated with a warming-related increase of atmospheric moisture content (e.g., *Casanueva et al.*, 2014; *Schmidli et al.*, 2007). Therefore, the increase of moisture due to intensified warming (*Trenberth*, 2011) may cause stronger changes in convective precipitation than in large-scale precipitation (e.g. *Casanueva et al.*, 2014). Similar connections could be applied to the area of the Netherlands.

The tendency of the *R99p* indicate that stations Bergen op Zoom and Delft have a significant positive trend by respectively 0.80 and 1.03 mm per year ($p < 0.01$), while six of the stations display a significant positive trend at $p < 0.05$. The stations De Bilt, Goedereede, and Middelburg have a significant

positive trend at a significance level of 90% ($p < 0.1$). The stations Poortugaal and Zwolle show not significant decreasing trend. Positive tendency of $R99p$ is observed for 93% of the analyzed stations.

Certain model simulations suggest that more extreme precipitation scenarios will have significant consequences for soil water dynamics at both shallow and deep soil depths. Because more extreme precipitation patterns represent permanent, as opposed to transient, changes in terrestrial ecosystems (e.g., those related to disturbances), resource levels will also be chronically altered either directly, through soil water dynamics, or indirectly, through the effects of soil water on the availability of other resources (Knapp *et al.*, 2008; Bosco *et al.*, 2015). The investigation of the extreme precipitation parameters is of great importance for the Netherlands, since the intensity of rainfall is one of the main factors driving soil water erosion processes.

The results for the $PRCPTOT$ are shown in Fig. 5f. All of the stations display a positive trend. For four of the stations this trend is significant at the given significance level of 99% ($p < 0.01$), while six stations have a significant trend at $p < 0.05$. The stations Schagen and Veendam have a significant positive trend respectively by 1.47 and 1.73 mm per year at $p < 0.1$.

These results are in agreement with previous studies, which pointed out that for the European continent, a growing intensity of heavy precipitation over the last five decades can be expected. Klein-Tank and Können (2003) reported primarily positive linear trends in extreme precipitation indices up to 5% per decade from their analysis of daily station data for the period 1945–1995. Similar conclusions were derived on the continental scale, and various regional studies (Easterling *et al.*, 2000; Trenberth *et al.*, 2007; Frei and Schär, 2001; Groisman *et al.*, 2005; Zolina *et al.*, 2005, 2008; Brunetti *et al.*, 2004, 2006; Moberg *et al.*, 2006; Alexander *et al.*, 2006). Van Minnen *et al.* (2013) pointed out that the frequency in which extreme precipitations in the Netherlands take place have increased since the last century. This happened primarily in winter and predominantly in the western part of the Netherlands. The respective authors explain the increase in extreme precipitation primarily by an increase in the amount of rain during already rainy days. The results from this study support the findings of the respective authors.

Using standardized indices for extreme climate events that have been defined by ETCCDI, a comprehensive understanding of variation patterns in precipitation extremes is gained for the Netherlands. The results of the precipitation extremes are in good agreement with the results of other studies conducted for the Netherlands and the European continent as well. In a majority of cases in this study, most precipitation indices suggest that there is an increase not only in the amount, but also in the intensity of precipitation. Changes in precipitation extremes were examined and evaluated in this study, because this approach can provide a more detailed insight of driving factors of rainfall erosivity, its spatial distribution, and impact. The main reason for

this lays in the fact that heavy precipitation events rank among the natural hazards with the most disastrous impact on human societies and anthropogenic systems in general.

4. Conclusions

The potential of rain to generate soil erosion is known as rainfall erosivity, and its estimation is fundamental for the understanding of climatic vulnerability of a given region. Also, the occurrence of extreme events and their impacts on society have become a fundamental issue due to the greater climate variability effects on them (e.g., very heavy precipitation episodes). Observation of rainfall erosivity in the Netherlands was carried out on the basis of the analysis of rainfall aggressiveness trends, extreme precipitation indices, and their spatial variability for the period 1957–2016. This study presents the first results of combined rainfall erosivity and extreme precipitation indices for the investigated area. The analysis, applied to the present climate conditions, reveal necessary information which can be used by decision makers on various levels, for the development of prevention activities and for the promotion of mitigation measures at all levels.

The results of this study indicate that, on an annual basis, the *PCI* values range within a moderate precipitation concentration distribution class, but trend analyses implies a shift from moderate to irregular distribution for the future period. However, during the dry season (April-September), the supra-seasonal *PCI* values are ranging between the uniform precipitation distribution and the moderate precipitation concentration class. Trend analysis implies a shift from being partly in the uniform and moderate class to being completely in the moderate distribution class for the future period. The supra-seasonal *PCI* values for the wet season (October-March) indicate a moderate precipitation concentration. When observing the results for the different seasons, it can be concluded that the winter season (December-February) indicates much higher *PCI* values than the other seasons. Since all the observed seasonal *PCI* values weight below 10, it can be concluded that there is a uniform precipitation distribution within the investigated area.

The *MFI* values for the Netherlands suggest that the largest part of the area falls within the low erosivity class (with values ranging from 78 to 90). Only the regions in northern, central, and western parts of the country (30% of stations analyzed in this study) fall in the moderate erosivity class with values ranging from 90 to 97. However, trend analysis implies a shift from being largely in the low erosivity class to being completely in the moderate erosivity class in the future, thus indicating an increase in rainfall erosivity.

The precipitation extremes suggest that both the amount and the intensity of precipitation are increasing, which is in a good agreement with the studies conducted for the Netherlands, as well as the ones done for the entire European

continent. The results of this study suggest that the climate conditions in the Netherlands are changing, and that this change might have a negative influence on the rainfall erosivity for the country.

The results of this study can contribute to the erosivity studies, since the focus is given to the dynamics of the main climatological agent of erosion – the precipitation. Hence, utilization of the more complex and sensitive indices such as EI_{30} along with physically based models for deriving soil erosion rates (e.g., RUSLE), can provide a more suitable approach for detailed rainfall erosivity estimation in some future studies. Since erosion is highly dependent on topography and land use, the next stage of the investigation of these parameters could be oriented towards incorporation into the GIS environment in order to determine erosion potential and its spatial causality.

Acknowledgements: This research was supported by Projects 176020 and 43002 of the Serbian Ministry of Education, Science and Technological Development and by Project 142-451-2511/2017-02 of Provincial Secretariat for Science and Technological Development, Vojvodina Province. Part of the research was supported by the HUSRБ/1602/11/0057 – WATER@RISK – Improvement of drought and excess water monitoring for supporting water management and mitigation of risks related to extreme weather conditions. Authors are grateful to the anonymous reviewer/s whose comments and suggestions greatly improved the manuscript.

References

- Alexander, L. V., Zhang, X., Peterson, T. C., Caesar, J., Gleason, B., Klein Tank, A.M.G., Haylock, M., Collins, D., Trewin, B., Rahimzadeh, F., Tagipour, A., Rupa Kumar, K., Revadekar, J., Griffiths, G., Vincent, L., Stephenson, D.B., Burn, J., Aguilar, E., Brunet, M., Taylor, M., New, M., Zhai, P., Rusticucci, M., and Vazquez-Aguirre, J.L., 2006: Global observed changes in daily climate extremes of temperature and precipitation. *J. Geophys. Res: Atmospheres* 111, D05109.
- Alexandersson, H., 1986: A homogeneity test applied to precipitation data. *J. Climatology* 6, 661–675.
<https://doi.org/10.1002/joc.3370060607>
- Apaydin, H., Erpul, G., Bayramin, I., and Gabriels, D., 2006: Evaluation of indices for characterizing the distribution and concentration of precipitation: A case for the region of Southeastern Anatolia Project, Turkey. *J. Hydrology* 328, 726–732.
<https://doi.org/10.1016/j.jhydrol.2006.01.019>
- Arnoldus, H. M., 1980: An approximation of the rainfall factor in the Universal Soil Loss Equation. In: (Eds. de Boodts M, Gabriels D.) Assessments of Erosion. John Wiley and Sons Ltd., Chichester, 127–132.
- Attema, J.J., Loriaux, J.M., and Lenderink, G., 2014: Extreme precipitation response to climate perturbations in an atmospheric mesoscale model. *Environ. Res. Letters* 9, 1–12.
<https://doi.org/10.1088/1748-9326/9/1/014003>
- Basarin, B., Lukic, T., Pavic, D., and Wilby, R.L., 2016: Trends and multi-annual variability of water temperatures in the river Danube, Serbia. *Hydrol. Proc.* 30, 3315–3329.
<https://doi.org/10.1002/hyp.10863>
- Basarin, B., Lukic, T., Mesaros, M., Pavic, D., Dordevic, J., and Matzarakis, A., 2017: Spatial and temporal analysis of extreme bioclimate conditions in Vojvodina, Northern Serbia. *Int. J. Climatol* 38, 142–157. <https://doi.org/10.1002/joc.5166>
- Berger, F. and Rey, F., 2004: Mountain protection forests against natural hazards and risks: new French developments by integrating forests in risk zoning. *Nat. Hazards* 33, 395–404.
<https://doi.org/10.1023/B:NHAZ.0000048468.67886.e5>

- Blinkov, I.*, 2015: The Balkans: The most erosive part of Europe?. *Glasnik Šumarskog fakulteta* 111, 9–20.
- Brunetti, M., Maugeri, M., Monti, F., and Nanni, T.*, 2004: Changes in daily precipitation frequency and distribution in Italy over the last 120 years. *J. Geophys. Res. Atmospheres* 109, D05102 <https://doi.org/10.1029/2003JD004296>
- Brunetti, M., Maugeri, M., Nanni, T., Auer, I., Böhm, R., and Schöner, W.*, 2006: Precipitation variability and changes in the greater Alpine region over the 1800–2003 period. *J. Geophys. Res. Atmospheres* 111, D11107. <https://doi.org/10.1029/2005JD006674>
- Boardman, J. and Poesen, J.*, 2006: Soil erosion in Europe: major processes, causes and consequences. Wiley. 477–487. <https://doi.org/10.1002/0470859202>
- Bosco, C., de Rigo, D., Dewitte, O., Poesen, J., and Panagos, P.*, 2015: Modelling soil erosion at European scale: towards harmonization and reproducibility. *Nat. Hazards Earth Syst. Sci.* 15, 225–245. <https://doi.org/10.5194/nhess-15-225-2015>
- Buishand, T.A., De Martino, G., Spreeuw, J.N., and Brandsma, T.*, 2013: Homogeneity of precipitation series in the Netherlands and their trends in the past century. *Int. J. Climatol.* 33, 815–833. <https://doi.org/10.1002/joc.3471>
- Burrough, P.A.*, 1986: Principles of geographical information systems for land resources assessment. Clarendon, Oxford.
- Casanueva V.A., Rodríguez-Puebla, C., Frías, M.D., and González-Reviriego, N.*, 2014: Variability of extreme precipitation over Europe and its relationships with teleconnection patterns. *Hydrol. Earth Syst. Sci.* 18, 709–725. <https://doi.org/10.5194/hess-18-709-2014>
- CBS* 2017. Bevolking; kerncijfers. <http://statline.cbs.nl/statweb/publication/?vw=tanddm=slnlandpa=37296nedandd1=0-2,8-13,19-21,25-35,52-56,68andd2=0,10,20,30,40,50,60,64-65andhd=151214-1132andhdr=glandstb=t> (Last access June 26, 2017)
- Collins, F.C. and Bolstad, P.V.*, 1996: A comparison of spatial interpolation techniques in temperature estimation. Proceedings of the Third International Conference/Workshop on Integrating GIS and Environmental Modeling, Santa Fe, New Mexico, January 21–25, 1996. Santa Barbara, California: National Center for Geographic Information Analysis (NCGIA).
- Costea, M.*, 2012: Using the Fournier indexes in estimating rainfall erosivity. Case study – the Secul Mare basin. *Aerul si Apa: Componente ale Mediului* 1, 313–320.
- Christensen, J.H., Hewitson, A., Busuioc, A., Chen, X., Gao, I., Held, R., Jones, R. K., Kolli, W.T., Kwon, R., Laprise, V., Magaña Rueda, L., Mearns, C.G., Menendez, J., Ranen, A., Rinke, A., Sarr, A., and Whetton, P.*, 2007: Regional climate projections. In (Eds. Solomon, S., Quin, D., Manning, M., Chen, Z., Marquis, M., Averyt, K.B., Tignor, M., Miller, H.L.) Climate Change 2007: The Physical Science Basis. Contribution of Working Group I to the Fourth Assessment Report of the Intergovernmental Panel on Climate Change. Cambridge University Press: Cambridge and New York, NY, 848–940.
- Diodato, N. and Bellocci, G.*, 2007: Estimating monthly (R) USLE climate input in a Mediterranean region using limited data. *J. Hydrology* 345, 224–236. <https://doi.org/10.1016/j.jhydrol.2007.08.008>
- Donat, M. G., Alexander, L. V., Yang, H., Durre, I., Vose, R., and Caesar, J.*, 2013: Global land-based datasets for monitoring climatic extremes. *Bull. Amer. Meteorol. Soc.* 94, 997–1006. <https://doi.org/10.1175/BAMS-D-12-00109.1>
- Easterling, D.R., Meehl, G.A., Parmesan, C., Changnon, S.A., Karl, T.R., and Mearns, L.O.*, 2000: Climate extremes: observations, modeling, and impacts. *Science* 289-5487, 2068–2074.
- Ferro, V., Porto, P., and Yu, B.*, 1999: A comparative study of rainfall erosivity estimation for southern Italy and southeastern Australia. *Hydrol. Sci. J.* 44, 3–24. <https://doi.org/10.1080/02626669909492199>
- Franke, R.*, 1982: Scattered data interpolation: tests of some methods. *Math. Comput.* 38, 181–200.
- Franke, R. and Nielson, G.*, 1991: Scattered data interpolation and applications: a tutorial and survey. In (Eds: Hagen H, Roller D) Geometric modelling: methods and applications. Springer, Berlin, 131–160.

- Frei, C. and Schär, C., 2001:* Detection probability of trends in rare events: Theory and application to heavy precipitation in the Alpine region. *J. Climate* 14, 1568–1584.
[https://doi.org/10.1175/1520-0442\(2001\)014<1568:DPOTIR>2.0.CO;2](https://doi.org/10.1175/1520-0442(2001)014<1568:DPOTIR>2.0.CO;2)
- Gabriels, D., 2001:* Rain erosivity in Europe. In: *Man and Soil in the Third Millennium*, III International Congress of European Society for Soil Conservation. 31–43.
- Gares, P.A., Sherman, D.J., and Nordstrom, K.F., 1994:* Geomorphology and natural hazards. *Geomorphology* 10, 1–4, 1–18.
- Gilbert, R.O., 1987:* Statistical methods for environmental pollution monitoring. Van Nostrand Reinhold, New York, 1-336.
- Gregori, E., Costanza, M., and Zorn, G., 2006:* Assessment and classification of climatic aggressiveness with regard to slope instability phenomena connected to hydrological and morphological processes. *J. Hydrology* 329, 489–499.
<https://doi.org/10.1016/j.jhydrol.2006.03.001>
- Groisman, P.Y., Knight, R.W., Easterling, D.R., Karl, T.R., Hegerl, G.C., and Razuvayev, V.N., 2005:* Trends in intense precipitation in the climate record. *J. Climate* 18, 1326–1350.
<https://doi.org/10.1175/JCLI3339.1>
- Handmer, J.W., Dovers, S., and Downing, T.E., 1999:* Societal Vulnerability to Climate Change and Variability. *Mitig. Adaptat. Strategies Glob. Change* 4, 267–281.
<https://doi.org/10.1023/A:1009611621048>
- Hernando, D. and Romana, M.G., 2015:* Estimating the rainfall erosivity factor from monthly precipitation data in the Madrid Region (Spain). *J. Hydrol. Hydromechanics* 63, 55–62.
<https://doi.org/10.1515/johh-2015-0003>
- IPCC 2007.* Climate change 2007: the physical science basis. Cambridge University Press, Cambridge, UK.
- IPCC 2012.* Summary for Policymakers. In (Eds.: Field, C.B., Barros, V., Stocker, T.F., Qin, D., Dokken, D.J., Ebi, K.L., Mastrandrea, M.D., Mach, K.J., Plattner, G.-K., Allen, S.K., Tignor, M., and Midgley, P.M.) Managing the Risks of Extreme Events and Disasters to Advance Climate Change Adaptation, , A Special Report of Working Groups I and II of the Intergovernmental Panel on Climate Change, Cambridge University Press, Cambridge, UK, and New York, NY, USA, 1–19.
- IPCC 2013. Climate Change 2013. The Scientific Basis*, Cambridge University Press, New York, NY.
- Iskander, S.M., Rajib, M.A., and Rahman, M.M., 2014:* Trending regional precipitation distribution and intensity: use of climatic indices. *Atmosph. Climate Sci.* 4, 385–393.
<https://doi.org/10.4236/acs.2014.43038>
- Kendall, M.G., 1976:* Rank Correlation Methods. 4th Ed. Griffin.
- Kirkby, M.J. and Neale, R.H., 1987:* A Soil Erosion Model Incorporating Seasonal Factors. In (Ed. Gardiner V) International geomorphology, Vol. II. John Wiley and Sons Ltd, Chichester: 179–210.
- Klein-Tank, A.M.G., Wijngaard, J.B., Können, G.P., Bohm, R., Demare, G., Gocheva, A., Mileta, M., Pashiardis, S., Hejkrlik, L., Kern-Hansen, C., Heino, R., Bessemoulin, P., Muller-Westermeier, G., Tzanakou, M., Szalai, S., Pals-dotir, T., Fitzgerald, D., Rubin, S., Capaldo, M., Maugeri, M., Leitass, A., Bukantis, A., Aberfeld, R., Van Engelen, A.F.V., Forland, E., Mietus, M., Coelho, F., Mares, C., Razuvayev, V., Nieplova, E., Cegnar, T., Lopez, J.A., Dahlstrom, B., Moberg, A., Kirchhofer, W., Ceylan, A., Pachaliuk, O., Alexander, L.V., and Petrovic, P., 2002:* Daily dataset of 20th-century surface air temperature and precipitation series for the European Climate Assessment. *Int. J. Climatol.* 22, 1441–1453. <https://doi.org/10.1002/joc.773>
- Klein-Tank, A.M.G. and Können, G.P., 2003:* Trends in indices of daily temperature and precipitation extremes in Europe, 1946–99. *J. Climate* 16, 3665–3680.
[https://doi.org/10.1175/1520-0442\(2003\)016<3665:TIIODT>2.0.CO;2](https://doi.org/10.1175/1520-0442(2003)016<3665:TIIODT>2.0.CO;2)
- Knapp, A. K., Beier, C., Briske, D. D., Classen, A. T., Luo, Y., Reichstein, M., Melinda D. Smith, M.D., Smith, S.D., Bell, J.E., Fay, P.F., Heisler, J.L., Leavitt, S.W., Sherry, R., Smith, B., Weng, E., 2008:* Consequences of more extreme precipitation regimes for terrestrial ecosystems. *AIBS Bull.* 58, 811–821.
- Lam, N.S., 1983:* Spatial interpolation methods: a review. *Amer. Cartogr.* 10, 129–149.
<https://doi.org/10.1559/152304083783914958>

- Lambert, A.M.*, 1971: The making of the Dutch landscape: an historical geography of the Netherlands. Seminar Press Ltd, 1–412.
- Lenderink, G., van Meijgaard, E., and Selen, F.*, 2009: Intense coastal rainfall in the Netherlands in response to high sea surface temperatures: analysis of the event of August 2006 from the perspective of a changing climate. *Clim. Dynam.* 32, 19–33.
<https://doi.org/10.1007/s00382-008-0366-x>
- Loureiro, N.D. and Coutinho, M.D.*, 2001: A new procedure to estimate the RUSLE EI30 index, based on monthly rainfall data and applied to the Algarve region, Portugal. *J. Hydrology* 250, 12–18.
[https://doi.org/10.1016/S0022-1694\(01\)00387-0](https://doi.org/10.1016/S0022-1694(01)00387-0)
- de Luis, M., Gonzales-Hidalgo J.C., and Longares, L.A.*, 2010: Is rainfall erosivity increasing in Mediterranean Iberian Peninsula. *Land Degradat. Develop.* 21, 139–144.
- de Luis, M., Gonzales-Hidalgo, J.C., Brunetti, M., and Longares, L.A.*, 2011: Precipitation concentration changes in Spain 1946–2005. *Nat. Haz. Earth Syst. Sci.* 11, 1259–1265.
<https://doi.org/10.5194/nhess-11-1259-2011>
- Lujan, D.L. and Gabriels, D.*, 2005: Assessing the rain erosivity and rain distribution in different agro-climatological zones in Venezuela. *Sociedade and Natureza- Special Issue* 1, 16–29.
- Lukić, T., Leščešen, I., Sakulski, D., Basarin, B., and Jordaan, A.*, 2016: Rainfall erosivity as an indicator of sliding occurrence along the southern slopes of the Bačka loess plateau: a case study of the Kula settlement, Vojvodina (North Serbia). *Carpathian J. Earth Environ. Sci.* 11, 303–318.
- Mann, H.B.*, 1945: Non-parametric tests against trend. *Econometrica* 13, 245–259.
<https://doi.org/10.2307/1907187>
- Markantonis, V., Meyer, V., and Schwarze, R.*, 2012: Valuating the intangible effects of natural hazards-review and analysis of the costing methods. *Nat. Haz. Earth Syst. Sci.* 12, 1633–1640.
<https://doi.org/10.5194/nhess-12-1633-2012>
- Martinez-Casanovas, J.A., Ramos, M.C., and Ribes-Dasi, M.*, 2002: Soil erosion caused by extreme rainfall events: mapping and quantification in agricultural plots from very detailed digital elevation models. *Geoderma* 105, 125–140. [https://doi.org/10.1016/S0016-7061\(01\)00096-9](https://doi.org/10.1016/S0016-7061(01)00096-9)
- Mather, A. S.*, 1982: The changing perception of soil erosion in New Zealand. *Geographic. J.* 148, 207–218. <https://doi.org/10.2307/633772>
- McCullagh, M.J.*, 1988: Terrain and surface modelling systems: theory and practice. *Photogrammetric Rec.* 12, 747–779. <https://doi.org/10.1111/j.1477-9730.1988.tb00627.x>
- Meijer, H.*, 1985: Compact geography of the Netherlands. ERIC Clearinghouse. Fifth edition.
- Mello, C.R., Viola, M.R., Beskow, S., and Norton, L.D.*, 2013: Multivariate models for annual rainfall erosivity in Brazil. *Geoderma* 202–203, 88–102. <https://doi.org/10.1016/j.geoderma.2013.03.009>
- Michiels, P., Gabriels, D., and Hartmann, R.*, 1992: Using the seasonal and temporal precipitation concentration index for characterizing monthly rainfall distribution in Spain. *Catena* 19, 43–58.
[https://doi.org/10.1016/0341-8162\(92\)90016-5](https://doi.org/10.1016/0341-8162(92)90016-5)
- Moberg, A., Jones, P. D., Lister, D., Walther, A., Brunet, M., Jacobit, J., Lisa V. Alexander, Paul M. Della-Marta, P.M., Luterbacher, J., Yiou, P., Chen, D., Klein Tank, A.M.G., Saladie, O., Sigro, J., Aguilar, E., Alexandersson, H., Almarza, C., Auer, I., Barriendos, M., Begert, M., Bergstrom, H., Bohm, R., Butler, C.J., Caesar, J., Drebs, A., Founda, D., Gerstengarbe, F.W., Micela, G., Maugeri, M., Osterle, H., Pandzic, K., Petrakis, M., Srnec, L., Tolasz, R., Tuomenvirta, H., Werner, P.C., Linderholm, H., Philipp, A., Wanner, H., and Xoplaki, E.*, 2006: Indices for daily temperature and precipitation extremes in Europe analyzed for the period 1901–2000. *J. Geophys. Res.: Atmospheres* 111, D22106. <https://doi.org/10.1029/2006JD007103>
- Oduro-Afriyie, K.*, 1996: Rainfall erosivity map for Ghana. *Geoderma* 74, 161–166.
[https://doi.org/10.1016/S0016-7061\(96\)00054-7](https://doi.org/10.1016/S0016-7061(96)00054-7)
- Oliver, J.E.*, 1980: Monthly precipitation distribution: A comparative index. *Prof. Geographer* 32, 300–309. <https://doi.org/10.1111/j.0033-0124.1980.00300.x>
- Pilz, J. and Spöck, G.*, 2007: Why Do We Need and How Should We Implement Bayesian Kriging Methods. *Stoch. Environ. Res. Risk Assess.* 22, 621–632.
<https://doi.org/10.1007/s00477-007-0165-7>

- Rawat, P.K., Tiwari, P.C., Pant, C.C., Sharama, A.K., and Pant, P.D.*, 2011: Modelling of stream runoff and sediment output for erosion hazard assessment in Lesser Himalaya: need for sustainable land use plan using remote sensing and GIS: a case study. *Nat. Hazards* 59, 1277–1297. <https://doi.org/10.1007/s11069-011-9833-5>
- Renard, K.G. and Freimund, J.R.*, 1994: Using monthly precipitation data to estimate the r-factor in the revised USLE. *J. Hydrology* 157, 287–306. [https://doi.org/10.1016/0022-1694\(94\)90110-4](https://doi.org/10.1016/0022-1694(94)90110-4)
- Renes, J.*, 1988: De geschiedenis van het Zuidlimburgse Cultuurlandschap. Van Gorcum, Assen.
- Schmidli, J., Goodess, C.M., Frei, C., Haylock, M.R., Hundecha, Y., Ribalaygua, J., and Schmitt, T.*, 2007: Statistical and dynamical downscaling of precipitation: An evaluation and comparison of scenarios for the European Alps. *J. Geophys. Res.: Atmospheres* 112, D04105.
- Sfîru, R., Cárdei, P., Herea, V., and Ertekin, C.*, 2011: Calculation of rainfall erosion intensity (rainfall erosivity) in Valea Călugărească wine growing area. *INMATEH – Agric. Engin.* 34, 23–28.
- Trenberth, K.E., Jones, P.D., Ambenje, P., Bojariu, R., Easterling, D., Tank, A.K., Parker, D., Rahimzadeh, F., Renwick, J.A., Rusticucci, M., Soden, B. and Zhai, P.*, 2007: Observations: Surface and Atmospheric Climate Change, chap. 3 of Climate Change 2007: The Physical Science Basis. In (Eds. Solomon, S., Qin, D., Manning, M., Marquis, M., Averyt, KB, Tignor, M., Miller, HL and Chen, Z.) Contribution of Working Group I to the Fourth Assessment Report of the Intergovernmental Panel on Climate Change. 235–336.
- Trenberth, K. E.*, 2011: Changes in precipitation with climate change. *Climate Res.* 47, 123–138. <https://doi.org/10.3354/cr00953>
- Vallejo, V.R., Diaz-Fierros, F., and De la Rosa, D.*, 2005: Impactos sobre los recursos edaficos. In (Ed. Moreno, J.M.) Evaluacion Preliminar General de Los Impactos en Espanapor Efecto del Cambio Climatico. Ministerio de Medio Ambiente: Madrid. (In Spain)
- Van den Hurk, B., Siegmund, P., Klein-Tank, A., Attema, J., Bakker, A., Beersma, J., Bessembinder, J., Boers, J., Brandsma, T., van den Brink, T., Drijfhout, S., Eskes, H., Haarsma, R., Hazeleger, W., Jilderda, R., Katsman, C., Lenderink, G., Loriaux, J., van Meijgaard, E., van Noije, T., van Oldenborgh, G., Selten, F., Siebesma, P., Sterl, A., de Vries, H., van Weele, M., de Winter, R., and van Zadelhoff, G.*, 2015: KNMI14: climate change scenarios for the 21st century. Technical report, Technical report Royal Netherlands Meteorological Institute, The Netherlands.
- Van Haren, R., Oldenborgh, G., Lenderink, G., Collins, M., and Hazeleger, W.*, 2013: SST and circulation trend biases cause an underestimation of European precipitation trends. *Clim. Dynam.* 40, 1–20. <https://doi.org/10.1007/s00382-012-1401-5>
- Van Minnen, J., Ligtvoet, W., van Bree, L., de Hollander, G., Visser, H., van der Schrier, G., and Klein-Tank, A.M.G.*, 2013: The effects of climate change in the Netherlands 2012. PBL, Utrecht.
- Van Oldenborgh, G.J., and Van Ulden, A.A.D.*, 2003: On the relationship between global warming, local warming in the Netherlands and changes in circulation in the 20th century. *Int. J. Climatol.* 23, 1711–1724. <https://doi.org/10.1002/joc.966>
- Von Storch H. and Navarra, A.*, 1995: Analysis of Climate Variability Applications of Statistical Techniques. Springer-Verlag Berlin Heidelberg New York. <https://doi.org/10.1007/978-3-662-03167-4>
- Watson, D.F. and Philip, G.M.*, 1987: Neighbourhood based interpolation. *Geobyte* 2, 12–16.
- Wijngaard, J.B. and Klein-Tank, A.M., Können, G.P.*, 2003: Homogeneity of 20th century European Daily Temperature and Precipitation series. *Int. J. Climatol.* 23, 679–692.
- Winteraeken, H. J., Spaan, W. P.*, 2010: A new approach to soil erosion and runoff in south Limburg - The Netherlands. *Land Degradat. Develop.* 21, 346–352.
- Wischmeier, W.H. and Smith, D.D.*, 1978: Predicting Rainfall Erosion losses – A Guide to Conservation Planning, Agriculture Handbook. USDA. Washington, 1–51.
- Yue, B.J., Shi, Z.H., and Fang, N.F.*, 2014: Evaluation of rainfall erosivity and its temporal variation in the Yanhe River catchment of the Chinese Loess Plateau. *Nat. Hazards* 74, 585.
- Yue, S., Pilon, P., Phinney, B., and Cavadias, G.*, 2002: The influence of autocorrelation on the ability to detect trend in hydrological series. *Hydrol. Proc.* 16, 1807–1829.

- Zolina, O., Simmer, C., Kapala, A., and Gulev, S., 2005: On the robustness of the estimates of centennial-scale variability in heavy precipitation from station data over Europe. Geophys. Res. Lett. 32, L14707.*
- Zolina, O., Simmer, C., Kapala, A., Bachner, S., Gulev, S., Maechel, H., 2008: Seasonally dependent changes of precipitation extremes over Germany since 1950 from a very dense observational network. J. Geophys. Res. Atmospheres 113, D06110.*
- Zhao, C., Ding, Y., Ye, B., Yao, S., Zhao, Q., Wang, Z., and Wang, Y., 2011: An analyses of long-term precipitation variability based on entropy over Xinjiang, northwestern China. Hydrol. Earth Syst. Sci. Discuss. 8, 2975–2999.*

IDŐJÁRÁS

*Quarterly Journal of the Hungarian Meteorological Service
Vol. 122, No. 4, October – December, 2018, pp. 433–452*

Analysis of extreme precipitation over the Peripannonian region of Bosnia Hercegovina

Tatjana Popov*, Slobodan Gnjato, and Goran Trbić

*University of Banja Luka,
Faculty of Natural Sciences and Mathematics,
Department of Geography,
Mladena Stojanovića 2, 78000 Banja Luka,
Republic of Srpska, Bosnia and Herzegovina;*

Corresponding author E-mail: tatjana.popov@pmf.unibl.org

(Manuscript received in final form December 15, 2017)

Abstract—Changes in extreme precipitation indices over the Peripannonian region of Bosnia and Herzegovina were examined. Data on daily precipitation during the period 1961–2016 from four meteorological stations were used for the calculation of 13 indices recommended by the Expert Team on Climate Change Detection and Indices (ETCCDI) for the climate change assessment. The precipitation change assessment covered trend analysis and analysis of changes in distribution. Determined patterns of change were neither spatially nor temporally coherent. The estimated trends in extreme precipitation indices were mixed in sign and mostly insignificant. Moreover, no significant changes in distribution of majority indices were determined. However, the upward trends in heavy precipitation indices RX1day, RX5day, R95p, and R99p indicate changes towards more intense precipitation. Understanding patterns of precipitation changes is of a great pertinence in many applied studies: flood risks management, agricultural planning, water resources management, environment conservation, etc.

Key-words: extreme precipitation indices, trend, probability density functions, generalized extreme value distribution, climate change, Peripannonian region (Bosnia and Herzegovina)

1. Introduction

Understanding changes in extreme precipitation events is of great importance in many applied studies due to their disproportionately strong impact on society and ecosystems compared to changes in mean precipitation (*Hartmann et al.*,

2013). Although studies around the world determined mixed-in-sign and mostly insignificant trends in mean precipitation (*Hartmann et al.*, 2013), the precipitation averaged over the Northern Hemisphere mid-latitudes has increased since the middle of the 20th century (*IPCC*, 2014).

Global scale studies indicate that changes in precipitation extremes are in general consistent with a wetter climate (*Alexander et al.*, 2006; *Donat et al.*, 2013). Further, there are more regions in the world where heavy precipitation events increased than those where they decreased (*IPCC*, 2014). The substantial increase in annual heavy precipitation events was also found over many mid-latitude regions (*Hartmann et al.*, 2013). Despite the general increase, trends observed around the world were less spatially coherent, a small scale and with a low level of statistical significance (*Alexander et al.*, 2006; *Kiktev et al.*, 2003).

Most of extreme precipitation indices displayed changes towards more intense precipitation over numerous world regions (*Donat et al.*, 2013). On a global scale, annual maximum daily precipitation (RX1day) increased by 5.73 mm on average during the last 110 years (*Asadieh and Krakauer*, 2015). The highest 5-day precipitation (RX5day) showed a general increase (although insignificant) over many world regions (*Alexander et al.*, 2006; *Kiktev et al.*, 2003). Globally averaged, the annual number of days with precipitation, i.e., wet days (R1mm), significantly increased ($p < 0.05$) (*Kiktev et al.*, 2003), whereas the annual number of very wet days (R10mm) displayed insignificant upward trends during the past 60 years (*Alexander et al.*, 2006; *Donat et al.*, 2013). In that period, the contribution from very wet days (R95p) also displayed an upward tendency (*Donat et al.*, 2013). Wetter conditions also suggest a steady decline in the number of consecutive dry days (CDD) since the 1960s (*Alexander et al.*, 2006; *Frich et al.*, 2002). *Alexander et al.* (2006) determined changes in the distributions of all these indices in the last quarter of the 20th century compared to the period 1901–1950. The observed changes in distributions were also consistent with tendency towards wetter conditions. Findings of these global scale studies (trends mixed in sign, mostly insignificant, and spatially incoherent) were confirmed by numerous regional and local studies all over the world – in America (*Powell and Keim*, 2015; *Skansi et al.*, 2013), Asia (*Tian et al.*, 2017; *Sheikh, et al.*, 2015; *Balling et al.*, 2016), Africa (*Ongoma et al.*, 2016; *Filahi et al.*, 2016), Australia (*Alexander and Arblaster*, 2017). Similar results were also obtained for Europe – at the continental level (*Chen et al.*, 2015; *Klein Tank and Können*, 2003) and in its various regions – over the Iberian Peninsula (*de Lima et al.*, 2015; *Bartolomeu et al.*, 2016), Central and Western Europe (*Lupikasza et al.*, 2011; *Moberg and Jones*, 2005), Carpathian Basin (*Bartholy and Pongrácz*, 2007), and Balkan Peninsula (*Kioutsioukis et al.*, 2010). Studies detected the increase in frequency or intensity of heavy precipitation over the continent (*Hartmann et al.*, 2013). Continentally averaged, most of extreme precipitation indices (R95p, R95ptot, RX5day, R10mm, and R20mm) have increased significantly (only RX1day

displayed insignificant trend) since the middle of the 20th century (*Klein-Tank* and *Können*, 2003). However, the observed trends were not spatially coherent (*Klein-Tank* and *Können*, 2003). Significant upward tendency in RX5day and simple daily intensity index (SDII) was determined over much of Europe (*Donat et al.*, 2013; *Frich et al.*, 2002; *Kiktev et al.*, 2003; *Alexander et al.*, 2006). Coherent patterns of positive change in R10mm were also determined (*Frich et al.*, 2002). The central part of Europe was one of the world regions with major increases in the fraction of precipitation from events wetter than the 95th percentile (R95p%) (*Frich et al.*, 2002). Shorter duration of dry spells was detected in many regions (*Kiktev et al.*, 2003; *Donat et al.*, 2013). *Casanueva et al.* (2014) found that trends in precipitation extremes were more significant than those in mean precipitation (especially for R95p). They stated that this is in agreement with the Clausius–Clapeyron relation that describes how a warmer atmosphere can hold more water vapor, which produces in turn more intense precipitation (*Casanueva et al.*, 2014).

Unlike the consistent warming trend regionally reported for extreme temperature indices (*Lakatos et al.*, 2016; *Bartholy* and *Pongrácz*, 2007; *Gavrilov et al.*, 2016; *Branković et al.*, 2013), studies on extreme precipitation indices over the Pannonian Basin determined spatially incoherent, mainly weak and mixed-in-sign trends (*Bartholy* and *Pongrácz*, 2007; *Lakatos et al.*, 2011; *Dumitrescu et al.*, 2015; *Unkašević* and *Tošić*, 2011; *Gajić-Čapka et al.*, 2015). However, they generally suggest that precipitation intensity had regionally increased. Research on changes in extreme precipitation indices over the Bosnia and Herzegovina part of the region has been scarce so far (e.g., *Popov et al.*, 2017), and this kind of study has not been previously performed for this area. Previous national scale studies primarily focused on precipitation spatial distribution (*Mihailović et al.*, 2015) and changes in drought occurrence patterns (*Ducić et al.*, 2014). The knowledge about extreme precipitation is very important for impact assessment studies as well as for development and implementation of efficient adaptation and mitigation strategies. Given the existing gap in the knowledge, this study aims to analyze changes in precipitation extremes during the period 1961–2016 using 11 indices recommended by the joint CCI/CLIVAR/JCOMM Expert Team on Climate Change Detection and Indices (ETCCDI) for the climate change assessment. The main goal was to determine trends in extreme precipitation indices and changes in their distributions.

2. Study area

The Peripannonic region of Bosnia and Herzegovina represents the southern rim of the Pannonian Basin. It is located in the northern part of Bosnia and Herzegovina's territory at latitudes $43^{\circ}57'22''$ – $45^{\circ}16'35''\text{N}$ and longitudes

$15^{\circ}43'49''$ – $19^{\circ}37'25''$ E (Fig. 1). It covers 37% of the country total area (18951.4 km^2). The study area encompasses the lowland of the Sava River basin (and basins of its tributaries Una, Vrbas, Bosna, and Drina) up to 200 m and the southern rim of the Pannonian Basin with hills, low ore and flysch mountains, and horst mountains from 200 to 800 m (in some locations up to 1000 m). Towards the south, it gradually enters the Dinaric Alps range covering the central part of Bosnia and Herzegovina. Western parts of the region are slightly cooler than the eastern. Average annual temperature increases from $10.2\text{ }^{\circ}\text{C}$ in the west to an $11.3\text{ }^{\circ}\text{C}$ in the east (Trbić, 2010). In the lowland area along the Sava River, annual precipitation decreases from $\sim 900\text{ mm}$ in the west to $\sim 700\text{ mm}$ in the east. From this lowland area, the precipitation increases to 1000 – 1200 mm towards the mountainous rim areas in the south (Trbić, 2010). The primary precipitation maximum occurs in June, whereas minimum is recorded in October.

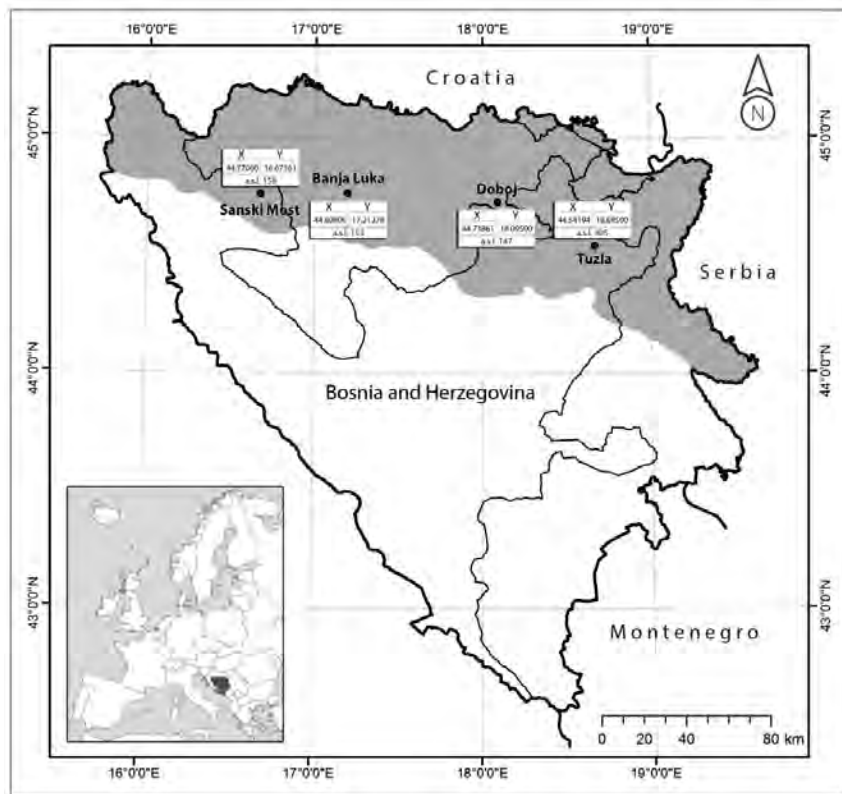


Fig. 1. Geographical location of the study area with the coordinates of the meteorological stations used in the study.

3. Data and methods

Analysis of extreme precipitation during the period of 1961–2016 was performed based on climatological datasets of daily precipitation from four meteorological stations located in different parts of the Peripannonian region: Sanski Most (SM), Banja Luka (BL), Doboj (DB), and Tuzla (TZ) (*Fig. 1*). Data were provided by the *Federal Hydrometeorological Institute* and the *Hydrometeorological Service of the Republic of Srpska*. In the observed period, there were short interruptions in measurements during the war period (at Sanski Most station in November and December 1992 and November 1996; at Tuzla station from July 1992 to July 1993; at Doboj station during the entire war period of 1992–1996). However, RCLimDex software can run if there are some missing values (Zhang and Yang, 2004). Data quality control was performed in RCLimDex. A few outliers (defined as values outside a range of 4 standard deviations of the climatological mean value for the day) were found and checked. The basic statistical parameters of the input precipitation series used in the study are given in *Table 1*.

Table 1. Statistical parameters of annual precipitation time series used in the study

Variable	SM	BL	DB	TZ	REGION
Mean (mm)	1041.9	1040.4	929.3	905.7	979.3
Standard deviation (mm)	159.7	184.9	192.1	166.1	161.7
Coefficient of variation (%)	15.3	17.8	20.7	18.3	16.5
Maximum (mm)	1543.3	1686.2	1494.5	1353.1	1519.3
Minimum (mm)	605.8	588.2	504.1	566.1	566.1
Skewness	0.230	0.474	0.706	0.503	0.471
Kurtosis	1.562	1.945	0.980	1.052	2.036

Mean annual and seasonal precipitation amounts during the observed period (1961–2016) are given in *Table 2*. For comparison, their average values in the period 1961–1990 are also showed. The regionally averaged, mean annual precipitation is 979 mm. In general, the precipitation decreases from the western (~1040 mm) to the eastern (~905 mm) parts of the region. Although precipitation is relatively distributed evenly throughout the year, the maximum occurs in the summer season (~280 mm).

Table 2. Annual and seasonal mean precipitation amounts in 1961–2016 (a) and 1961–1990 (b) (mm)

Index	SM		BL		DB		TZ		REGION	
	a	b	a	b	a	b	a	b	a	b
Winter	226	214	227	220	198	188	184	186	209	202
Spring	264	262	266	264	232	221	228	229	248	244
Summer	272	293	284	299	274	263	284	289	279	286
Autumn	281	254	266	246	228	200	212	192	247	223
Year	1042	1023	1040	1029	929	870	906	894	979	954

Unlike the consistent warming trend recorded for temperature (*Trbić et al.*, 2017), precipitation does not show spatially and temporally coherent trends. The annual and seasonal precipitation amounts displayed trends of both signs, but all insignificant (Table 3). The strongest positive trend in annual precipitation was registered in Doboj (19.85 mm per decade), whereas the most prominent negative trend was detected in Banja Luka (-7.79 mm per decade). The seasonal trend analysis showed that negative trends were registered in summer over the entire region (most pronounced in Sanski Most and Banja Luka -14.0 mm per decade), whereas in other parts of the year the upward tendency was registered, except in winter in Tuzla (-4.59 mm per decade). In autumn and spring, the most pronounced trends were found at Sanski Most (11.12 mm per decade) and Doboj (8.44 mm per decade), respectively.

Table 3. Decadal trends in mean annual and seasonal precipitation amounts in 1961–2016

Station	Winter		Spring		Summer		Autumn		Year	
	slope	p-value	slope	p-value	slope	p-value	slope	p-value	slope	p-value
SM	4.93	0.338	2.09	0.740	-14.05	0.094	11.12	0.140	4.35	0.719
BL	1.36	0.839	0.48	0.927	-14.00	0.177	7.00	0.312	-7.79	0.656
DB	0.44	0.919	8.44	0.193	-3.72	0.651	8.47	0.155	19.85	0.238
TZ	-4.59	0.433	2.06	0.827	-3.38	0.636	9.29	0.118	-0.57	0.961
REGION	0.79	0.873	2.66	0.596	-8.87	0.326	8.46	0.103	3.24	0.687

The selected precipitation indices (*Table 4*) can be divided into 4 different categories (*Alexander et al., 2006*):

1. Absolute extreme indices representing the maximum precipitation values (RX1day, Rx5day, and SDII).
2. Absolute-based (fixed) threshold indices defined as the number of days on which a precipitation value falls above fixed thresholds (R1mm, R10mm, and R20mm).
3. Percentile-based (non-fixed) threshold indices defined as the precipitation amounts exceeding fixed percentile thresholds (in this study 95th and 99th were chosen for the analysis, with the period 1961–1990 as a base period for determining its frequency distribution) (R95p and R99p).
4. Duration-based indices (i.e., spell indices) defined as periods of excessive wet or dry periods (CDD and CWD).

Table 4. Definitions of precipitation indices used in the study (ETCCDI, 2009)

Index	Descriptive name	Definition	Units
PRCPTOT	Annual total wet-day precipitation	Annual total precipitation in wet days (days with precipitation $\geq 1\text{mm}$)	mm
RX1day	Highest 1-day precipitation amount	Monthly maximum 1-day precipitation	mm
RX5day	Highest 5-day precipitation amount	Monthly maximum consecutive 5-day precipitation	mm
SDII	Simple precipitation intensity index	Annual total precipitation divided by the number of wet days in the year	mm/day
R1mm	Number of wet days	Annual count of days when precipitation $\geq 1\text{mm}$	days
R10mm	Number of heavy precipitation days	Annual count of days when precipitation $\geq 10\text{mm}$	days
R20mm	Number of very heavy precipitation days	Annual count of days when precipitation $\geq 20\text{mm}$	days
R95p	Very wet days	Annual total precipitation when precipitation $>95\text{th}$ percentile	mm
R99p	Extremely wet days	Annual total precipitation when precipitation $>99\text{th}$ percentile	mm
CDD	Consecutive dry days	Maximum number of consecutive days with precipitation $<1\text{mm}$	days
CWD	Consecutive wet days	Maximum number of consecutive days with precipitation $\geq 1\text{mm}$	days

An overview of the average annual values of extreme precipitation indices during the periods of 1961–2016 and 1961–1990 is given in *Table 5*.

Table 5. Average annual values of extreme precipitation indices in 1961–2016 (a) and 1961–1990 (b)

Index	SM		BL		DB		TZ		REGION	
	a	b	a	b	a	b	a	b	a	b
PRCTOT	1025.9	1007.5	1022.8	1012.2	904.1	853.5	892.8	876.0	958.6	932.6
RX1day	51.8	54.0	55.4	54.4	48.8	44.9	48.9	46.1	42.2	40.0
RX5day	92.6	94.3	96.9	95.1	85.1	74.6	84.8	77.5	81.2	73.9
SDII	9.1	8.9	9.2	9.0	8.2	7.8	8.0	7.9	7.3	7.1
R1mm	113.1	114.2	111.2	113.0	109.6	109.9	111.3	111.8	130.3	132.2
R10mm	35.8	34.8	35.5	35.2	30.5	28.8	29.5	29.3	31.8	30.8
R20mm	12.9	12.8	13.3	12.6	9.9	8.9	9.6	9.0	8.6	7.5
R95p	231.2	218.9	232.9	212.1	220.1	176.1	210.2	190.7	224.2	185.2
R99p	69.8	64.5	74.4	65.5	82.1	50.4	71.1	54.5	70.9	54.0
CDD	21.9	21.5	22.9	21.4	23.7	24.0	22.8	22.4	20.7	20.7
CWD	7.0	6.8	6.8	6.4	6.4	6.0	6.3	6.4	7.6	7.4

The extreme precipitation indices were calculated using the RCLimDex (1.0) software package developed at the Climate Research Branch of Meteorological Service of Canada (*Zhang and Yang*, 2004). Trend slope estimate and its statistical significance were also computed in RCLimDex by linear least square method and locally weighted linear regression (dashed line on plots) (*Zhang and Yang*, 2004). Calculations were made by stations individually and then averaged for the whole Peripannonic region of Bosnia and Herzegovina.

In order to further examine the changes in the extreme precipitation, probability density functions (pdfs) for each index (regionally averaged) were calculated for two sub-periods: 1961–1990 and 1991–2016. Two-tailed nonparametric Kolmogorov–Smirnov test was performed by the XLSTAT Version 2014.5.03 software to test whether distribution of the indices changed significantly between the two specified periods. Moreover, the maximum likelihood estimation (MLE) method was used for estimating changes in generalized extreme value (GEV) distribution functions parameters (location, shape, and scale) of the annual maximum precipitation. R package extRemes created at the National Center for Atmospheric Research of the USA was used for performing this extreme value analysis (*Gilleland and Katz*, 2016).

4. Results

Decadal trends in the annual extreme precipitation indices in the period 1961–2016 are shown by stations in *Table 6*. *Fig. 2* displays annual trends averaged for the whole region. The obtained results suggest a general increase in the precipitation intensity. Moreover, growing maximum duration of both dry and wet periods indicates increased precipitation variability. However, compared to the observed trends in mean and extreme temperatures (*Trbić et al.*, 2017; *Popov et al.*, 2018), less spatially coherent patterns of change were registered.

Table 6. Decadal trends in extreme precipitation indices in 1961–2016

Index	SM		BL		DB		TZ	
	slope	p-value	slope	p-value	slope	p-value	slope	p-value
PRCTOT	7.07	0.601	-1.61	0.916	20.84	0.202	7.83	0.580
RX1day	-1.55	0.310	-0.04	0.984	2.28	0.112	1.38	0.286
RX5day	0.26	0.914	-0.14	0.962	6.84	0.010	4.73	0.095
SDII	0.16	0.049	0.06	0.513	0.21	0.029	0.09	0.343
R1mm	-1.51	0.196	-1.23	0.288	-0.82	0.472	-0.70	0.501
R10mm	0.57	0.293	0.08	0.898	0.56	0.366	0.06	0.908
R20mm	-0.07	0.836	0.15	0.658	0.40	0.264	0.25	0.436
R95p	7.34	0.395	6.77	0.494	21.06	0.056	10.29	0.306
R99p	1.01	0.857	1.05	0.865	18.88	0.012	9.97	0.136
CDD	0.52	0.314	1.31	0.022	0.02	0.974	0.58	0.302
CWD	0.15	0.242	0.26	0.132	0.23	0.088	-0.07	0.634

Most of the estimated trend values were not statistically significant. PRCPTOT (annual total of precipitation on wet days) displayed predominantly positive trends in the range of 7.07–20.84 mm per decade, except in Banja Luka, where a weak downward tendency was registered (-1.61mm per decade).

The peak annual daily precipitation showed very weak trends that were mixed in sign. Maximum 1-day precipitation (RX1day) had been increasing in the eastern parts of the region (1.38–2.28 mm per decade), whereas a slight decrease was registered in the west (e.g., -0.04mm per decade in Banja Luka). The increasing tendency was somewhat stronger for the RX5day – e.g., statistically significant trend in the range of 6.84 mm per decade was determined for Doboj area. Although simple precipitation intensity index (SDII) showed upward trends over the entire region, the estimated trend values were significant only at Doboj and Sanski Most stations (0.16 mm/day per decade and 0.21 mm/day per decade, respectively).

Absolute-based (fixed) threshold indices displayed very weak and insignificant trends. The negative trends in the annual number of wet days

(R1mm) (ranging from -0.70 to -1.51 days per decade) and the upward trends in the annual number of heavy precipitation days (R10mm) and very heavy precipitation days (R20mm) (in the range of 0.06 – 0.57 and 0.15 – 0.40 days per decade, respectively) suggest changes towards more intense precipitation (although mainly insignificant).

Decadal trends in the annual percentile-based indices were also consistent with stated. The contribution from the very wet days (R95p) and extremely wet days (R99p) to the annual precipitation total increased over the entire region, although trends were mostly insignificant. Statistically significant positive trends in the annual R95p and R99p were registered only in Doboј – in the range of 21.06 mm per decade and 18.88 mm per decade, respectively. All trends indicating increase in either the frequency or intensity of heavy precipitation were generally most prominent precisely in Doboј area. Exceptionally high precipitation, which caused catastrophic flooding over this area, had been recorded several times since the beginning of the 21st century. The most disastrous floods occurred in May and August 2014, when in just a few days, 17% and 14% of average annual precipitation in the period 1961–1990 was registered. Before that, similar weather conditions had been registered in June 2010, when in only two days, 20% of the total annual precipitation was recorded.

Both duration-based indices, CDD and CWD, displayed positive trends over the region (but predominantly insignificant). A very weak negative trend was determined only for CWD in Tuzla. The maximum number of consecutive dry days (CDD) showed particularly prominent positive trend in Banja Luka (1.31 days per decade). The upward trend in the maximum duration of consecutive wet days (CWD) during the observed period was the most significant ($p < 0.1\%$) in Doboј, 0.23 days per decade.

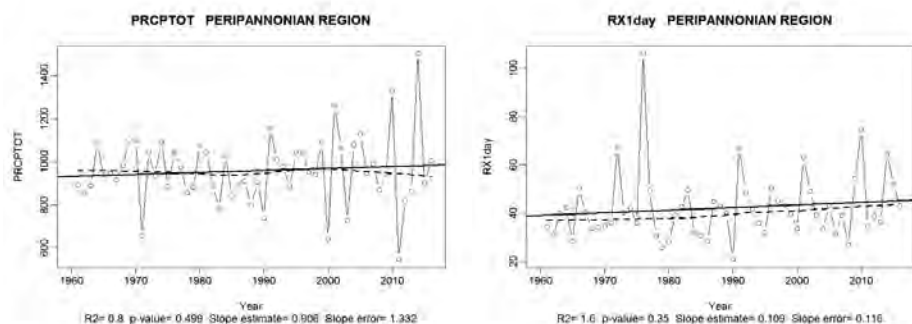


Fig. 2. Linear trends in extreme precipitation indices in 1961–2016. (Continued on the following page.)

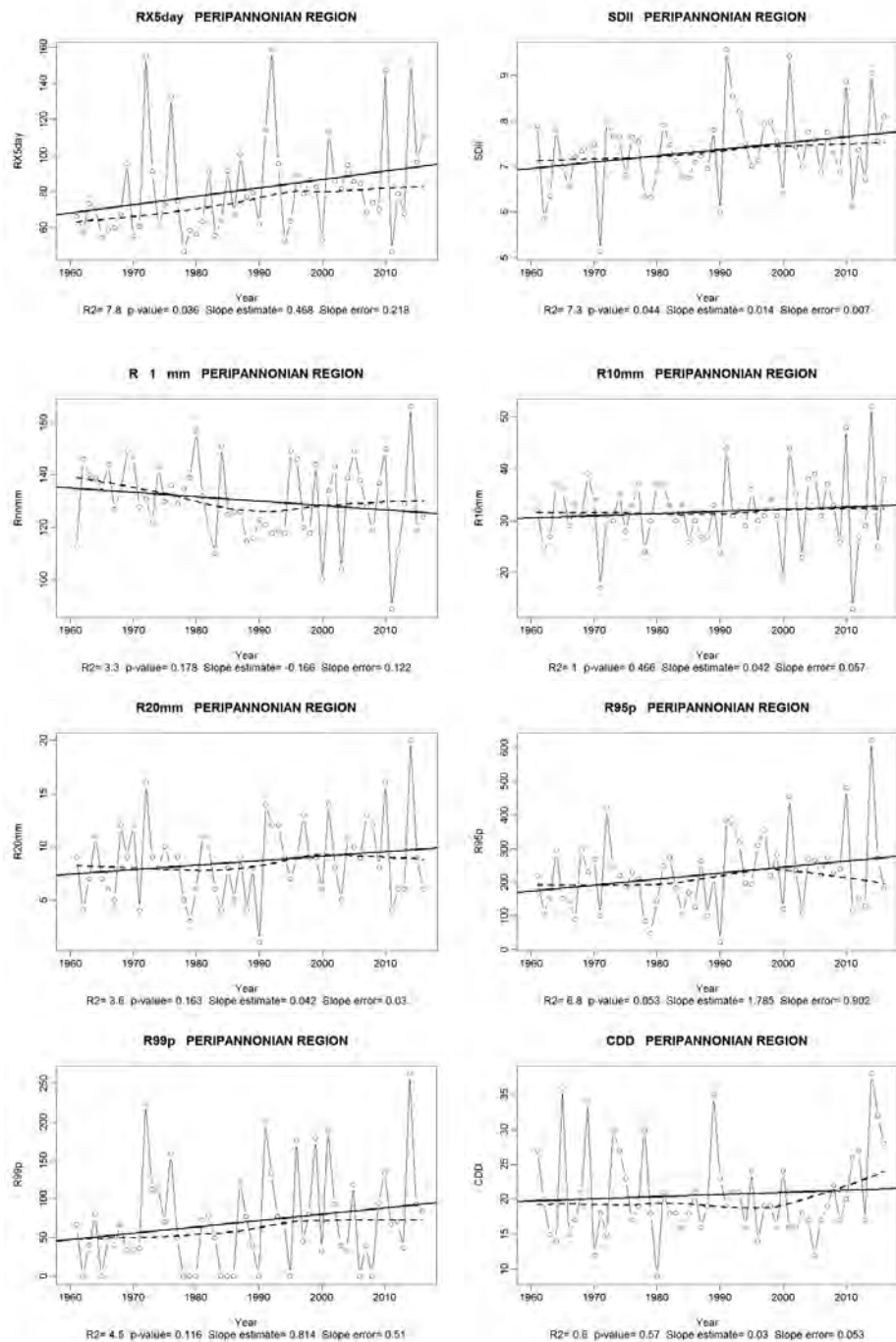


Fig. 2. (Continued on the following page.)

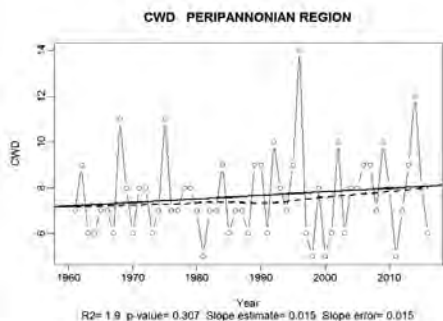


Fig. 2. (Continued from the previous page.)

The analysis of deviations of annual extreme precipitation indices from the thirty-year period (1961–1990) averages (*Fig. 3*) showed that the increase in heavy precipitation (e.g. in R95p and R99p) has become more pronounced since the beginning of the 21st century. In that period, maximum 1-day and 5-day precipitations were also dominantly above the 1961–1990 period averages. A noticeable increase in the inter-annual precipitation variability was also observed in this period – a year with precipitation far above the average was often followed by a year with extremely low precipitation or vice versa (e.g., 2000–2001 and 2010–2011). In 2001, annual values of PRCTOT, R10mm, R20mm, RX1day, and RX5day were 2.0–2.3 times higher than in 2000, whereas the contribution of R95p and R99p was 4-fold and 6-fold, respectively. In the very dry year 2011, the number of wet days with precipitation were 41% less, while the precipitation amount was 59% less than in the very wet 2010.

Changes in the probability distribution functions (pdfs) of the annual extreme precipitation indices in the period 1991–2016 compared to the reference period 1961–1990 are displayed in *Fig. 4*.

In terms of the probability distributions, the results also very clearly show that heavy precipitation indices SDII, RX1day, RX5day, R20mm, R95p, and R99p shifted to the right, to higher index values (i.e., to increased heavy precipitation events). However, the Kolmogorov–Smirnov test results showed that distributional changes between the two specified periods were mostly insignificant. However, significant distributional shifts were determined for heavy precipitation indices RX5day, R95p, and R99p. For the majority of indices, changes were particularly pronounced in the upper tail of distribution. This was especially the case with the maximum duration of consecutive days with precipitation (CWD) and heavy precipitation indices SDII, R10mm, R20mm, R95p, and R99p.

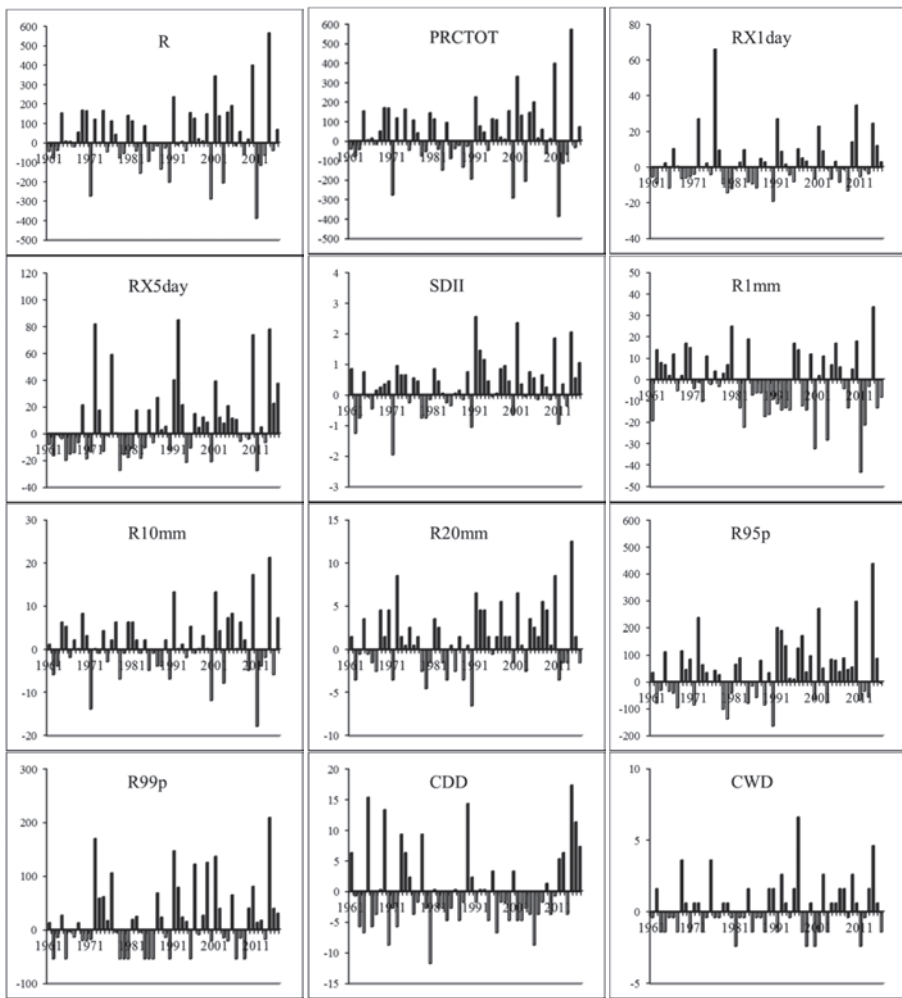


Fig. 3. Annual deviations of mean precipitation and extreme precipitation indices from the averages of the period 1961–1990.

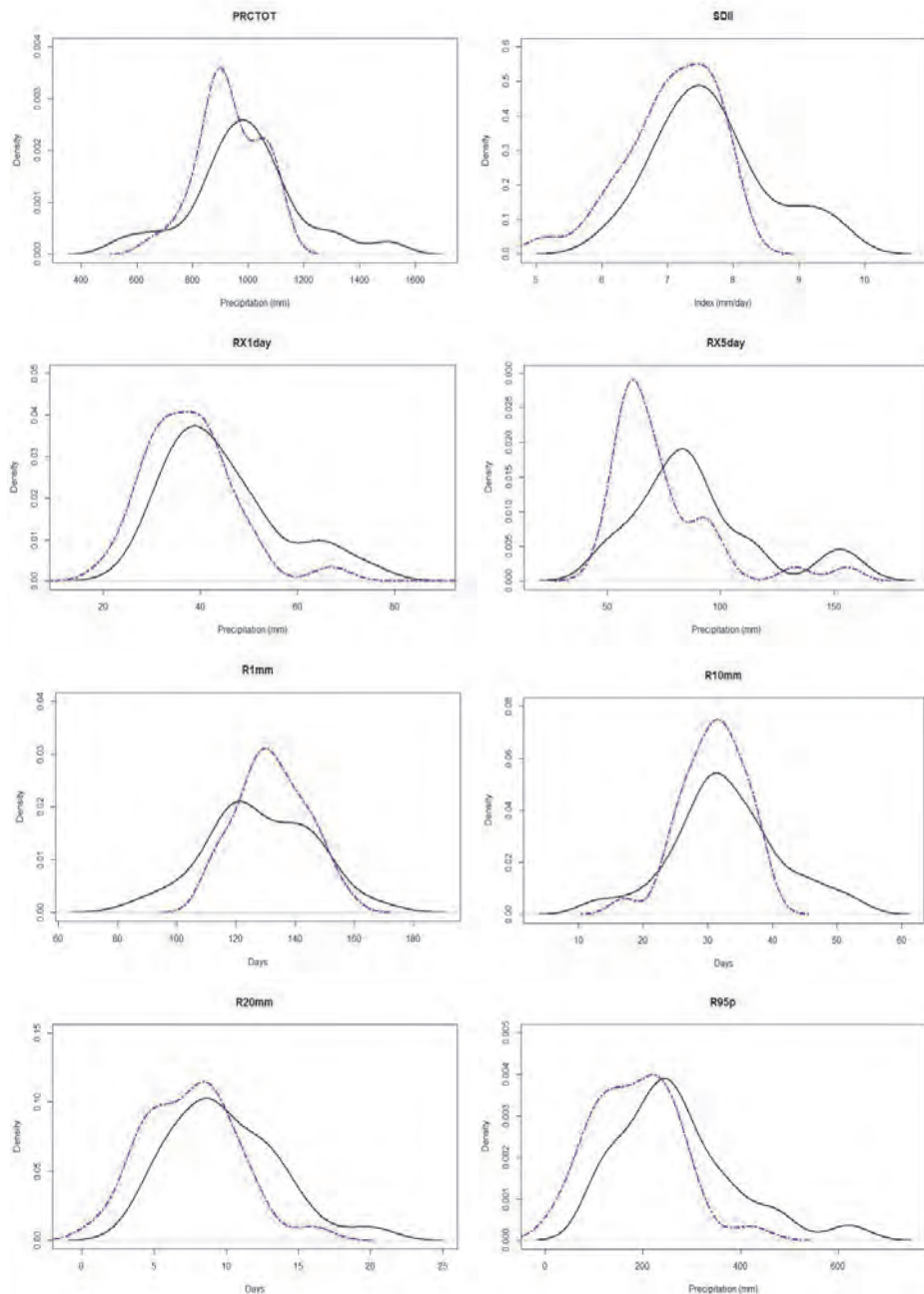


Fig. 4. Probability distribution functions of extreme precipitation indices for the two sub-periods: 1961–1990 (dashed line) and 1991–2016 (solid line).

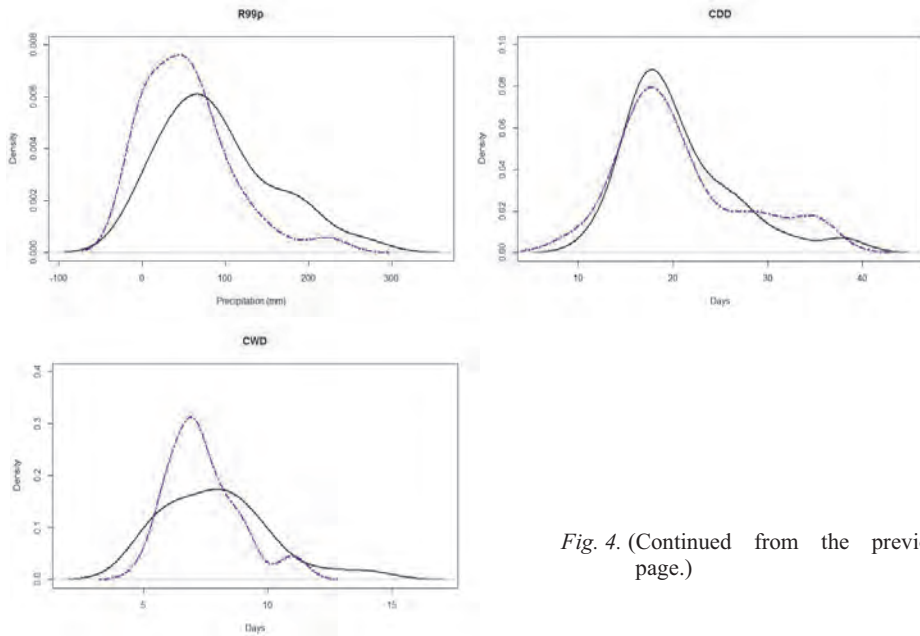


Fig. 4. (Continued from the previous page.)

In addition, the analysis of the GEV distribution parameters of annual maximum precipitations showed that the location parameter value increased in the period 1991–2016 (*Table 7*), which also indicates an increase in the precipitation intensity. Higher value of the distribution scale parameter suggests that the precipitation variability also increased in the latter period. This is consistent with the changes in the probability distributions of annual total of precipitation in wet days – the lower tail of PRCTOT distribution shifted towards drier conditions, whereas the upper tail of distribution shifted towards wetter conditions. Estimated 2-year and 20-year return levels also increased compared to the reference period. Results of the study carried out over Europe for the period 1951–2010 also determined that, despite a considerable decadal variability, 5-, 10-, and 20-year events of the 1-day (but also 5-day) precipitation for the first 20-year period generally became more common during this 60-year period (*Van den Besselaar et al.*, 2013). For all analyzed regions, seasons, and return periods, the median reduction in the return period between the first and last 20-year periods was about 21% (a decrease ranged from ~2% to ~58%) (*Van den Besselaar et al.*, 2013).

Table 7. Estimated GEV distribution functions parameters and return levels fitted to the annual maximum precipitation

Parameter	1961–1990	1991–2016
Location	33.74	38.92
Scale	8.446	8.637
Shape	0.137	0.075
Estimated return levels		
2-year	36.91	42.13
20-year	64.68	67.66
100-year	87.82	86.38

5. Discussion

Although observed trends were spatially incoherent and mainly statistically insignificant, the results indicate a general increase in the extreme precipitation (in its intensity, frequency, or duration). Similar patterns of change with trends spatially and temporally mixed-in-sign and mostly insignificant, had been determined in other studies carried out in the Pannonian and Peripannonic regions. A regional scale study determined that the intensity and frequency of extreme precipitation increased between 1976 and 2001 (*Bartholy and Pongrácz*, 2007). The significant mean tendency during the period 1946–2001 displayed CDD, RX5day, and R1mm (*Bartholy and Pongrácz*, 2007). It should be noted that the strongest upward trends were detected for extreme indices indicating very intense or large precipitation (i.e., R95p, R20mm, and R95) (*Bartholy and Pongrácz*, 2007). Local scale studies found spatially incoherent and mainly insignificant patterns of change. Increase in the proportion of heavy precipitation events in total precipitation was registered over most areas in Hungary (*Lakatos et al.*, 2011). Over this area, the number of wet days decreased annually, whereas mixed-in-sign trends were detected for RX1day (in the range from -15mm to +10mm) (*Lakatos et al.*, 2011). SDII increased in the summer season (*Lakatos et al.*, 2011). The annual precipitation extremes showed mixed signals and no significant trends at majority of stations in Romania for all indices examined in the study of *Dumitrescu et. al.* (2015). Increase in the R10mm and R20mm was found in the Pannonian region of Romania (*Dumitrescu et. al.*, 2015). Over this area, about one third of the stations registered significant SDII trends (20% increasing and 12% decreasing) (*Dumitrescu et. al.*, 2015). Heavy precipitation indices R95p and R20mm displayed upward trends over almost the entire territory of Serbia, including northern Pannonian part of the country (*Unkašević and Tošić*, 2011). During the 20th century, the average annual precipitation on the wettest day over Serbia increased by nearly 9% (*Unkašević*

and *Tošić*, 2011). Over the mainland of Croatia, the R95p showed mostly positive trends, whereas trends in RX1day and RX5day were mixed in sign, but weak in magnitude (*Gajić-Čapka et al.*, 2015). The seasonal SDII trend analysis revealed mixed-in-sign and mainly insignificant trends, except in summer, when negative trends were detected (*Gajić-Čapka et al.*, 2015). Although changes in precipitation sums showed no significant tendencies over the southern Poland in the part of period 1971–2010, an increase in R1mm and a decrease in R20mm were observed (*Skowera et al.*, 2016).

The expected changes in the annual precipitation indices by the end of the 21st century (2071–2100) will be small, but generally consistent with the detected trends in the last quarter of the 20th century (*Pongrácz et al.*, 2009). Strong positive and negative changes in the monthly precipitation indices are projected to occur in winter and summer, respectively – the increase in the extreme precipitation events will exceed 50% in January, whereas drought is projected to become more intense in July (*Pongrácz et al.*, 2009). The frequency of extreme precipitation will generally increase over the entire region, except in summer, when decreasing trend is very likely to occur (e.g., R10mm and R20mm are projected to decrease in July and August relative to the 1961–1990 reference period) (*Bartholy et al.*, 2015). The projected increase in the heavy precipitation indices R95p and R99p fractions will be generally higher in winter and autumn, whereas the smallest increases are projected to occur in the summer and spring seasons (*Bartholy et al.*, 2015). Results of *Pongrácz et al.* (2014) clearly imply that future summers will be considerably drier. In this part of the year, drought-related climate indices are projected to significantly increase over the region by the end of the 21st century. In accordance with the indicated increase in dryness, R1mm is projected to decrease and CDD to increase in this season (*Pongrácz et al.*, 2014).

6. Conclusion

Recent trends in the 11 extreme daily precipitation indices over the Peripannonic region of Bosnia and Herzegovina were calculated for the period 1961–2016 using the RClimDex (1.0) software. The examined indices displayed mainly weak, insignificant, and mixed-in-sign trends. The analysis of probability density functions also confirmed that for the majority of indices there were not significant changes in extreme precipitation indices in the period 1991–2016 compared to the period 1961–1990. However, the obtained results suggest a general increase in heavy precipitation over the study area. The upward trends in heavy precipitation events such as RX1day, RX5day, SDII, R10mm, R20mm, R95p, and R99p indicate changes towards more intense precipitation. The increase in intense precipitation has become more pronounced since the beginning of the 21st century. In addition, a noticeable increase in inter-annual precipitation variability was observed in this period.

This kind of study should contribute to overcoming the existing gap in knowledge about recent changes in extreme precipitation over this part of the Pannonian Basin. The obtained results are in accordance with the results of similar studies in other parts of the region. Moreover, the results confirm the findings of the previous studies, that changes in precipitation were not coherent at a regional scale – as opposed to the coherent and significant temperature trends (i.e., warming trend) (Lakatos *et al.*, 2016; Bartholy and Pongrácz, 2007).

The future research should be focused on several major issues regarding the results: 1) projections of future changes in extreme precipitation indices and 2) impact assessment studies, given that the observed changes in extreme precipitation events (but also the changes anticipated by the end of the 21st century) could have strong influence on socio-economic and natural systems. Understanding the patterns of extreme precipitation change will be of a great pertinence in many applied studies – in flood risks management, agricultural planning, water resources management, environment conservation, etc. The third major issue is the development and implementation of efficient adaptation and mitigation strategies in various sectors. As such, there is a growing need for a more detailed knowledge on extreme precipitation patterns of change.

References

- Alexander, L.V. and Arblaster, J.M., 2017: Historical and projected trends in temperature and precipitation extremes in Australia in observations and CMIP5. *Weather Climate Extr.* 15, 34–56. <https://doi.org/10.1016/j.wace.2017.02.001>
- Alexander, L.V., Zhang, X., Peterson, T.C., Caesar, J., Gleason, B., Klein Tank, A.M.G., Haylock, M., Collins, D., Trewin, B., Rahimzadeh, F., Tagipour, A., Rupa Kumar, K., Revadekar, J., Griffiths, G., Vincent, L., Stephenson, D.B., Burn, J., Aguilar, E., Brunet, M., Taylor, M., New, M., Zhai, P., Rusticucci, M. and Vazquez-Aguirre, J.L., 2006: Global Observed Changes in Daily Climate Extremes of Temperature and Precipitation. *J. Geophys. Res.* 111, D05109. <https://doi.org/10.1029/2005JD006290>
- Asadieh, B. and Krakauer, N.Y., 2015: Global trends in extreme precipitation: climate models versus observations. *Hydrol. Earth Syst. Sci.* 19, 877–891. <https://doi.org/10.5194/hess-19-877-2015>
- Balling Jr., R.C., Kiany, M.S.K., Sen Roy, S. and Khoshhal, J., 2016: Trends in extreme precipitation indices in Iran: 1951–2007. *Adv. Meteorol.* 2016, Article ID 2456809.
- Bartholy, J. and Pongrácz, R., 2007: Regional analysis of extreme temperature and precipitation indices for the Carpathian Basin from 1946 to 2001. *Glob. Planet. Change* 57, 83–95. <https://doi.org/10.1016/j.gloplacha.2006.11.002>
- Bartholy, J., Pongrácz, R. and Kis, A., 2015: Projected changes of extreme precipitation using multi-model approach. *Időjárás* 119, 129–142.
- Bartolomeu, S., Carvalho, M.J., Marta-Almeida, M., Melo-Gonçalves, P. and Rocha, A., 2016: Recent trends of extreme precipitation indices in the Iberian Peninsula using observations and WRF model results. *Physics and Chem. Earth, Parts A/B/C* 94, 10–21. <https://doi.org/10.1016/j.pce.2016.06.005>
- Branković, Č., Cindrić, K., Gajić-Čapka, M., Güttler, I., Pandžić, K., Patarčić, M., Srnec, L., Tomašević, I., Vučetić, V. and Zaninović, K., 2013: Sixth National Communication of the Republic of Croatia under the United Nation Framework Convention on the Climate Change (UNFCCC) Selected Sections in Chapters: 7. Climate Change Impacts and Adaptation Measures 8. Research, Systematic Observation and Monitoring. Meteorological and hydrological service of Croatia, Zagreb.

- Casanueva, A., Rodríguez-Puebla, C., Frías, M.D. and González-Reviriego, N., 2014: Variability of extreme precipitation over Europe and its relationships with teleconnection patterns. *Hydrol. Earth Syst. Sci.* 18, 709–725. <https://doi.org/10.5194/hess-18-709-2014>
- Chen, D., Walther, A., Moberg, A., Jones, P., Jacobbeit, J. and Lister, D., 2015: European trend atlas of extreme temperature and precipitation records. Springer, Dordrecht.
- Donat, M.G., Alexander, L.V., Yang, H., Durre, I., Vose, R., Dunn, R.J.H., Willett, K.M., Aguilar, E., Brunet, M., Caesar, J., Hewitson, B., Jack, C., Klein Tank, A.M.G., Kruger, A.C., Marengo, J., Peterson, T.C., Renom, M., Oria Rojas, C., Rusticucci, M., Salinger, J., Elrayah, A.S., Sekele, S.S., Srivastava, A.K., Trewin, B., Villarroel, C., Vincent, L.A., Zhai, P., Zhang, X. and Kitching, S., 2013: Updated analyses of temperature and precipitation extreme indices since the beginning of the twentieth century: the Hadex2 dataset. *Journal of Geophysical Research: Atmospheres* 118, 1–16.
- Ducić, V., Burić, D., Trbić, G. and Cupać, R., 2014: Analysis of precipitation and droughts on BIH territory based upon Standardized Precipitation Index (SPI). *Herald* 18, 53–70.
- Dumitrescu, A., Bojariu, R., Birisan, M. V., Marin, L. and Manea, A., 2015: Recent climatic changes in Romania from observational data (1961–2013). *Theor. Appl. Climatol.* 122, 111–119. <https://doi.org/10.1007/s00704-014-1290-0>
- ETCCDI, 2009: Climate Change Indices, Definitions of the 27 Core Indices. Retrieved on February 8 2017 from http://etccdi.pacificclimate.org/list_27_indices.shtml
- Filahi, S., Tanarhte, M., Mouhir, L., El Morhit, M. and Tramblay, Y., 2016: Trends in indices of daily temperature and precipitations extremes in morocco. *Theor. Appl. Climatol.* 124, 959–972. <https://doi.org/10.1007/s00704-015-1472-4>
- Frich, P., Alexander, L.V., Della-Marta, P., Gleason, B., Haylock, M., Klein Tank, A.M.G. and Peterson, T., 2002: Observed coherent changes in climatic extremes during the second half of the twentieth century. *Climate Res.* 19, 193–212. <https://doi.org/10.3354/cr019193>
- Gajić-Čapka, M., Cindrić, K. and Pasarić, Z., 2015: Trends in precipitation indices in Croatia, 1961–2010. *Theor. Appl. Climatol.* 121, 167–177. <https://doi.org/10.1007/s00704-014-1217-9>
- Gavrilov, M.B., Tošić, I., Marković, S.B., Unkašević, M. and Petrović, P., 2016: Analysis of annual and seasonal temperature trends using the Mann-Kendall test in Vojvodina, Serbia. *Időjárás* 120, 183–198.
- Gilleland, E. and Katz, R.W., 2016: extRemes 2.0: an extreme value analysis package in R. *J. Stat. Software* 72, 1–39. <https://doi.org/10.18637/jss.v072.i08>
- Hartmann, D.L., Klein Tank, A.M.G., Rusticucci, M., Alexander, L.V., Brönnimann, S., Charabi, Y., Dentener, F.J., Dlugokencky, E.J., Easterling, D.R., Kaplan, A., Soden, B.J., Thorne, P.W., Wild, M. and Zhai, P.M., 2013: Observations: atmosphere and surface. In (Eds.: Stocker, T.F., Qin, D., Plattner, G.K., Tignor, M., Allen, S.K., Boschung, J., Nauels, A., Xia, Y., Bex, V. and Midgley, P.M.) Climate change 2013: the physical science basis, Contribution of Working Group I to the Fifth Assessment Report of the Intergovernmental Panel on Climate Change. Cambridge University Press, Cambridge. 159–254
- IPCC, 2014: Climate change 2014: synthesis report. Contribution of Working Groups I, II and III to the Fifth Assessment Report of the Intergovernmental Panel on Climate Change (Eds. Core Writing Team, Pachauri, R.K., & Meyer, L.A.) IPCC, Geneva.
- Kiktev, D., Sexton, D.M.H., Alexander, L. and Folland, C.K., 2003: Comparison of modeled and observed trends in indices of daily climate extremes. *J. Climate* 16, 3560–3571. [https://doi.org/10.1175/1520-0442\(2003\)016<3560:COMAOT>2.0.CO;2](https://doi.org/10.1175/1520-0442(2003)016<3560:COMAOT>2.0.CO;2)
- Kioutsioukis, I., Melas, D. and Zerefos, C., 2010: Statistical assessment of changes in climate extremes over Greece (1955–2002). *Int. J. Climatol.* 30, 1723–1737. <https://doi.org/10.1002/joc.2030>
- Klein-Tank, A.M.G. and Könen, G.P., 2003: Trends indices of daily temperature and precipitation extremes in Europe, 1946–99. *J. Climate* 16, 3665–3680. [https://doi.org/10.1175/1520-0442\(2003\)016<3665:TIIODT>2.0.CO;2](https://doi.org/10.1175/1520-0442(2003)016<3665:TIIODT>2.0.CO;2)
- Lakatos, M., Bihari, Z., Szentimrey, T., Spinoni, J. and Szalai, S., 2016: Analyses of temperature extremes in the Carpathian region in the period 1961–2010. *Időjárás* 120, 41–51.
- Lakatos, M., Szentimrey, T. and Bihari, Z., 2011: Application of gridded daily data series for calculation of extreme temperature and precipitation indices in Hungary. *Időjárás* 115, 99–109.

- de Lima, M.I.P., Santo, F.E., Ramos, A.M. and Trigo, R.M., 2015: Trends and correlations in annual extreme precipitation indices for mainland Portugal, 1941–2007. Theor. Appl. Climatol.* 119, 55–75. <https://doi.org/10.1007/s00704-013-1079-6>
- Łupikasza, E.B., Hänsel, S. and Matschullat, J., 2011: Regional and seasonal variability of extreme precipitation trends in southern Poland and central-eastern Germany 1951–2006. Int. J. Climatol.* 31, 2249–2271. <https://doi.org/10.1002/joc.2229>
- Mihailović, D.T., Drešković, N. and Mimić, G., 2015: complexity analysis of spatial distribution of precipitation: an application to Bosnia and Herzegovina. Atmos. Sci. Lett.* 16, 324–330. <https://doi.org/10.1002/asl2.563>
- Moberg, A. and Jones, P.D., 2005: Trends in indices for extremes in daily temperature and precipitation in central and western Europe, 1901–99. Int. J. Climatol.* 25, 1149–1171. <https://doi.org/10.1002/joc.1163>
- Ongoma, V., Chen, H. and Omonya, G.W., 2016: Variability of extreme weather events over the Equatorial East Africa, a case study of rainfall in Kenya and Uganda. Theor. Appl. Climatol.* 131, 295–308. <https://doi.org/10.1007/s00704-016-1973-9>
- Pongrácz, R., Bartholy, J. and Kis, A., 2014: Estimation of future precipitation conditions for Hungary with special focus on dry periods. Időjárás 118, 305–321.*
- Pongrácz, R., Bartholy, J., Gelybó, G. and Szabó, P., 2009: Detected and expected trends of extreme climate indices for the Carpathian Basin. In (Eds. Střelcová, K., Mátyás, C., Kleidon, A., Lapin, M., Matejka, F., Blaženec, M., Škvarenina, J. and Holécy, J.) *Bioclimatology and Natural Hazards*. Springer, Dordrecht. 15–28. https://doi.org/10.1007/978-1-4020-8876-6_2*
- Popov, T., Gnjato, S., Trbić, G. and Ivićević, M., 2018: Recent Trends in Extreme Temperature Indices in Bosnia and Herzegovina. Carpathian J. Earth and Environ. Sci.* 13, 211–224.
- Popov, T., Gnjato, S., Trbić, G. and Ivićević, M., 2017: Trends in Extreme Daily Precipitation Indices in Bosnia and Herzegovina. Collection of Papers - Faculty of Geography at the University of Belgrade 65, online first (<http://zbornik.gef.bg.ac.rs/pdf/radovi/182.pdf>)*
- Powell, E.J. and Keim, B.D., 2015: Trends in daily temperature and precipitation extremes for the Southeastern United States: 1948–2012. J. Climate* 28, 1592–1612. <https://doi.org/10.1175/JCLI-D-14-00410.1>
- Sheikh, M.M., Manzoor, N., Ashraf, J., Adnan, M., Collins, D., Hameed, S., Manton, M. J., Ahmed, A.U., Baidya, S.K., Borgaonkar, H.P., Islam, N., Jayasingheharachchi, D., Kothawale, D.R., Premalal, K.H.M.S., Revadekar, J.V. and Shrestha, M.L., 2015: Trends in extreme daily rainfall and temperature indices over South Asia. Int. J. Climatol.* 35, 1625–1637. <https://doi.org/10.1002/joc.4081>
- Skansi, M.M., Brunet, M., Sigro, J., Aguilar, E., Groening, J.A.A., Bentancur, O.J., Castellon Geier, Y.R., Correa Amaya, R.I., Jacome, H., Malheiros Ramos, A., Oria Rojas, C., Pasten, A.M., Mitro, S.S., Villaroel Jimenez, C., Martinez, R., Alexander, L.V. and Jones, P.D., 2013: Warming and wetting signals emerging from analysis of changes in climate extreme indices over South America. Glob. Planet. Change* 100, 295–307. <https://doi.org/10.1016/j.gloplacha.2012.11.004>
- Skowera, B., Kopcińska, J.J. and Bokwa, A., 2016: Changes in the structure of days with precipitation in southern Poland in 1971–2010. Időjárás* 120, 365–381.
- Tian, J., Liu, J., Wang, J., Li, C., Nie, H. and Yu, F., 2017: Trend analysis of temperature and precipitation extremes in major grain producing area of China. Int. J. Climatol.* 37, 672–687. <https://doi.org/10.1002/joc.4732>
- Trbić, G., 2010: Ecoclimatological Regionalisation of the Peripannonian Rim in the Republic of Srpska. Geographic society of the Republic of Srpska, Banja Luka. (in Serbian)*
- Trbić, G., Popov, T. and Gnjato, S., 2017: Analysis of air temperature trends in Bosnia and Herzegovina. Geographica Pannonica* 21, 68–84. <https://doi.org/10.5937/GeoPan1702068T>
- Unkašević, M. and Tošić, I., 2011: A statistical analysis of the daily precipitation over Serbia: trends and indices. Theor. Appl. Climatol.* 106, 69–78. <https://doi.org/10.1007/s00704-011-0418-8>
- van den Besselaar, E.J.M., Klein Tank, A.M.G. and Buishand, T.A., 2013: Trends in European precipitation extremes over 1951–2010. Int. J. Climatol.* 33, 2682–2689.
- Zhang, X. and Yang, F., 2004: RClimDex (1.0) User Manual. Climate Research Branch Environment Canada, Downsview, Ontario, Canada.*

IDÓJÁRÁS

*Quarterly Journal of the Hungarian Meteorological Service
Vol. 122, No. 4, October – December, 2018, pp. 453–462*

Methodology of objective three-dimensional identification and tracking of cyclones and anticyclones in the low and middle troposphere

Evhen V. Samchuk

*Ukrainian Hydrometeorological Institute
Nauky av., 37, 03028 Kyiv, Ukraine*

Authors E-mail: evhen.samchuk@gmail.com

(Manuscript received in final form October 25, 2017)

Abstract — Extratropical cyclones and anticyclones are the main objects in researches of the large-scale atmospheric circulation processes in midlatitudes. In this context, new data which can improve our knowledge about their typical places of origin, tracks, and lifetime characteristics were critical.

The purpose of this research is to analyze existing methods and algorithms, used for cyclone and anticyclone identification and tracking, and to develop a three-stage methodology of baric systems identification in the low and middle troposphere based on a three-dimensional approach.

This research utilizes 40-year-long datasets of sea level pressure and geopotential height of three standard pressure levels up to 500 hPa covering the Northern hemisphere down to 20°N.

This paper presents a newly developed unified baric systems identification and tracking methodology. It is based on a step-by-step identification of isolated clusters of low and high sea level pressure and geopotential height throughout the low and middle troposphere from the ground level to 500 hPa pressure level. Centers of clusters on different levels for each moment of time are combined in a single vertical profile which represents one certain baric system. Tracking of the baric system movement is realized with nearest neighbor method, improved for more accurate detection and tracking of fast-moving short-living cyclones. In the process, a software was developed for the purposes of the automatic identification of baric systems in the Northern Hemisphere and for creating sets of cinematic schemes of natural synoptic periods. Also, a database of the baric systems existed during on the period of 1976–2015 on the Northern Hemisphere was created.

Key-words: objective identification, baric system, cyclone, anticyclone, reanalysis, trajectories, software.

1. Introduction

Among all processes occurring in the atmosphere, cyclonic and anticyclonic activities are the most fundamental and persistent. It includes formation, evolution, movement and decline of cyclones and anticyclones in the lower and middle troposphere in the midlatitudes of the Northern Hemisphere. This process provides transportation and distribution of atmospheric energy, heat, and moisture on the global scale, so objective knowledge of its progress is vital for description and systematization of the different weather regimes. The best way of this systematization in the traditions of the soviet synoptic school, which is still represented at the Ukrainian weather service, is a compiling of the so-called 'joint kinematic maps' of the natural synoptic periods. Despite of the critical importance of such activities in understanding of the state of the atmosphere and its tendencies, it is still fully performed in manned mode without any automation.

On the one hand, identification and tracking of extratropical cyclones is heavily studied due to their significant role in a wide spectrum of weather phenomena. Thus, there is no surprise that in the last 20 years numerous different methods of cyclone identification and tracking were developed and applied (*Alpert et al.*, 1990; *Murray and Simmonds*, 1991; *Keonig et al.*, 1993; *Hodges*, 1994; *Serreze*, 1995; *Sinclair*, 1997; *Sickmoller et al.*, 2000; *Klawa and Ulbrich*, 2003; *Hanson et al.*, 2004; *Bengtsson et al.*, 2006; *Wernli and Schwierz*, 2006; *Raible et al.*, 2008; *Inatsu*, 2009). Each of them is based on different perceptions of what cyclone is, and utilizes different atmospheric variables, such as sea level pressure (*Benestad and Chen*, 2006), its gradient (*Leckebusch et al.*, 2006), geopotential height of 1000 (*Blender and Schuber*, 2000) and 850 hPa (*Hewson and Titley*, 2010) pressure levels, Laplasian of the geopotential height (*Balabukh*, 2005; *Neu U. et al.*, 2010; *Trigo*, 2011) and potential vorticity (*Kew et al.*, 2010). Each of these methods has its limitations, determining conditions under which localized baric system could be ignored, such as distance of day-to-day displacement, duration of existence, or elevation above sea level of the region of baric system existence (*Pinto et al.*, 2005). On the other hand, results provided by these methods are hard to intercompare.

Also, the most frequently used variable in these methods is a sea level pressure, while higher levels of troposphere are ignored. Besides, a very few information about anticyclone identification and tracking methods can be found due to their less dangerous overall impact on weather.

Taking all into account the above mentioned facts, the necessity of a reliable and universal methodology of three-dimensional identification of both cyclone and anticyclone became clear.

The full-scale methodology of the three-dimensional baric systems identification consists of three stages:

1. Localization of the low and high pressure centers in the sea level pressure (SLP) fields and on the pressure surfaces (850, 700, and 500 hPa).

2. Combination of the centers into a vertical profile of a single baric system.
3. Tracking of baric system movement and evolution during its whole lifecycle.

2. Initial data and methods

This research utilizes the 40-year-long NCEP/NCAR Reanalysis dataset, including 4-time daily sea level pressure (SLP) fields, and the geopotential height of the 850, 700, and 500 hPa pressure surfaces (ESRL: PSD: NCEP/NCAR Reanalisis 1). The period of interest is from 1976 to 2015, and the research region includes part of the Northern Hemisphere from 20°N to the north. All algorithms are realized with C# programming language under .NET platform using Windows Forms technology. GDI+ programming interface was used for maps composition and graphics visualization.

3. Localization of the pressure centers

Fig. 1 shows a part of the region of interest and also represents every grid node within it. It is important to emphasize that each square on the map represents one single node of a grid, which means that the node's actual position is referred to as the center of a square. Numbers near the x and y axis refers to the numbers of grid columns and rows inside the original dataset correspondently. Every number (N) can be translated into latitude or longitude using Eqs. (1) and (2):

$$\varphi = -2.5N + 90^\circ. \quad (1)$$

$$\lambda = 2.5N. \quad (2)$$

Also it is necessary to explain such a large region of interest in this research. While other identification methods has been tested on relatively small regions, such as Europe or the North Pacific region, in this case the Northern Hemisphere was chosen in order to avoid unnecessary accuracy drops even in face of the bigger amount of data to analyze and time to spend. The reason of this choice is inside of the form the logical representation of initial data. Dataset transfer data are derived from the Earth's spherical surface into a two-dimensional array, each cell of which represent a single node of a grid.

In case of an array, which covers the whole Northern Hemisphere, the left side of this rectangle is actually a continuation of the right one. But in the logic model there are two opposite sides of the region of interest, so any analysis of the geometric shape of the SLP or the geopotential field, performed on limited area without taking this data feature into account, leads to a critical failure on both left and right edges. The method of center's localization, described below, does take this feature into account, so on one hand it is protected from erroneous detection, and on the other

hand it covers entire hemisphere, allowing further study of atmospheric circulation in any region on demand.

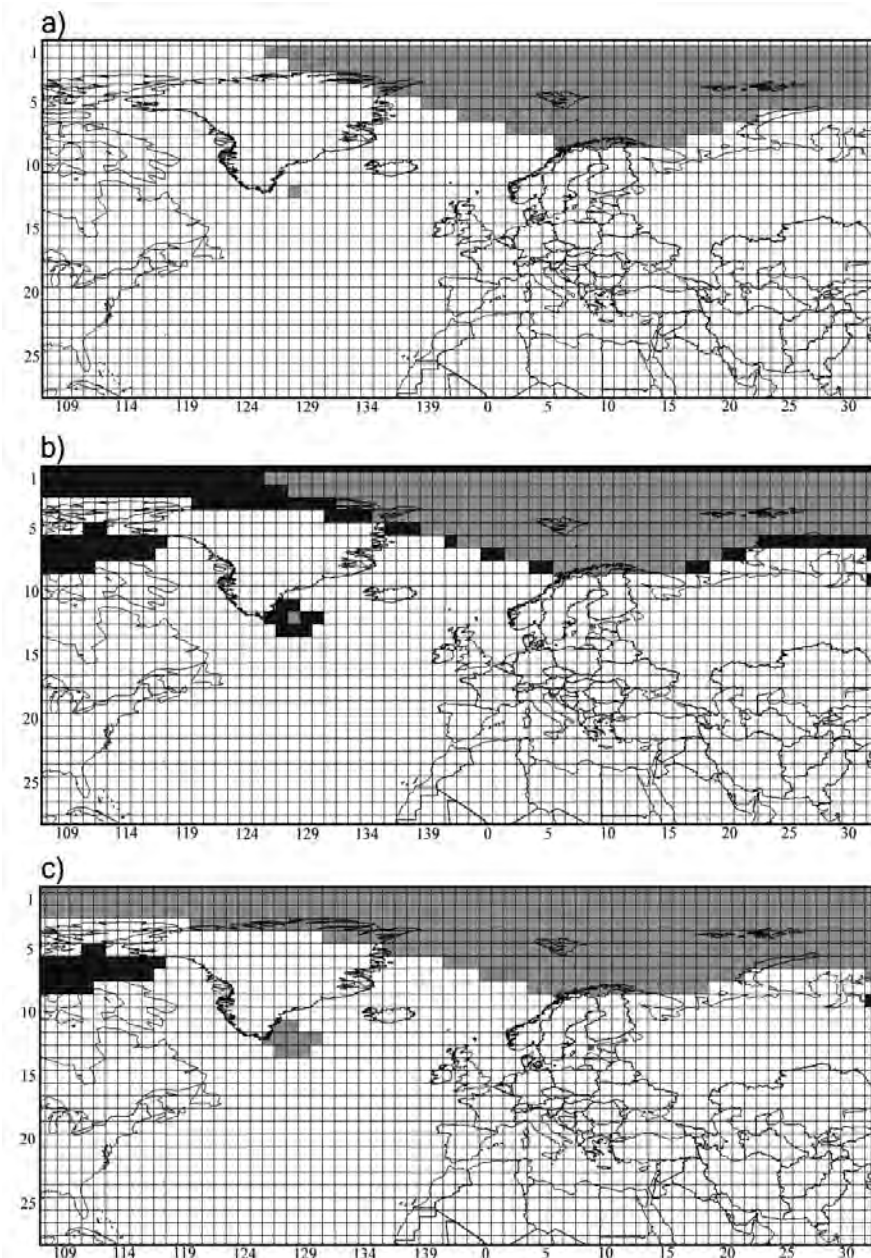


Fig. 1. Stages of grid nodes filtering during the localization of the pressure centers.

The first stage is accomplished through the method of regular grid nodes filtering. Employment of this method will be demonstrated on the localization of low-pressure centers in the SLP field. All statements are applicable to the localization of the rest types of centers with few clauses, which will be mentioned later.

Localization of a low-pressure center in the SLP field is performed through the allocation of isolated low-pressure clusters via regular grid nodes iterative filtering. The first step is calculating of pressure minima within the grid, which hereinafter will be a reference value. Then this value is replaced with the nearest number that is greater than it and is a multiple of 5 (according to the rules of hemisphere-scale SLP charts composing isobar values which are always a multiple of 5). Then, among all nodes of grid, only those are picked into the initial array for analysis, in which the pressure is less than reference value (*Fig. 1a, light gray squares*). At this stage of progress, nodes, contained in the initial array are divided into separate clusters. Each cluster contains nodes that directly adjoin each other and does not adjoin nodes from any other clusters. As it can be seen from *Fig. 1a*, initial array was divided into two separate clusters – one in the polar region and the other one, which contains only one grid node, near Greenland.

For each of these clusters, the node with the local minima of pressure and the node, representing the geometrical center of the cluster, are designated. Grid node of a cluster with coordinates (φ_g, λ_g) which satisfies condition (Eq.(3)) is marked as the geometrical center of the cluster:

$$\sum_{i=1}^n \sqrt{(\varphi_g - \varphi_i)^2 + (\lambda_g - \lambda_i)^2} = \min. \quad (3)$$

For now, only the deepest centers of the grid are picked up, so the reference value is incremented by 5 hPa, and the clusterization procedure repeats. Thus, beginning from the second procedure iteration, additional node filtering are involved. Because of the repetitive picking of the previously analyzed nodes, fresh-composed clusters will consist of grid nodes, which were already used on the previous iteration or directly adjoin them. (*Fig. 1b, dark gray squares*). To avoid this, all nodes, adjoining previously composed clusters, are ignored and only previously uncharted centers are brought to the analysis (*Fig. 1c, dark gray squares*). Applying this additional filtering allows to decrease the time expenses by 5 times, which is vital in case of lack of computing resources and large time periods to process. As a result, the analysis of a single field takes nearly 1 second even on low-end computers, independently from the field structure and the seasons of the year. The described clusterization procedure is repeated until the reference value is lower than 1020 hPa, which is the boundary between cyclonic and anticyclonic fields.

The identification procedure has a few features while applying in different conditions. Thus, when localizing high-pressure centers in the SLP field, firstly the grid pressure maxima is picked up as reference value, and then it is iteratively decreased to 1020 hPa. On the pressure surfaces, the reference value decreases and increases by 4 geopotential decameters. Besides, there is no field division into cyclonic and anticyclone parts, and both high- and low-pressure centers localized through all available reference values from grid minima to maxima.

Results of the center localization on each level are stored in the database, which contains information about every localized center, such as its type (low- or high-pressure), pressure level, where center has been localized, coordinates of grid node with extreme pressure value within every unique cluster, as well as coordinates of its geometrical center.

There is a reason why the terms ‘cyclone’ and ‘anticyclone’ were avoided previously. Centers, localized on the first stage of the baric system identification, cannot be directly associated with a particular cyclone or anticyclone, because these centers are only the grid nodes, outlined with isoline. Thus, the question of belonging of each center to the real baric system remains uncertain on this stage. This uncertainty resolves on the next stage of the baric systems’ identification, where the composition of their vertical profile is taking place.

4. Composing of the baric system profile

Vertical profile is a source of valuable characteristics of the baric system. First of all, it describes its vertical extension, which allow us to assign the examined system to one of the principal groups: low, middle, high, or upper baric system. Also, the profile's tilt angle is specific for each stage of the baric system lifetime. Profile of a new-formed baric system has significant slant on the higher levels, but on the later stages it is negligible. Last, but not least: composing a vertical profile allows us to operate with such terms as ‘cyclone’ and ‘anticyclone’, which were avoided earlier, and to treat identified structures as full-scale baric systems, which exists not only on one particular level, but in a whole thickness of the low and middle troposphere.

Algorithm of the baric system profile composition uses characteristics of the previously localized centers as raw data. The geometrical location of the center, localized in the SLP field, became the first point of the profile. After that, the algorithm searches for centers suitable for the current profile, on each of the rest levels. The only condition of including a center into profile is localization of one within a radius of 500 km from the previous profile point. After that the centers selected by the profile completion are removed from the initial array, the procedure is repeated until all centers are involved in profiles, independently from the level where profile composition begins. The result of this procedure is an array of the profile entities. Each profile entity contains detailed

characteristics of each profile point as well as generic characteristics of each profile, such as type, number of involved levels, and averaged geographical coordinates of profile which represent the general position of a baric system in the atmosphere. Also, all profiles which involve only one level are removed from the result collection.

5. Baric system tracking

The final stage of the baric system identification implies the nearest neighbor method also known as NN-method (*Fix and Hodges, 1951*) for cyclones and anticyclones tracking, using baric systems coordinates obtained on the previous stage. From this point, coordinates of each baric system will be mentioned as ‘nodes’. By this approach, every node can be included into a trajectory when its distance from the previous and next trajectory nodes is minimal. The maximum distance between trajectory nodes is limited to 700 km. This distance corresponds to a baric system movement speed of 110 km/h, which surely exceeds the actual velocities of fast-moving cyclones, preventing trajectory division. Analysis of manually composed cyclone and anticyclone tracks showed that in nearly 35% of cases, the opposite issue takes place when two cyclones tracks are composed into a single one when one of them declines nearby another. Low time resolution (12 hours and more) of initial data promotes this issue as well. This is the reason why the nearest neighbor method was improved with one significant modification to prevent such issues. Beginning from the second node of any trajectory, additional movement direction verification is applied to prevent combining two different cyclones into one trajectory. This verification checks directions of the cyclone movement on two adjacent sections of the trajectory. If movement directions on these sections are opposite or directed closely opposite one to another, the last node is not included into the trajectory, but trajectory compositions are continued. The distance limit increases by 1.5 times, and the next node of trajectory is picked up among centers of the next time stamp. If the algorithm is unable to find the next trajectory node under this condition, the trajectory composition interrupts completely, and the distance limit returns to the original value. Also, all trajectories that last for less than 24 hours are ignored. Similarly to the first two stages of the baric system identification, results of trajectory composition are stored in the database.

6. Accuracy assessment

Objective assessment of the accuracy of the described methodology is obviously complicated, because each stage itself also demands accuracy assessment. Due to lack of similar researches, dedicated to the same period and region, accuracy

assessment was performed through visual control of correspondence between the location of identified centers on each pressure level and its actual location on the map. The comparison covers the whole year of 2015 and involves almost six thousands unique maps of SLP (4 maps per day) and geopotential height on three pressure levels (12 maps per day). This verification has demonstrated a weak spot of the localization algorithm associated with the features of input data. In cases, when gridded data contain single nodes which can be outlined with isolines, excessive center localization takes place. It is caused by the incapability of displaying nodes with grid translation into conical projection during the map composition. However, it decreases the accuracy of center localization only by 5% in the SLP field and less than 1% on the rest of the pressure levels (*Table 1*). Nevertheless, it can not affect the accuracy of the baric system identification, because such erroneously localized centers will not be included into the vertical profile.

Table 1. Accuracy of the localization of high- and low-pressure centers on each level

Level	Low-pressure centers		Accuracy [%]	High-pressure centers		Accuracy [%]
	Total	Excessive		Total	Excessive	
SLP	12838	510	96.2	10854	595	94.8
H850	12468	124	99.0	7680	80	99.0
H700	10534	110	99.0	5290	37	99.3
H500	10663	105	99.0	3775	32	99.2

Due to modifications applied to the NN-method, tracking efficiency has been significantly improved, especially in cases of several intensive, fast-moving cyclones, which develop and decline nearby to each others. The increased criteria, applied to anticyclone tracking, prevent fragmentation of long-living stationary anticyclone trajectory caused by center displacement. The discovered issues affect only the first stage of the entire procedure and can be ignored. Thus, overall climatology of both cyclone and anticyclone activities sustain minimal impact.

7. Conclusions

The developed methodology reflects new perspective on the baric system identification and tracking with classic synoptic perception of cyclones and anticyclones as three-dimensional structures, covering few vertical levels at once. This approach appears in a multi-staged algorithm, which provides reliable data about the lifetime characteristics of cyclones and anticyclones. The reliability of the results is provided through objective limitations, derived from issues, found during analysis of manually performed identification procedure. The assessment of the new identification methodology's accuracy showed it extremely high precision compared to the manual identification. Also, algorithm optimization tends to decrease the time expense, allowing running identification procedure on big time periods without any necessity for a powerful computer. The developed database (with generic and detailed characteristics of the cyclones and anticyclones, which existed in the Northern Hemisphere in the period of 1976–2015) can be used for the further study of any kind of specific types of the large-scale atmospheric processes, such as atmospheric blocking, southern cyclones, etc.

References

- Alpert P., Neeman B.U., and Shay-El Y., 1990: Climatological analysis of Mediterranean cyclones using ECMWF data. Tellus 42A, 65–77.*
- Balabukh V., 2005: Objective identification of synoptic-scale baric systems. Taras Shevchenko Nat. Univ. Kyiv Bull. 51, 49–50.*
- Benestad, R.E. and Chen, D., 2006: The use of a calculus-based cyclone identification method for generating storm statistics. Tellus 58A, 473–486.
<https://doi.org/10.1600-0870.2006.00191.x>*
- Bengtsson, L.K., Hodges K.I., and Roeckner, E., 2006: Storm tracks and climate change. J.Climate 19, 3518–3543. <https://doi.org/10.1175/JCLI3815.1>*
- Blender, R. and Schubert, M., 2000: Cyclone tracking indifferent spatial and temporal resolutions. Month. Weather Rev. 128, 377–384.
[https://doi.org/10.1175/1520-0493\(2000\)128<0377:CTIDSA>2.0.CO;2](https://doi.org/10.1175/1520-0493(2000)128<0377:CTIDSA>2.0.CO;2)*
- ESRL: PSD: NCEP/NCAR Reanalisisys 1:
<https://www.esrl.noaa.gov/psd/data/gridded/data.ncep.reanalysis.html>*
- Fix E. and Hodges, J.L., 1951: Discriminatory analysis, nonparametric discrimination, consistency properties. U.S. Air Force School of Aviation Medicine, Randolph Field, Texas, Project 21-49-004, Contract AF 41(128)-31, Rep. 4, 1951.*
- Hanson, C.E., Palutikof, J.P., and Davies, T.D., 2004: Objective cyclone climatologies of the North Atlantic – a comparision between ECMWF and NCEP reanalysis. Climate Dynam. 22, 757–769. <https://doi.org/10.1007/s00382-004-0415-z>*
- Hewson, T.D. and Titley H. A., 2010: Objective identification, typing and tracking of the complete life-cycles of cyclonic features at high spatial resolution. Meteorol. Appl. 17, 355–381.
<https://doi.org/10.1002/met.204>*
- Hodges, K.I., 1994: A general method for tracking analysis and its applications to meteorological data, Month. Weather Rev. 122, 2573–2586.
[https://doi.org/10.1175/1520-0493\(1994\)122<2573:AGMFTA>2.0.CO;2](https://doi.org/10.1175/1520-0493(1994)122<2573:AGMFTA>2.0.CO;2)*

- Inatsu, M.*, 2009: The neighbor enclosed area tracking algorithm for extratropical wintertime cyclones. *Atmos. Sci. Lett.* 10, 267–272. <https://doi.org/10.1002/asl.238>
- Kew, S.F., Sprenger, M., and Davies, H.C.*, 2010: Potential vorticity anomalies of the lower most stratosphere: A 10-yr winter climatology. *Month. Weather Rev.* 138, 1234–1249. <https://doi.org/10.1175/2009MWR3193.1>
- Keonig, W., Sausen, R., and Sielmann, F.*, 1993: Objective identification of cyclones in GCM simulations. *J. Climate*, 6, 2217–2231. [https://doi.org/10.1175/1520-0442\(1993\)006<2217:OIOCIG>2.0.CO;2](https://doi.org/10.1175/1520-0442(1993)006<2217:OIOCIG>2.0.CO;2)
- Klawa, M. and Ulbrich, U.*, 2003: A model for the estimation of storm losses and the identification of severe winter storms in Germany. *Nat. Haz. Earth Syst. Sci.* 3, 725–732. <https://doi.org/10.5194/nhess-3-725-2003>
- Leckebusch, G.C., Koffi, B., Ulbrich, U., Pinto, J.G., Span-Gehl, T., and Zacharias, S.*, 2006: Analysis of frequency and intensity of winter storm events in Europe on synoptic and regional scales from a multi-model perspective, at synoptic and regional scales. *Climate Res.* 31, 59–74. <https://doi.org/10.3354/cr031059>
- Murray, R.J. and Simmonds, I.*, 1991: A numerical scheme for tracking cyclone centres from digital data, part 1: development and operation of the scheme. *Australian Meteorol. Mag.* 39, 155–156.
- Neu, U., Akperov, M.G.; Bellenbaum, N.; Benestad, R., Blender, R., Caballero, R., Cocozza, A., Dacre, H.F., Feng, Y., Fraedrich, K., Griege, J., Gulev, S., Hanley, J., Hewson, T., Inatsu, M., Keay, K., Kew, S.F., Kindem, I., Leckebusch, G.C., Liberato, M.L.R., Lionello, P., Mokhov, I.I., Pinto, J.G., Raible, C.C., Reale, M., Rudeva, I., Schuster, M., Simmonds, I., Sinclair, M., Sprenger, M., Tilinina, N.D., Trigo, I.F., Ulbrich, S., Ulbrich, U., Wang, Xi.L., and Wernli, H.*, 2013: IMILAST: A Community Effort to Intercompare Extratropical Cyclone Detection and Tracking Algorithms. *Amer. Meteorol. Soc.* 94, 529–547. <https://doi.org/10.1175/BAMS-D-11-00154.1>
- Pinto, J.G., Spangehl, T., Ulbrich, U., and Speth, P.*, 2005: Sensitivities of a Cyclone Detection and Tracking Algorithm: Individual Tracks and Climatology. *Meteorol. Zeitschrift* 14, 823–838. <https://doi.org/10.1127/0941-2948/2005/0068>
- Raible, C., Della-Marta, P.M., Schewierz, C., Wernli, H., and Blender, R.*, 2008: Northern hemisphere extratropical cyclones: A comparison of detection and tracking methods and different reanalysis. *Month. Weather Rev.* 136, 880–897. <https://doi.org/10.1175/2007MWR2143.1>
- Serreze, M.C.*, 1995: Climatological aspects of cyclone development and decay in the Arctic. *Atmos.–Ocean* 33, 1–23. <https://doi.org/10.1080/07055900.1995.9649522>
- Sickmoller, M., Blender, R., and Fraedrick, K.*, 2000: Observed winter cyclone tracks in the northern hemisphere in reanalysed ECMWF data. *Quart. J. Roy. Meteorol. Soc.* 126, 591–620. <https://doi.org/10.1002/qj.49712656311>
- Sinclair, M.R.*, 1997: Objective identification of cyclones and their circulation intensity and climatology. *Weather Forecast.* 12, 595–612. [https://doi.org/10.1175/1520-0434\(1997\)012<0595:OIOCAT>2.0.CO;2](https://doi.org/10.1175/1520-0434(1997)012<0595:OIOCAT>2.0.CO;2)
- Trigo, R. and Klaus, M.*, 2011: An exceptional winterstorm over northern Iberia and southern France. *Weather* 66, 330–334. <https://doi.org/10.1002/wea.755>
- Wernli H. and Schwierz C.*, 2006: Surface cyclones in the ERA-40 data set (1958–2001). Part 1: Novel identification method and global climatology. *J. Atmos. Sci.* 63, 2486–2507. <https://doi.org/10.1175/JAS3766.1>

IDÓJÁRÁS

VOLUME 122 * 2018

EDITORIAL BOARD

- ANTAL, E. (Budapest, Hungary)
BARTHOLY, J. (Budapest, Hungary)
BATCHVAROVA, E. (Sofia, Bulgaria)
BRIMBLECOMBE, P. (Hong Kong, SAR)
CZELNAI, R. (Dörgicse, Hungary)
DUNKEL, Z. (Budapest, Hungary)
FERENCZI, Z. (Budapest, Hungary)
GERESDI, I. (Pécs, Hungary)
HASZPRA, L. (Budapest, Hungary)
HORVÁTH, Á. (Siófok, Hungary)
HORVÁTH, L. (Budapest, Hungary)
HUNKÁR, M. (Keszthely, Hungary)
LASZLO, I. (Camp Springs, MD, U.S.A.)
MAJOR, G. (Budapest, Hungary)
MÉSZÁROS, E. (Veszprém, Hungary)
MÉSZÁROS, R. (Budapest, Hungary)
- MIKA, J. (Eger, Hungary)
MERSICH, I. (Budapest, Hungary)
MÖLLER, D. (Berlin, Germany)
PINTO, J. (Res. Triangle Park, NC, U.S.A.)
PRÁGER, T. (Budapest, Hungary)
PROBÁLD, F. (Budapest, Hungary)
RADNÓTI, G. (Reading, U.K.)
S. BURÁNSZKI, M. (Budapest, Hungary)
SZALAI, S. (Budapest, Hungary)
SZEIDL, L. (Budapest, Hungary)
SZUNYOGH, I. (College Station, TX, U.S.A.)
TAR, K. (Debrecen, Hungary)
TÄNCZER, T. (Budapest, Hungary)
TOTH, Z. (Camp Springs, MD, U.S.A.)
VALI, G. (Laramie, WY, U.S.A.)
WEIDINGER, T. (Budapest, Hungary)

Editor-in-Chief
LÁSZLÓ BOZÓ

Executive Editor
MÁRTA T. PUSKÁS

BUDAPEST, HUNGARY

AUTHOR INDEX

- Anda, A. (Keszthely, Hungary).....41, 203
Baćević, N. (Kosovska Mitrovica, Serbia) ..259
Bartoszek, K. (Lublin, Poland).....101
Basarin, B. (Novi Sad, Serbia).....321, 409
Berbeć, T. (Puławy, Poland)361
Bielec-Bąkowska, Z. (Sosnowiec, Poland) .375
Birkás, M. (Gödöllő, Hungary)31
Bjeljac, D. (Novi Sad, Serbia)321, 409
Bocheva, L. (Sofia, Bulgaria).....177
Bodor, P. (Budapest, Hungary)217
Bogatchev, A. (Sofia, Bulgaria)237
Bonta, I. (Budapest, Hungary).....59
Builtjes, P.J.H. (Utrecht, Netherlands).....119
Chervenkov, H. (Sofia, Bulgaria).....305
Csáki, P. (Sopron, Hungary)81
Czekierda, D. (Warszawa, Poland).....145
Dimitrova, T. (Sofia, Bulgaria)177
Đorđević, J. (Novi Sad, Serbia).....321
Đorđević, T. (Novi Sad, Serbia)321
Doroszewski, A. (Puławy, Poland)361
Gavrilov, M.B. (Novi Sad, Serbia).....409
Gelybó, Gy. (Budapest, Hungary).....119
Gerhátné Kerényi, J. (Budapest, Hungary)1
Grijato, S. (Banja Luka, Bosnia Herzegovina) ..433
Gorgieva, V. (Sofia, Bulgaria)305
Gospodinov, I. (Sofia, Bulgaria)177
Gribovszki, Z. (Sopron, Hungary).....15, 81
Guenther, A.B. (Irvine, USA)119
Hammer, T. (Veszprém, Hungary).....159
Herceg, A. (Sopron, Hungary)81
Hristov, H. (Sofia, Bulgaria)237
Ihász, I. (Budapest, Hungary).....59
Ivanović, R. (Kosovska Mitrovica, Serbia) .259
Jandžiković, B. (Kosovska Mitrovica, Serbia)...259
Jolánkai, M. (Gödöllő, Hungary)31
Kalicz, P. (Sopron, Hungary)81
Kapros, Z. (Gödöllő, Hungary)345
Kassai, K.M. (Gödöllő, Hungary)31
Kazandjiev, V. (Sofia, Bulgaria)305
Kocsis, T. (Budapest, Hungary)203
Koźmiński, C. (Szczecin, Poland).....393
Krępa-Adolf, E. (Krakow, Poland).....375
Kucserka, T. (Keszthely, Hungary).....41
Ladányi, M. (Budapest, Hungary).....217
Lázár, I. (Debrecen, Hungary).....285
Lukić, T. (Novi Sad, Serbia)321, 409
Maris, T. (Novi Sad, Serbia).....409
Marković, S.B. (Novi Sad, Serbia)409
Mátrai, A. (Budapest, Hungary)59
Matzarakis, A. (Freiburg, Germany)321
Mesaroš, M. (Novi Sad, Serbia)409
Mesterházy, I. (Budapest, Hungary)217
Mészáros, R. (Budapest, Hungary)217
Michalska, B. (Szczecin, Poland)393
Micić, T. (Novi Sad, Serbia)321, 409
Milosavljević, S. (Kosovska Mitrovica, Serbia)259
Nieróbca, A. (Puławy, Poland)361
Nikolić, M. (Belgrade, Serbia).....259
Palarz, A. (Krakow, Poland)145
Pavić, D. (Novi Sad, Serbia).....409
Penchev, R. (Sofia, Bulgaria)177
Penjišević, I. (Kosovska Mitrovica, Serbia) ...259
Piotrowicz, K. (Krakow, Poland).....375
Pongrácz, R. (Budapest, Hungary)217
Popov, T. (Banja Luka, Bosnia Herzegovina)..433
Pósá, B. (Gödöllő, Hungary)31
Samchuk, E.V. (Kiev, Ukraine)453
Simeonov, P. (Sofia, Bulgaria)177
Simon, B., (Keszthely, Hungary).....41
Soós, G. (Keszthely, Hungary)41
Stamenković, I. (Novi Sad, Serbia).....321
Stojićević, G. (Novi Sad, Serbia)321
Sulikowska, A. (Krakow, Poland)145
Szinetár, M.M. (Sopron, Hungary)81
Szintai, B. (Budapest, Hungary)59
Szinyei, D. (Veszprém, Hungary).....119
Szűcs, M. (Budapest, Hungary)59
Tar, K. (Debrecen, Hungary)285
Tarnawa, Á. (Gödöllő, Hungary)31
Tóth, E. (Budapest, Hungary)119
Trájer, A.J. (Veszprém, Hungary)159
Trbić G. (Banja Luka, Bosnia Herzegovina).....433
Turnipseed, A.A. (Boulder, USA)119
Ustrnul, Z. (Warszawa, Poland).....145
Vukoičić, D. (Kosovska Mitrovica, Serbia) ...259
Wypych, A. (Krakow, Poland)145
Żyłowska, K. (Puławy, Poland)361

TABLE OF CONTENTS

I. Papers

<i>Anda, A., Simon, B., Soós, G., and Kucserka, T.:</i> Estimation of natural water body's evaporation based on Class A pan measurements in comparison to reference evapotranspiration	41
<i>Bartoszek, K.:</i> The long-term relationships between air flow indices and air temperature over South-East Poland	101
<i>Basarin, B., Lukić, T., Bjelajac, D., Micić, T., Stojićević, G., Stamenković, I., Đorđević, J., Đorđević, T., and Matzarakis, A.:</i> Bioclimatic and climatic tourism conditions at Zlatibor Mountain (Western Serbia)	321
<i>Bielec-Bąkowska, Z., Piotrowicz, K., and Krępa-Adolf, E.:</i> Trends in the frost-free season with parallel circulation and air-mass statistics in Poland.....	375
<i>Bocheva, L., Dimitrova, T., Penchev, R., Gospodinov, I., and Simeonov, P.:</i> Severe convective supercells outbreak over western Bulgaria on July 8, 2014	177
<i>Chervenkov, H., Kazandjiev, V., and Gorgieva, V.:</i> Application of the crop model WOFOST in grid using meteorological input data from reanalysis and objective analysis	305
<i>Csáki, P., Szenetár, M.M., Herceg, A., Kalicz, P., and Gribovszki, Z.:</i> Climate Change Impacts on the Water Balance - Case Studies in Hungarian Watersheds	81
<i>Doroszewski, A., Żyłowska, K., Nieróbca, A., and Berbęć, T.:</i> Agricultural autumn drought and crop yield in 2011 in Poland.....	361
<i>Gerhátné Kerényi, J.:</i> Application of remote sensing for the determination of water management parameters, Hydrology SAF	1
<i>Gribovszki, Z.:</i> Validation of diurnal soil moisture dynamic-based evapotranspiration estimation methods	15
<i>Hristov, H. and Bogatchev, A.:</i> An assessment of daily extreme temperature forecasts – stations average view	237
<i>Ihász, I., Mátrai, A., Szintai, B., Szűcs, M., and Bonta, I.:</i> Application of European numerical weather prediction models for hydrological purposes	59
<i>Jolánkai, M., Kassai, K.M., Tarnawa, Á., Pósa, B., and Birkás, M.:</i> Impact of precipitation and temperature on the grain and protein yield of wheat (<i>Triticum aestivum</i> L) varieties	31
<i>Kapros, Z.:</i> A dynamic data-driven forecast prediction methodology for photovoltaic power systems.....	345
<i>Kocsis, T. and Anda, A.:</i> Parametric or non-parametric: results of time series analyzation of rainfall at a Hungarian meteorological station.....	203
<i>Koźmiński, C. and Michalska, B.:</i> Wind Speed and Direction on the Polish Baltic Coast and Conditions for Recreation.....	393
<i>Lukić, T., Basarin, B., Micić, T., Bjelajac, D., Maris, T., Marković, S.B., Pavić, D., Gavrilov, M.B., and Mesaroš, M.:</i> Rainfall erosivity and extreme precipitation in the Netherlands	409
<i>Mesterházy, I., Mészáros, R., Pongrácz, R., Bodor, P., and Ladányi, M.:</i> The analysis of climatic indicators using different growing season calculation methods – an application to grapevine grown in Hungary	217
<i>Popov, T., Gnjato, S., and Trbić G.:</i> Analysis of extreme precipitation over the Peripannonian region of Bosnia Hercegovina.....	433
<i>Samchuk, E.V.:</i> Methodology of objective three-dimensional identification and tracking of the cyclones and anticyclones in the low and middle troposphere	453
<i>Szinyei, D., Gelybó, Gy., Guenther, A.B., Turnipseed, A.A., Tóth, E., and Builtjes, P.J.H.:</i> Evaluation of ozone deposition models over a subalpine forest in Niwot Ridge, Colorado.....	119

<i>Tar, K.</i> and <i>Lázár, I.</i> : Statistical structure of day by day alteration of daily average wind speeds	285
<i>Trájer, A.J.</i> and <i>Hammer, T.</i> : Expected changes in the length of <i>Anopheles maculipennis</i> (Diptera: Culicidae) larva season and the possibility of the re-emergence of malaria in East Central Europe and the North Balkan Region	159
<i>Vuković, D., Milosavljević, S., Penjišević, I., Bačević, N., Nikolić, M., Ivanović, R., and Jandžiković, B.</i> : Spatial analysis of air temperature and its impact on the sustainable development of mountain tourism in Central and Western Serbia.....	259
<i>Wypych, A., Ustrnul, Z., Czekierda, D., Palarz, A., and Sulikowska, A.</i> : Extreme precipitation events in the Polish Carpathians and their synoptic determinants.....	145

SUBJECT INDEX

A

agricultural drought	361
air masses	375
ALADIN	59, 217
<i>Anopheles maculipennis</i>	159
ANOVA	217, 237
anticyclone	453
aquatic macrophytes	41
AROME	59
assessment	237
atmospheric	
- circulation	375
- drought	361

B

Balaton Lake	41, 81, 203
Balkan, North	159
Baltic sea coast	361, 375, 393
baric system	453
bioclimate	321, 393
Bonferroni's correction	217
Bosnia Hercegovina	433
Budyko model	81
Bulgaria	177, 237, 305

C

Carpathian Basin	31, 159
Carpathians, Poland	145
Central and Eastern Europe	159
circulation	
- atmospheric	145
- index	101
climate	
- change	41, 15, 31,
- 59, 81, 217, 409, 433	
- hazard	409
- indicators	217, 409
- modeling	59, 217
- runoff model	81
- tourism	259, 321
- water balance	361
climatological leaflet	321
coniferous forest	119
convective storms	177
crop	
- model	305
- year	31
- yield	31, 361
crop simulation	305
CTIS	321
cyclone	453

D		
daily		flux, ozone forecast
- average wind speed	285	- dynamic data-driven
- extreme temperature	237	- ensemble
day-to-day changes of wind speed	285	- extreme temperature
data-driven forecast	345	forest
density function	433	frost
deposition model	119	- first fall
discharge areas	15	- last spring
distribution, generalized extreme value	433	frost-free season
diurnal signal	15	
Doppler radar	177	
drought	1	G
- agricultural	361	genetic algorithm
- atmospheric	361	geopotential height
		geostrophic flow
E		grape production
ECMWF	59, 305	gridded crop simulation
ecological modeling	159	growing season calculation
EFAS (flood awareness)	59	groundwater discharge
energy strategy	345	
ensemble forecast	59	H
E-OBS	305	hailstorm
equivalent peak load hour	345	hazards, climate
ERA-Interim	305	Hill index
erosion	409	H-SAF
error		Huglin index
- estimation	285	Hungary
- mean	237	41, 1, 15, 31,
- mean absolute	237	81, 203, 159, 345, 217, 285
evaluation	237	hydrological validation
evaporation	41	1
- Class A pan	41	hydrology
evapotranspiration	41, 15, 81	1, 59
- model CREMAP	81	hydrothermal coefficient
extreme		217
- events	145, 217, 237	I
- precipitation indices	409, 433	index
- value distribution	433	- agricultural drought
		- air flow
F		- circulation
Flood	1, 59	- extreme precipitation
- awareness system	59	- heliothermal
flow, geostrophic	101	- Hill
		- Huglin
		- leaf area
		- modified Fournier
		- NAO
		101

-	standardized evapotranspiration		non-hydrostatic model	59
		361	the Netherlands	409
-	thermal climate	321		
-	Thorntwaite	41		
			O	
K			objective identification	453
Kendall's tau	203		ozone	
Keszthely	41, 203		- deposition model	119
			- fluxes	119
L			P	
lake evaporation	41		peak load hour	345
leaf model	119		Penman-Monteith formula	41, 15
			Péczely's macrosynoptic situations	285
			Peripannonian region	433
M			phenology	217
macrophytes	41		photovoltaic system	345
malaria	159		physiologically equivalent temperature	
Mann-Kendall trend test	203, 259			321
mean absolute error	237		<i>Plasmodium vivax</i>	159
model			Poland	101, 145,
- ALADIN	59, 217		361, 375, 393	
- AROME	59		power prediction	345
- big leaf	119		precipitation	41, 1, 59
- climate-runoff	81		- changes	203
- deposition	119		- extremes	145, 217,
- ECMWF	59		361, 409, 433	
- ecological	159		- long-time series	203
- evapotranspiration	81		- totals	145
- hydrological watershed	81		PRECIS model	217
- numerical weather prediction			pressure	
	59, 177		- long-time series	453
- PRECIS	217		probability	59, 433
- RegCM	217		- density function	433
- REMO climate	159			
- WOFOST	305			
- WRF	177			
modified Fournier index	409		Q	
mosquitoes	159			
			R	
			radar analyses	177
N			rainfall erosivity	409
national energy strategy	345		reanalysis	453
nitrogen supply	31		REMO model	159
Nivot Ridge, Colorado	119		remote sensing	1
			runoff	81

S	U		
satellite	1	Ukraine	453
Sen's slope estimator	203	U.S.A.	119
Serbia	259, 321, 409		
Shuttleworth formula	41	V	
small-scale photovoltaic system	345	validation	1
snow	1	- hydrological	1
soil moisture	1, 15	verification	237
Sopron Hills	15	<i>Vitis vinifera</i>	217
split cells	177	vorticity	101
statistical estimation	285		
storm, severe convective	177	W	
supercell	177	water balance	81, 361
sustainable development	345, 259	- climatic (CWB)	361
synoptic analysis	145, 375	water budget, simplified	41
synoptic situation types	375	watershed	1, 59, 81, 203
		weather	
		- crop yield	31
T		White method	15
temperature		wine production	217
- extremes	217, 237	wind	
- long-time series	101	- bioclimatic conditions	393
- mean monthly	159	- daily average	285
- physiologically equivalent	321	- day-to-day changes	285
- spatial analysis	259	- geostrophic	101
thermal		- speed and direction	393
- climate index	321	winter wheat	31
- sensation	393	WOFOST crop model	305
Thorntwaite index	41	WRF-ARW model	177
trend analysis	203, 259, 433		
three body scatter signature	177		
time series		Y	
- precipitation	203, 217	yield	305, 361
- temperature	101, 217, 259	- grain	31
tourism	259, 321	- protein	31
- Baltic coast in Poland	393		
- mountain	259, 321		
- zones	259, 321		
trajectories	453		
		Z	

INSTRUCTIONS TO AUTHORS OF *IDŐJÁRÁS*

The purpose of the journal is to publish papers in any field of meteorology and atmosphere related scientific areas. These may be

- research papers on new results of scientific investigations,
- critical review articles summarizing the current state of art of a certain topic,
- short contributions dealing with a particular question.

Some issues contain "News" and "Book review", therefore, such contributions are also welcome. The papers must be in American English and should be checked by a native speaker if necessary.

Authors are requested to send their manuscripts to

Editor-in Chief of IDŐJÁRÁS
P.O. Box 38, H-1525 Budapest, Hungary
E-mail: journal.idojaras@met.hu

including all illustrations. MS Word format is preferred in electronic submission. Papers will then be reviewed normally by two independent referees, who remain unidentified for the author(s). The Editor-in-Chief will inform the author(s) whether or not the paper is acceptable for publication, and what modifications, if any, are necessary.

Please, follow the order given below when typing manuscripts.

Title page should consist of the title, the name(s) of the author(s), their affiliation(s) including full postal and e-mail address(es). In case of more than one author, the corresponding author must be identified.

Abstract: should contain the purpose, the applied data and methods as well as the basic conclusion(s) of the paper.

Key-words: must be included (from 5 to 10) to help to classify the topic.

Text: has to be typed in single spacing on an A4 size paper using 14 pt Times New Roman font if possible. Use of S.I.

units are expected, and the use of negative exponent is preferred to fractional sign. Mathematical formulae are expected to be as simple as possible and numbered in parentheses at the right margin.

All publications cited in the text should be presented in the *list of references*, arranged in alphabetical order. For an article: name(s) of author(s) in Italics, year, title of article, name of journal, volume, number (the latter two in Italics) and pages. E.g., *Nathan, K.K.*, 1986: A note on the relationship between photosynthetically active radiation and cloud amount. *Időjárás* 90, 10–13. For a book: name(s) of author(s), year, title of the book (all in Italics except the year), publisher and place of publication. E.g., *Junge, C.E.*, 1963: *Air Chemistry and Radioactivity*. Academic Press, New York and London. Reference in the text should contain the name(s) of the author(s) in Italics and year of publication. E.g., in the case of one author: *Miller* (1989); in the case of two authors: *Gamov and Cleveland* (1973); and if there are more than two authors: *Smith et al.* (1990). If the name of the author cannot be fitted into the text: (*Miller, 1989*); etc. When referring papers published in the same year by the same author, letters a, b, c, etc. should follow the year of publication. DOI numbers of references should be provided if applicable.

Tables should be marked by Arabic numbers and printed in separate sheets with their numbers and legends given below them. Avoid too lengthy or complicated tables, or tables duplicating results given in other form in the manuscript (e.g., graphs). *Figures* should also be marked with Arabic numbers and printed in black and white or color (under special arrangement) in separate sheets with their numbers and captions given below them. JPG, TIF, GIF, BMP or PNG formats should be used for electronic artwork submission.

More information for authors is available: journal.idojaras@met.hu

Published by the Hungarian Meteorological Service

Budapest, Hungary

INDEX 26 361

HU ISSN 0324-6329